Justus-Liebig-Universität Gießen **Klinik Für Neurologie**

Modification of Neuroblastoma – immune interactions by Extracellular RNA (exRNA)

Inaugural Dissertation

Submitted to the

Faculty of Medicine

In partial fulfillment of the requirements for the

PhD - Degree

of the Faculties of Veterinary Medicine and Medicine

of the Justus-Liebig University Giessen, Germany

By

Tahira Zar

Giessen 2020

Germany

From the Department of Neurology of the Justus-Liebig University Giessen

Chairman: Prof. Dr. Manfred Kaps

First Supervisor and Committee member: Prof. Dr. Franz Blaes

Second Supervisor and Committee member: Prof. Dr. Albrecht Bindereif

Chairman and Committee member: Prof. Dr. Klaus-Dieter Schlüter

External Supervisor and Committee member: Prof. Dr. Michael Schroeter

Date of Doctoral Defense: 04.03.2021

I dedicate this thesis to my family,

I love you all dearly

and

I miss you Papa

Declaration

I hereby declare that the present thesis is my original work and that it has not been previously presented in this or any other university for any degree. I have also abided by the principles of good scientific conduct laid down in the charter of the Justus Liebig University of Giessen in carrying out the investigations described in the dissertation.

……

(Tahira Zar)

Giessen, Germany

INDEX

LIST OF ABBREVIATIONS

Aß	Amyloid-beta
AD	Alzheimer disease
ADCC	Antibody-dependent cell-mediated cytotoxicity
ALK	Anaplastic lymphoma kinase
AP-1	Adaptor protein 1
CARs	Chimeric antigen receptors
CMC	Complement-mediated cytotoxicity
CNS	Central nervous system
COG	Children's Oncology Group
CSF	Cerebrospinal fluid
CT	Computed tomography
CTL	Cytotoxic T lymphocyte
dsRNA	Double stranded RNA
EILP	Early innate lymphoid precursor
ELISA	Enzyme linked immunosorbent assay
EMT	Epithelial to mesenchymal transition
EVs	Extracellular vesicles
exRNA	Extracellular RNA
FACS	Fluorescence activated cell sorting
FOXP3	Forkhead Box P3
GTR	Gross total resection
HDACs	Histone deacetylases
HLA	Human leukocyte antigen
HVA	Homovanillic acid
IFN	Interferon
IFN-αβ	Interferon alpha beta

IFN-γ	Interferon Gamma
IL	Interleukin
ILC	Innate Lymphoid Cell
ILD	Interstitial lung disease
INRGSS	International Neuroblastoma Risk Group Staging System
INSS	International Neuroblastoma Staging System
IPF	Idiopathic pulmonary fibrosis
IRF-3	Interferon Regulatory Factor 3
LDH	Lactate dehydrogenase
lncRNA	Long non-coding RNA
MAC	Membrane attack complex
MIBG	Metaiodobenzylguanidine
miRNA	MicroRNA
MMPs	Matrix metalloproteinases
MRI	Magnetic resonance imaging
mRNA	Messenger RNA
MVB	Multivesicular bodies
NB	Neuroblastoma
ncRNA	Non-coding RNA
NF-κB	Nuclear Factor Kappa B
NK cells	Natural Killer cells
OMAS	Opsoclonus-myoclonus-ataxia syndrome
OMS	Opsoclonus myoclonus syndrome
PAMPs	Pathogen-associated molecular patterns
PB	Peripheral blood
PD	Parkinson disease
PHOX2B	Paired Like Homeobox 2B
PNS	Paraneoplastic syndromes

Poly (I:C)	Polyriboinosinic:polyribocytidylic acid
PRRs	Pattern-recognition receptors
RNA	Ribonucleic acid
siRNA	Small interfering RNA
STR	Subtotal resection
TFG-β	Transforming Growth Factor Beta
TICAM	Toll Like Receptor Adaptor Molecule 1
TLR-3	Toll-like receptor 3
TNF	Tumor Necrosis Factor
TRAIL	TNF-related apoptosis-inducing ligand
tRNA	Transfer RNA
US	Ultrasound

LIST OF FIGURES

LIST OF TABLES

1. INTRODUCTION

1.1 Neuroblastoma - Background

1.1.1 Definition

Neuroblastoma (NB) is the most common extracranial solid tumor of childhood and signifies a neoplastic expansion of neural crest cells in the developing sympathetic nervous system. The primary tumor can develop anywhere along sympathetic chain but often arises from the adrenal gland (Arendonk et al., 2018). Neuroblastoma accounts for approximately 8% of all childhood cancers and 15% of childhood cancer mortality (Smith et al., 2018). More than one third of patients are diagnosed during infancy, and approximately 90% are diagnosed before five years of age (Meany, 2019).

About 50% of cases present with metastases at the time of diagnosis, predominantly at bone marrow (70.5%), skeleton (55.7%), lymph nodes (30.9%), liver (29.6%), or intracranial (18.2%) (Morandi et al., 2018).

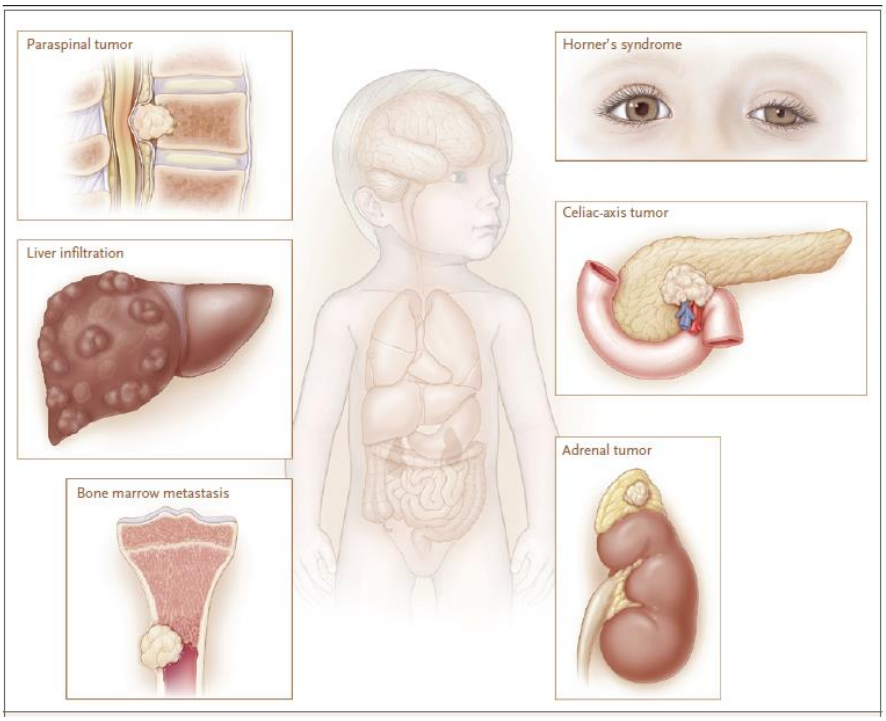

Figure 1. Clinical presentations of Neuroblastoma (Maris, 2010)

1.1.2 Disease Staging

The presurgical International Neuroblastoma Risk Group Staging System (INRGSS) (Cohn et al., 2009 and Monclair et al., 2009) based on the presence or absence of metastatic disease and radiographic characteristics of the primary tumor, has replaced the International Neuroblastoma Staging System (INSS), a post-surgical staging system (Brodeur et al., 1988).

The INRGSS differentiates locoregional tumors based on the absence (stage L1) or presence (stage L2) of image-defined risk factors, a measure of tumor invasiveness. Patients with distant metastatic disease are categorized into stage M disease, and the children with characteristic metastatic pattern of skin, liver and limited bone marrow involvement are classified as stage MS disease (Meany, 2019).

Table 1(a). International Neuroblastoma Risk Group Staging System (INRGSS) (Meany, 2019)

INRG Stage	Description
L1	Localized tumor not involving vital structures as defined by absence of an image-defined risk factor and confined to one body compartment.
L2	Locoregional tumor with presence of one or more image-defined risk factors.
M	Distant metastatic disease (except MS).
MS	Metastatic disease in children younger than 18 months with metastases confined to skin, liver, and/or bone marrow (bone marrow involvement should be limited to <10% of total nucleated cells on smears or biopsy). Primary tumor may be L1 or L2 as defined above.

Table 1(b). The International Neuroblastoma Staging System (INSS)

(Bethesda, 2002)

Stage/Prognostic Group	Description
Stage 1	Localized tumor with complete gross excision, with or without microscopic residual disease; representative ipsilateral lymph nodes negative for tumor microscopically (i.e., nodes attached to and removed with the primary tumor may be positive).
Stage 2A	Localized tumor with incomplete gross excision; representative ipsilateral nonadherent lymph nodes negative for tumor microscopically.
Stage 2B	Localized tumor with or without complete gross excision, with ipsilateral nonadherent lymph nodes positive for tumor. Enlarged contralateral lymph nodes must be negative microscopically.
Stage 3	Unresectable unilateral tumor infiltrating across the midline, with or without regional lymph node involvement; or localized unilateral tumor with contralateral regional lymph node involvement; or midline tumor with bilateral extension by infiltration (unresectable) or by lymph node involvement. The midline is defined as the vertebral column. Tumors originating on one side and crossing the midline must infiltrate to or beyond the opposite side of the vertebral column.
Stage 4	Any primary tumor with dissemination to distant lymph nodes, bone, bone marrow, liver, skin, and/or other organs, except as defined for stage 4S.
Stage 4S	Localized primary tumor, as defined for stage 1, 2A, or 2B, with dissemination limited to skin, liver, and/or bone marrow (by definition limited to infants younger than 12 months). Marrow involvement should be minimal (i.e., <10% of total nucleated cells identified as malignant by bone biopsy or by bone marrow aspirate). More extensive bone marrow involvement would be considered stage 4 disease. The results of the MIBG scan, if performed, should be negative for disease in the bone marrow.

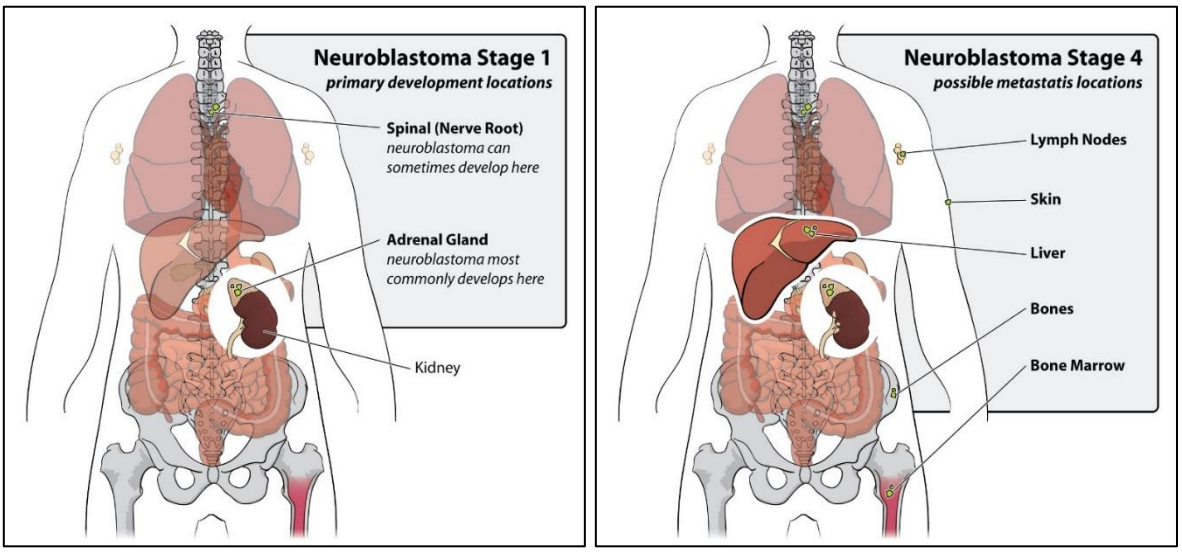

Figure 2. Staging of Neuroblastoma (https://cancerwall.com/neuroblastoma-symptoms-survival-rate-prognosis/)

1.1.3 Signs and Symptoms

The clinical symptoms are diverse and vary depending on the anatomic location of the tumor. The majority of tumors (65%) occur in the abdomen, most of which arise from the adrenal gland, resulting in symptoms of pain, distention, constipation or bowel, and/or bladder dysfunction (Swift et al., 2018). Extra-abdominal disease may occur in the paravertebral ganglia of the neck, chest or pelvis and result in a palpable mass, respiratory symptoms, neurologic compromise or spinal cord impingement. A common manifestation of superior cervical ganglion involvement is Horner syndrome (Ward et al., 2014 and Pollard et al., 2010).

At the time of diagnosis, more than half of the patients with neuroblastoma have metastatic disease. The typical metastatic sites are regional or distant lymph nodes, cortical bone, bone marrow, and liver while involvement of the lungs and brain is rare. Metastatic disease may result in symptoms such as fever, weight loss or fatigue as well

as pancytopenia, periorbital ecchymosis, and bone pain at the time of diagnosis (Meany, 2019).

A tumor may cause a swollen belly, leading to constipation in the abdomen. Likewise, a tumor in the chest and spinal cord may cause breathing problems and inability to walk respectively. A tumor around the eyes may cause bruising and swelling. Infiltration of the bone marrow may cause paleness from anemia. Systematic symptoms of fever, weight loss and fatigue often indicate bone marrow involvement and advanced disease (Newman et al., 2019).

1.1.4 Diagnosis and Evaluation

Metastatic disease may result in numerous symptoms at the time of diagnosis such as fever, weight loss or fatigue as well as pancytopenia, periorbital ecchymosis, and bone pain (Kalaskar et al., 2016). The current risk classification employs clinical factors at diagnosis (age, disease stage) and features of the tumor to assign suitable treatment to patients based on risk of disease recurrence. The risk categories such as non high risk neuroblastoma, low and intermediate, represent nearly half of all diagnosed patients (Meany, 2019).

Diagnosis of neuroblastoma is based on histologic conformation combined with histochemical profiling and imaging characteristics. Histologic confirmation is performed by acquiring an incisional biopsy of the primary tumor. For localized tumors, the incisional biopsy may also include a sampling of lymph nodes (Swift et al., 2018). To evaluate fully the extent of disease, bone marrow aspiration of two separate sites is needed. Immunohistochemical stains for biological markers such as neuron-specific enolase, S-100 protein, and chromogranin can be utilized in the histologic diagnosis of neuroblastoma (Rajwanshi et al., 2009).

Being derived from neural crest cells, neuroblastoma often expresses the enzymes required for catecholamine metabolism. Detection of elevated serum and urine levels of vanillylmandelic acid and homovanillic acid can provide chemical confirmation of disease. Although not specific for neuroblastoma, high vanillylmandelic acid and homovanillic acid

levels are present in approximately 75% of patients with neuroblastoma (LaBrosse et al., 1980). Detection of tumor cells in bone marrow and elevated urinary vanillylmandelic acid and homovanillic acid levels can lead to a diagnosis (Cohn et al., 2009).

Ultrasound (US) is usually the first examination performed when an abdominal mass is suspected in a child. US is typically followed by CT or MR imaging to further evaluate the extent of disease and contribute in staging. CT is quickly performed and widely available, with superior detection of calcifications. MR imaging is better for evaluating spinal involvement and does not involve use of ionizing radiation. Both modalities can also demonstrate metastasis to the liver, lymph nodes, bone, and skin (Papaioannou et al., 2005 and Kembhavi et al., 2015). Whole-body MR imaging can be a helpful diagnostic tool for imaging neuroblastomas in certain contexts (Swift et al., 2018).

Table 2. Initial Diagnostic Evaluation for Neuroblastoma (Newman et al., 2019)

Evaluation for Neuroblastoma	
History and physical examination	Painless abdominal, neck, or chest mass; mass effect from primary tumors (airway, spinal cord, adjacent organs), bone pain, limping (bone metastases), subcutaneous nodules, opsoclonus-myoclonus.
Cross-sectional Imaging (Chest/Abdomen/Pelvis) and MIBG	Solid tumor invading and displacing contiguous structures, encases major blood vessels, may have calcifications or necrosis, detect metastatic disease.
Laboratory studies	Elevated urine catecholamines (VMA and HVA), elevated serum ferritin, elevated LDH.
Tumor biopsy/resection and BM biopsies/aspirates	Neuroectodermal immature or differentiating small round blue cell histology, Homer Wright pseudorosettes.

1.1.5 Etiology

Neuroblastoma arises from abnormal growth of embryonic neural crest cells that make up the sympathetic ganglia and the adrenal medulla. This abnormal growth is caused by gene mutations, as in most cancers. As a starting point, the gene mutation may be germline (occurring in sperm or eggs, thus hereditable) or somatic (in other cells of the body, which become a tumor) (Sharma et al., 2018).

The origin of neuroblastoma tumorigenesis starts from the disrupted development of neural crest precursors (Louis et al., 2015). In some cases, hereditable gene mutations influence neuroblastoma. A germline mutation in the ALK oncogene is known as familial neuroblastoma, which presents itself with severe clinical features, such as younger age at diagnosis and bilateral adrenal tumors (Mossé et al., 2008). A PHOX2B loss of function mutation can result in neuroblastoma as one feature of congenital central hypoventilation syndrome (Di-Lascio et al., 2018).

Numerous neuroblastoma cases have somatic mutations present. Several genetic alterations have been identified, including gene amplification, chromosomal alterations, and gene polymorphisms. The most important biomarker in neuroblastoma, MYCN gene, is amplified in 25% cases (Huang et al., 2013). The ALK oncogene has gain of function somatic mutation in approximately 14% of neuroblastomas. MYCN and ALK amplifications are associated with aggressive tumor phenotype and poor prognosis (Sharma et al., 2018).

Recurrent loss or gain of chromosomal segments is found in almost all high risk neuroblastomas. For example, chromosome 17q occurs in approximately 80% of neuroblastomas, making it the most common genetic aberration (Colon et al., 2011). There are diverse genetic alterations possible, leading to a wide spectrum of clinical behavior of neuroblastomas (Van-Roy et al., 2009).

1.1.6 Treatment / Immunotherapy

In general, Immunotherapy for tumors is based on the possibility to exploit the host immune system to fight cancer. There are two main strategies of cancer immunotherapy: active and passive - based on their ability to engage the host immune system to fight cancer. Furthermore, both of them can be classified based on their antigen specificity (Galluzzi et al., 2014 and Lesterhuis et al., 2011).

The active immunotherapy involves the stimulation of the patient's immune system, with the purpose to trigger an immune response against cancer cells, finally leading to their destruction. Examples are tumor vaccines and check point inhibitors, which work upon the engagement of the host immune system (Pardoll, 2012 and Palucka et al., 2012). In contrast, passive immunotherapy makes use of the adoptive transfer of substances with immunomodulatory activity. Examples are tumor-targeting monoclonal antibodies (mAb) and adoptive transfer of T cells which are endowed with antineoplastic activity (Humphries, 2013 and Weiner, 2007).

The intensity of therapy in neuroblastoma differs significantly for patients in different risk groups (Table 3).

Table 3. Comparison of standard upfront treatment for patients with neuroblastoma (Meany, 2019)

Risk Classification	Standard Therapy
Low Risk	Observation
	Surgical resection
Intermediate Risk	Chemotherapy
	Surgical resection
High Risk	Chemotherapy
	Surgical resection
	Myeloablative chemotherapy with autologous stem cell transplant
	External beam radiation therapy
	Immunotherapy with differentiating agent

Treatment strategies are directed by the Children's Oncology Group (COG) risk stratification as low, intermediate and high risk groups.

1.1.6.1 Low Risk Neuroblastoma

Low risk disease including Stage 1 and asymptomatic Stage 2 disease has an excellent prognosis with nonmutilating surgery alone (Parikh et al., 2015). The aim is to decrease therapy for low risk patients to avoid long term complications while augmenting and targeting therapies for high risk patients to improve. The treatment for asymptomatic low risk patients with an estimated survival of >98% is often observation or surgical resection alone (Tolbert et al., 2018).

1.1.6.2 Intermediate Risk Neuroblastoma

Patients with intermediate risk group tumors that are not amenable for primary resection receive chemotherapy to stop speedy tumor progression, treat life-threatening symptoms, or improve tumor resectability. Chemotherapy (4–8 cycles) for debulking and metastatic remission, followed by surgery aiming at maximum safe resection, is the recommended approach (Luo et al., 2018).

1.1.6.3 High Risk Neuroblastoma

High risk NB patients who receive four cycles of chemotherapy before surgical resection have a superior overall survival (OS) rate than patients who receive 2 (Rojas et al., 2016). However, the 5-year OS rate of high risk patients remains around 40–50% (Pinto et al., 2015). Patients diagnosed with high risk factors often have poor prognosis. Study results indicate that local treatment with gross total resection (GTR)/subtotal resection (STR) with local irradiation may be safe and sufficient for preventing local recurrence in stage 4 NB patients who received delayed local treatment. (Rich et al., 2011).

1.1.6.4 Surgical Approach

For neuroblastomas requiring initiation of chemotherapy, tissue diagnosis has been achieved via an open biopsy. However, a minimally invasive approach (laparoscopy or thoracoscopy) is also widely used now. Similarly, open surgical resection is the traditional approach; likewise, a minimally invasive surgical approach is now being used more frequently for neuroblastoma resection (Arendonk et al., 2018).

1.1.6.5 Immunotherapy

Neuroblastoma can evade T cells recognition by downregulating or losing human leukocyte antigen (HLA) expression, thereby interfering with the afferent arm (priming through dendritic cells), the homing of T cells to neuroblastoma and the cytotoxic T lymphocyte (CTL) effector phase of adaptive immunity. Soluble inhibitors of the immune response (for example, FAS ligand (FASL) and gangliosides) are constantly released into the tumor stroma to impair cellular immunity (Cheever et al., 2009 and Cheung, 2013).

Furthermore, neuroblastoma silences natural killer (NK) cells and recruits pro-tumor macrophages. Myeloid suppressor cells and regulatory T cells can also suppress immunity (Yu et al., 2010). The lack of mutations in neuroblastoma, the immaturity of the immune system in young patients, the high disease burden in these patients and the intensive use of chemotherapy all combine to make neuroblastoma poorly immunogenic for T cells. Carbohydrate differentiation antigens (for example, GD2, GD3, all of which are classically T cell-independent antigens, offer alternative targets for antibody-based therapies (Yu et al., 2010). In the presence of monoclonal antibodies specific for GD2, neuroblastoma loses its defense and becomes highly susceptible to NK cell-mediated antibody-dependent cell-mediated cytotoxicity (NK-ADCC) (Schulz et al., 1984 and Kramer et al., 1998).

Even polyclonal T cells can be retargeted to kill neuroblastoma through monoclonal antibodies in the form of chimeric antigen receptors (CARs) or bispecific antibodies (anti-GD2 and anti-CD3). (Park et al., 2007 and Pule et al., 2008).

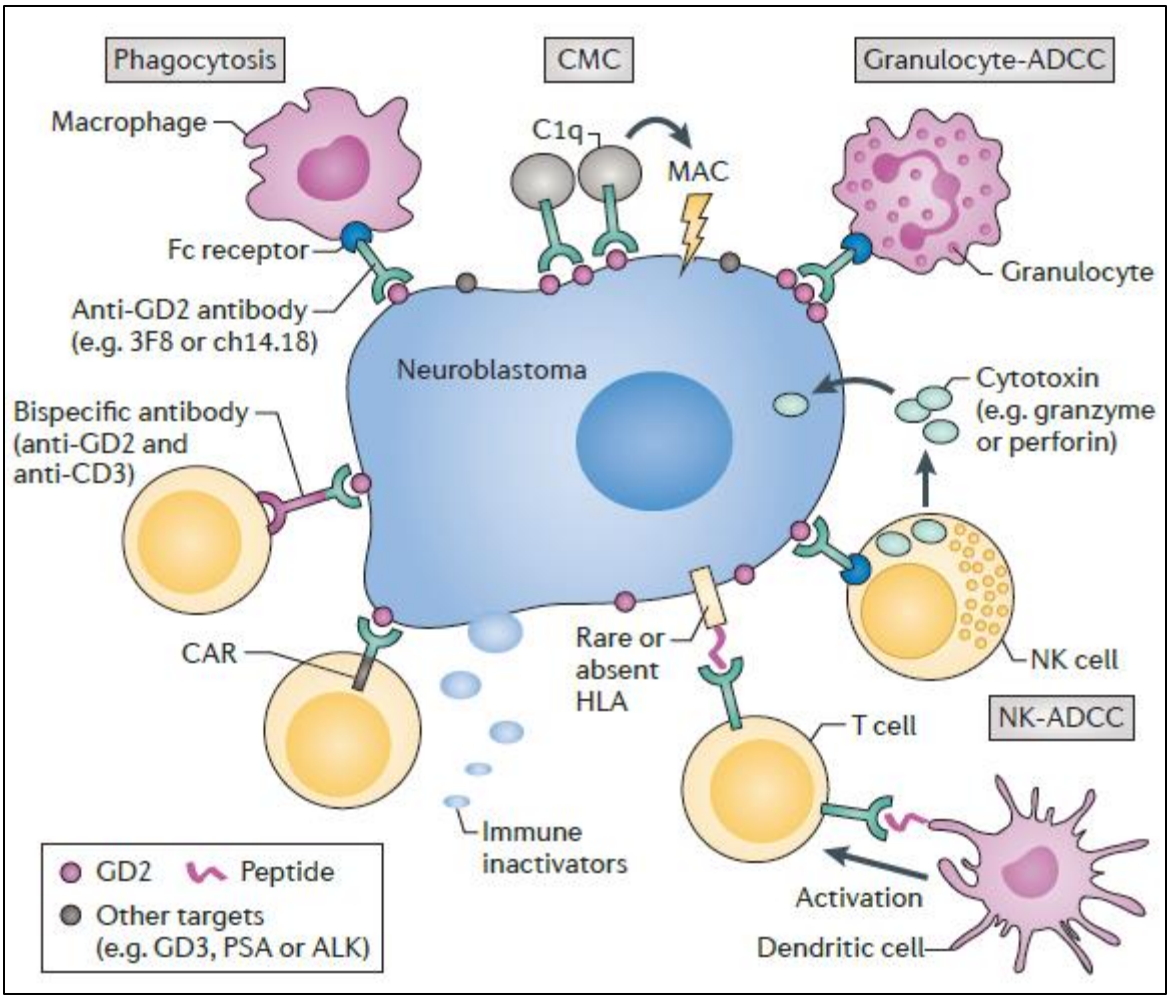

Figure 3. Immunotherapy of Neuroblastoma (Cheung, 2013)

1.1.7 Immunology of Neuroblastoma (Tumor immunology)

Clinically, neuroblastoma is known for heterogeneous clinical behavior, from spontaneous regression or differentiation, to persistent progression despite rigorous, multimodality therapy. However, it is the tendency of spontaneous regression that makes this tumor so captivating. Several mechanisms have been discussed in the process of spontaneous regression of neuroblastomas, for example, humoral or cellular immune responses, loss of telomerase activity or alterations in epigenetic regulation (Brodeur, 2014).

Since neuroblastoma can spontaneously regress, *de novo* antitumor immunity in patients seems a reasonable possibility. However, an active adaptive immunity against neuroblastoma has been difficult to demonstrate, especially in high-risk patients. This is not unexpected given the exceptionally large tumor bulk (both primary and metastatic) and its rapid proliferation, which can overpower the immature immune system in a child. The rareness of somatic mutations in neuroblastoma makes it poorly immunogenic. Moreover, neuroblastoma has built sophisticated immunosuppressive microenvironment that prevents the development of effective T cell immunity (Cheung, 2013).

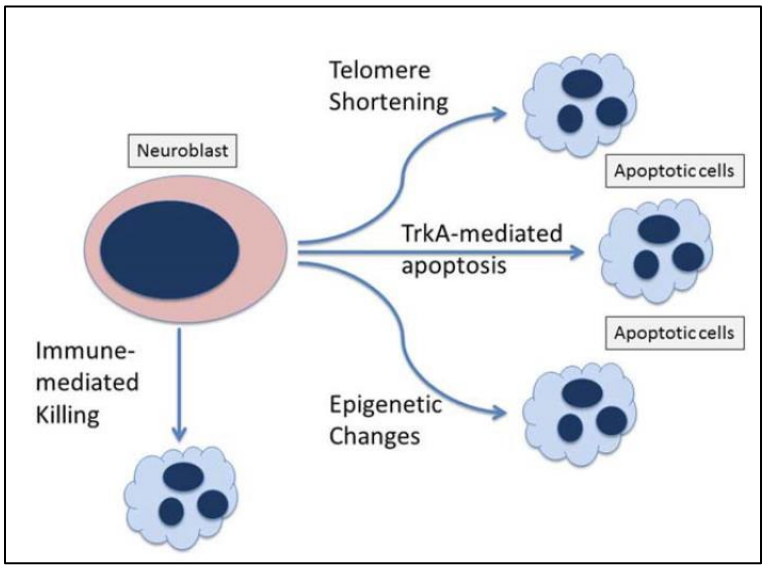

Figure 4. Mechanisms of neuroblastoma regression (Ratner, 2016)

Neuroblastoma cells evade T cells by downregulating human leukocyte antigen (HLA) (Raffaghello et al., 2005 and Coughlin et al. 2006) and adhesion molecules (Favrot et al. 1991 and Foreman et al., 1993). They express or release proteins to inhibit and kill T cells (Castriconi et al. 2004, Raffaghello et al. 2004, Morandi et al. 2012, Asgharzadeh et al. 2006 and Song et al. 2009). They even recruit tissue macrophages to disable these lymphocytes (Liu et al., 2012). Neuroblastomas downregulate HLA to escape T cells (Tarek et al. 2012 and Cheung et al. 2012). Clinically, neuroblastoma evades the immune system by escaping to sanctuaries such as the CNS, which is not accessible to circulating antibodies (Cheung et al., 2012).

Some patients with neuroblastoma develop a neurological paraneoplastic syndrome (PNS). The term paraneoplastic refers to a remote, not direct, effect of a tumor. Although the individual syndromes are rare, the concept of paraneoplastic syndromes (PNS) is well spread in the medical literature and frequently reviewed (Steinman L, 2014, Höftberger et al. 2015 and Graus, 2017). Underlying tumors vary considerably between different PNS, and some PNS may be induced by more than one tumor. PNS associated with neuroblastoma, is the most common solid pediatric tumor. The most frequent PNS in neuroblastoma is opsoclonus myoclonus syndrome (OMS). More than half of OMS patients have neuroblastoma (NB), and vice versa about 1-1.5% of the neuroblastoma patients develop OMS (Dale, 2003 and Pranzatelli, 2001). The typical symptoms of OMS include chaotic and synchronous eyes' movement (opsoclonus), spontaneous muscle jerking (myoclonus), ataxia and behavioral disturbance (Rudnick et al. 2001).

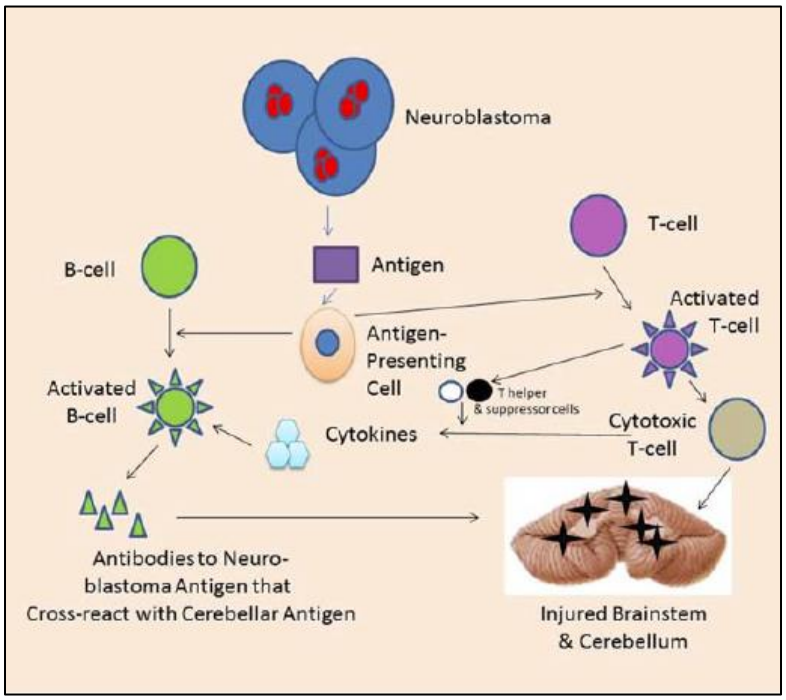

Figure 5. B-cell and T-cell involvement in the pathogenesis of opsoclonus-myoclonus-ataxia syndrome (OMAS) in neuroblastoma (Ratner, 2016)

OMS as a paraneoplastic syndrome is interesting in the discussion of tumor immunology, since these syndromes are thought to be the result of a cross-reactive immune response against antigens shared by the tumor and the nervous system (Korfei et al. 2005 and Blaes et al. 2005). Autoantibodies of OMS patients react with cerebellar neurons and neuroblastoma cells and one major antigen was recently identified as the orphan glutamate receptor delta2 (GluDelta2) (Berridge et al. 2018). Moreover, we could show, that these surface-binding autoantibodies can directly influence the ERK-1/2 pathway both in cerebellar and neuroblastoma cells (Fühlhuber et al. 2015). To be immunogenic, tumors have to provide special features, such as MHC class I expression and presentation of possible tumor antigens. Absent MHC class I expression allows neuroblastoma to escape immunological recognition (Seeger, 2011). However, under special circumstances, such as NK-cell secreted interferon-γ, MHC class I is upregulated on neuroblastoma cells (Spel et al. 2015).

1.2 Extracellular RNA (exRNA)

1.2.1 Definition

Cells can change their phenotypes through the secretion and uptake of RNA, thus implicating RNA molecules as critical mediators of intercellular communication (Baj-Krzyworzeka et al., 2006 and Valadi et al., 2007). Extracellular RNA (also known as exRNA or exosomal RNA) describes RNA species present outside of the cells from which they were transcribed. In humans, exRNAs have been discovered in bodily fluids such as venous blood, saliva, breast milk, urine, semen, menstrual blood, and vaginal fluid (Michael et al., 2010, Kosaka et al., 2010, Menke et al., 2004, Zubakov et al., 2010, Hanson et al., 2009 and Chen et al., 2008).

RNAs have a role in a multiple range of complex cellular functions, such as cell to cell communication. RNA can be exported from cells in extracellular vesicles or bound to lipids and proteins, to flow through the body and affect cells. These exRNAs may also be absorbed from food, the microbes in our bodies, or the environment, potentially eliciting a variety of biological responses. However, the actual impact of these exRNAs is not known (Wei et al., 2017).

The discovery of extracellular RNA (exRNA) as a signaling molecule implies an important change in our understanding of the regulatory role of RNA in cell biology and has a massive translational potential for human health. Moreover, extracellular RNA (exRNA) has emerged as an important transducer of intercellular communication (Li et al., 2018).

1.2.2 Types of exRNA

Extracellular RNA should not be seen as a category describing a set of RNAs with a specific biological function or belonging to a particular RNA family. Extracellular RNA defines a group of several types of RNAs that have various functions, yet they share a common aspect, which, in the case of exRNAs, is existence in an extracellular environment (Valadi et al., 2007). The following types of RNA are found outside the cell:

- Messenger RNA (mRNA)
- Transfer RNA (tRNA)
- MicroRNA (miRNA)
- Small interfering RNA (siRNA)
- Long non-coding RNA (lncRNA)

1.2.3 Extracellular RNA in Disease

Neurodegenerative diseases such as Parkinson disease (PD) and Alzheimer disease (AD) share a common disease signature; specifically, aggregation of disease-specific proteins that differ in composition dependent upon the respective disease (Ross et al., 2004 and Soto, 2003). Studies have shown that in AD, amyloid-β (Aß) peptides are packaged and released into the extracellular environment (Rajendran et al., 2006, Saman et al., 2012, Frost et al., 2009 and Gupta et al., 2014). An ongoing evaluation of cerebrospinal fluid (CSF) samples has thus far detected over 200 miRNAs functioning as exRNAs (Quinn et al., 2015).

Atherosclerosis is the main reason of ischemic diseases, such as myocardial infarction and stroke. The involvement of diverse exRNA species is emerging as critical mediators

of the mechanisms that control (ischemic) cardiovascular disease (Gama-Carvalho et al., 2014). miR-126 has an essential role in vessel development and endothelial cell repair (Urbich et al., 2008, Zernecke et al., 2009 and Kuhnert et al., 2008). It is highly expressed in endothelial cells and deficiency in its expression causes almost 50% embryonic mortality. Interestingly, apoptotic endothelial cells release microvesicles enriched with miR-126 that triggers CXCL12 production in the recipient vascular cells (Zernecke et al., 2009).

The most common interstitial lung disease (ILD) is idiopathic pulmonary fibrosis (IPF) (Nalysnyk et al., 2012). In IPF, miRNAs appear to have a pro-fibrotic role (Milosevic et al., 2012). miR-145 knockout mice can be protected from bleomycin-induced pulmonary fibrosis (Yang et al., 2013). In a separate study, inhibition of miR-21 resulted in a decrease of extracellular matrix proteins through the regulations of SMAD7 (Liu et al., 2010). miR-21-5p isolated from serum was found to be a predictor of IPF severity (Makiguchi et al., 2016). Similar to lung fibrosis, liver fibrosis is characterized by excessive scarring, caused by chronic inflammatory processes (Hautekeete et al., 1997). In a study, expression levels of miR-122 and miR-155 in serum/plasma correlated with liver damage regardless of the etiology of hepatocyte injury. miR-155 in particular appears to be a candidate biomarker of liver inflammation.

1.2.4 Roles of extracellular RNA in cancer progression

Vesicle shedding has been observed to occur in tumor cells for a number of different human cancer types (Skog et al., 2008, Peinado et al., 2012 and Di-Vizio et al., 2012). In fact, extracellular vesicles (EVs) have been isolated from both cultured tumor cells and biological samples, such as plasma, urine and ascites fluid of cancer patients, as well as controls (Skog et al., 2008, Al-Nedawi et al., 2008 and Peinado et al. 2012). An influence of tumor EVs on many aspects of cancer progression, such as invasiveness, angiogenesis, immune evasion, metastasis and coagulation has been observed (Kahlert et al., 2013, Ogorevc et al., 2013, Millimaggi et al., 2007 and Delves et al., 2007).

A specific example of the role of miRNA in cancer is exemplified by the ability of EV mediated transfer of miR-223 from activated macrophages to breast cancer cells with an associated increase in their invasiveness (Yang et al., 2011). Another study showed that miRNA increase in endothelial cells is mediated by EVs stimulated tumor angiogenesis (Delves et al., 2007). These studies represent key steps forward in interpreting contributions of specific RNA molecules transferred within EVs to cancer progression (Redzic et al., 2014).

1.2.5 Extracellular RNA as biomarkers for cancer

The presence of exRNAs from cancer cells in biofluids provides the potential for their use as biomarkers to provide a “snapshot” of the macromolecular composition of tumor cells. exRNAs are perfect biomarkers because they have the potential to be highly sensitive, prognostic, strong, translatable and most importantly minimally invasive (Redzic et al., 2014).

The use of exRNAs in biofluids as biomarkers of cancer is being discovered using several biofluids and types of cancer with analysis of levels and mRNA mutations, as well as levels of miRNAs and other non-coding RNAs. Abundant importance is currently being placed on levels of miRNAs in biofluids as a source of biomarkers for cancer (Wittmann et al., 2010). Studies have reported abnormal distinctive miRNA profiles in serum from patients with ovarian cancer (Taylor et al., 2008), lung cancer (Rabinowits et al., 2009) and esophageal squamous cell carcinoma (Takeshita et al., 2013), as well as in saliva from patients with oral cancer (Yoshizawa et al., 2013). Other cancers, including prostate (Nilsson et al. 2009 and Bryant et al., 2012), liver (Gailhouste et al. 2013) and colorectal cancer (Chiba et al., 2012).

1.2.6 Extracellular RNA as therapeutics for cancer

While considering the probable therapeutic impact of exRNA in cancer, it is of utmost importance to remember the large amount of information EVs normally contain in the form

of protein, lipid, DNA and RNA. One probable therapeutic approach would be to reduce the release of EVs from tumor cells, for example using short interfering RNAs (siRNAs) which downregulate Rab proteins involved in the MVB release process (Bobrie et al., 2012). EVs from normal cells on the other hand, such as immune cells, are seen as active components in fighting cancer with an important aspect being their RNA content, as found in EVs from immune cells (Redzic et al., 2014).

It can be envisioned in future approaches, the release of vesicles from the plasma membrane, such as by expression of oligomeric proteins (Fang et al., 2007), and elucidation of RNA sequence – protein binding combinations in the EVs that can load specifically engineered RNAs into the vesicles. Such RNAs could include mRNAs encoding therapeutic proteins, as above, as well as miRNA or other regulatory ncRNAs alone or in combination (Fang et al., 2007, EL-Andaloussi et al., 2013, Kosaka et al., 2013, Seow et al., 2009, Mobergslien et al., 2014 and Koppers-Lalic et al., 2013).

1.2.7 Toll-like receptor 3 signaling in RNA-induced immune responses

The immune system has developed a strategy for maintaining host homoeostasis through its interaction with environmental microbes. An array of PRRs (pattern-recognition receptors) in the innate immune system recognizes PAMPs (pathogen-associated molecular patterns) and induces anti-microbial immune responses (Janeway et al., 2002). Among the nucleic acid sensing TLRs, TLR3 that recognizes dsRNA has a unique expression profile and subcellular localization (Alexopoulou et al., 2001 and Matsumoto et al., 2002). Although TLR3s on the cell surface participate in dsRNA recognition (Matsumoto et al., 2002), TLR3-mediated signaling is initiated from endosomal compartments in either cell type (Matsumoto et al., 2003).

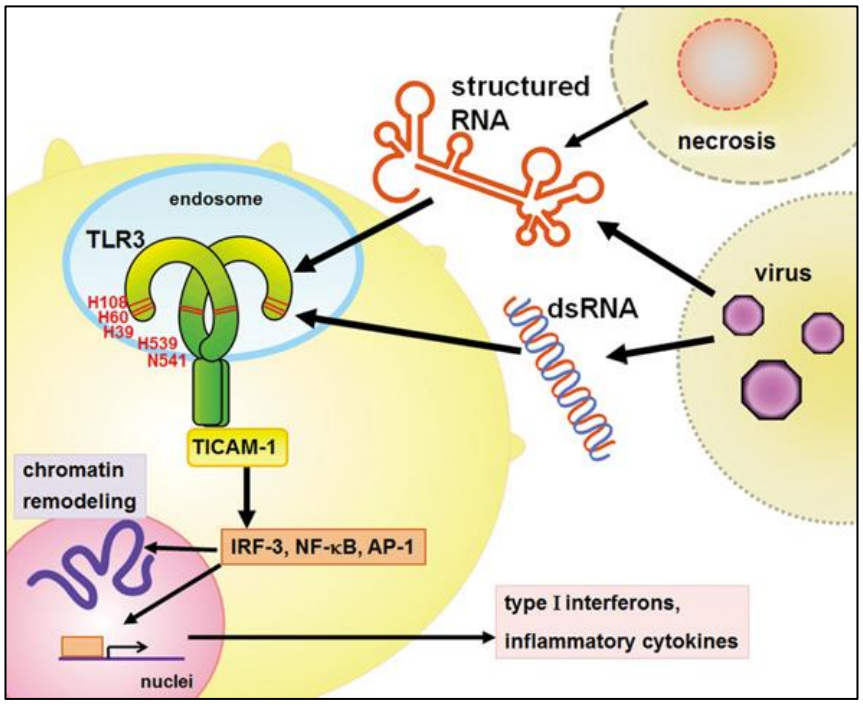

Figure 6. Model for dsRNA/structured RNA-induced TLR3-mediated immunity (Tatematsu et al., 2014)

Virus derived dsRNA and poly (I:C) (polyriboinosinic:polyribocytidylic acid), a synthetic dsRNA are TLR3 ligands (Alexopoulou et al., 2001 and Matsumoto et al., 2002). dsRNA exists as a viral genome or is generated in the cytosol during replication of positive-strand RNA viruses and DNA viruses (Weber et al., 2006). Thus, TLR3 appears to sense extracellular viral dsRNA released from infected cells and activates antiviral immunity (Matsumoto et al., 2011). Virus and host derived RNAs are released from necrotic cells, upon viral infection and sterile inflammation. In local environments, extracellular viral dsRNAs and virus/host derived structured RNAs are rapidly taken up into cells via endocytosis and delivered to endosomal TLR3. Once dsRNA/structured RNA oligomerizes TLR3, it recruits the adaptor protein TICAM-1 that activates the transcription factors, IRF-3, NF-κB and AP-1, leading to the production of type I IFNs and proinflammatory cytokines (Matsumoto et al., 2008 and Tatematsu et al., 2013).

1.3 Natural Killer Cells

1.3.1 Definition

Natural killer (NK) cells are innate immune cells that were first discovered in mice in 1975 (Fang et al., 2017). They are large granular lymphocytes that develop from an early innate lymphoid precursor (EILP) in the bone marrow and are known as the founding member of the Innate Lymphoid Cell (ILC) family. NK cells are capable of responding to virus infected and tumor cells (Müller-Hermelink et al., 2008). NK cells account for approximately 10% of lymphocytes in human peripheral blood (PB). There are various chemokine receptors expressed in NK cells and the distribution of NK cells differ among healthy tissues. Most NK cells are found in the PB, liver, spleen, and bone marrow and a small portion are present in the lymph nodes (Hazenberg et al., 2014, Caligiuri, 2008, Rezvani et al., 2017 and Campbell et al., 2013).

NK cells are part of the first line of defense that protects the body from pathogens and malignant transformation. When viruses infect normal cells, NK cells are activated to protect against abnormal and virus infected cells without prior sensitization (Cerwenka et al., 2016 and Hammer et al., 2018).

1.3.2 Functions of NK Cells

NK cell function is firmly regulated by a balance between positive and negative signals provided by a diverse range of cell surface receptors (Cerwenka et al., 2001). The activation of NK cells requires the action of pro-inflammatory cytokines in combination with cell surface receptors, such as IL-12, IL-15, IL-18, IL-21 and IFN-αβ. They can induce NK cell proliferation, as well as promoting NK cell cytotoxicity and/or production of IFN-γ (Biron et al., 1999).

NK cells do not express antigen-specific recognition receptors. There are two receptors with opposite functions on their surface. The first receptor can bind to its corresponding ligand on the surface of the target cell, activating the killing effects of NK cells. This receptor is called the activating NK cell receptor (Lanier, 2008). The other receptor, called the inhibitory NK cell receptor, inhibits the killing effect of NK cells (Lanier, 2008). The

activating and inhibitory receptor can recognize classical or non-classical major histocompatibility complex (MHC) class I molecules expressed on the surface of normal cells (Sivakumar et al., 1999 and Kumar, 2018). In virus infected cells and tumor cells, MHC class I molecules on the cell surface are lost or downregulated; activating NK cell receptors play a role in this process (Zhang et al., 2019). NK cells kill their target cells by release of cytotoxic granules containing perforin and granzymes, by the expression or release of TRAIL, FasL and TNF and by antibody-dependent cellular cytotoxicity (ADCC), resulting in apoptosis of the target cell (Farag et al., 2006 and Moretta et al., 2006).

1.3.3 Anti-tumor activities of NK Cells

When a normal cell transforms into a malignant cell, it requires numerous intrinsic oncogenic events for the cell to escape immune surveillance. The number of mutations that result in tumor transformation within an individual are 80 and affects the functionality of 6-7 signaling pathways (Forbes et al., 2011). However, there are several intrinsic barriers that inhibit the development of cancer (Smyth et al., 2006 and Vesely et al., 2011). There are two major challenges for immunosurveillance of malignantly transformed cells: (1) tumor cells originate from ‘self’ as well as their biochemical properties and their behavior differs only slightly from their healthy counterparts, and (2) tumor cells employ many tricks to actively evade detection and elimination by effector cells of the immune system (Vesely et al., 2011).

NK cells kill malignantly transformed cells after interaction of induced or overexpressed ligands with their activating receptors. This killing may happen, if MHC mediated inhibition is lowered by the downregulation of MHC class I molecules from the surface of malignantly transformed cells (Groth et al., 2011). A fine-tuned balance of activating and inhibitory signals facilitates NK cell recognition (Farag et al., 2006).

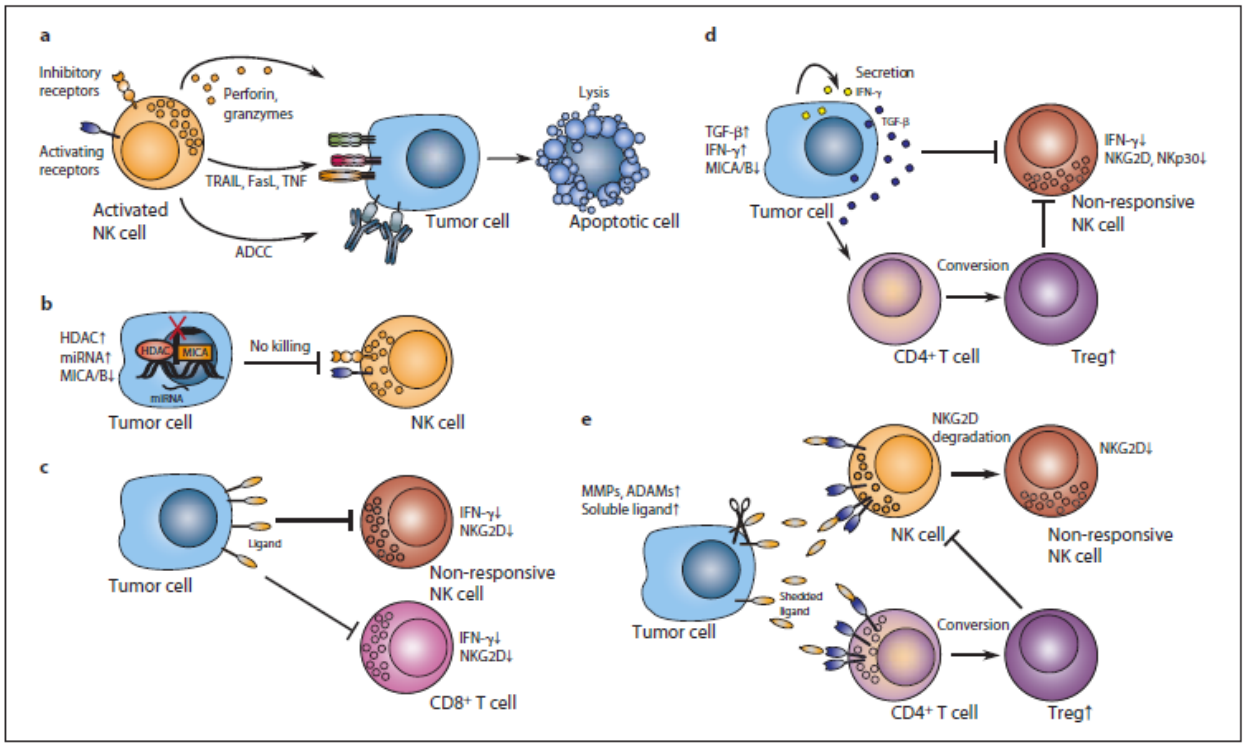

Figure 7. Strategies of tumor immune escape from NK cell-dependent Immunosurveillance (Groth et al., 2011)

2. AIMS OF THE THESIS

1. To study the pro-inflammatory effects of exRNA and other stimulants to human neuroblastoma cells.

2. To investigate the effect of exRNA on the susceptibility of neuroblastoma cells to immune cell killing by NK cells.

3. To investigate the differences in the effect of extracellular RNA (exRNA) on neuroblastoma cells and primary cultured autonomic (enteric) nervous system cells.

3. MATERIALS AND METHODS

3.1 Materials

3.1.1 Chemicals, acids and bases

Compounds	Company
Agarose	Bioline GmbH, Luckenwalde, Germany
Attune™ Focusing Fluid, 1X	Applied Biosystems, Darmstadt, Germany
Attune™ Wash Solution	Applied Biosystems, Darmstadt, Germany
Attune™ 10X Shutdown Solution	Applied Biosystems, Darmstadt, Germany
Attune™ Performance Tracking Beads	Applied Biosystems, Darmstadt, Germany
α-Cystein	Sigma-Aldrich Chemie GmbH, Taufkirchen, Germany
ß-Mercaptoethanol 50mM	Thermo Fisher Scientific, Darmstadt, Germany
Bovine Serum Albumin (BSA)	Sigma-Aldrich Chemie GmbH, Taufkirchen, Germany
BSA 35% in DPBS	Sigma-Aldrich Chemie GmbH, Taufkirchen, Germany
B27 supplement with retinoic acid	Thermo Fisher Scientific, Darmstadt, Germany
B27 supplement without retinoic acid	Thermo Fisher Scientific, Darmstadt, Germany
Calcein	Thermo Fisher Scientific, Darmstadt, Germany
DIG-labeled DNA Molecular Weight Marker VII (0.35-8.5 kb)	Roche, Mannheim, Germany
Distilled water (Ecostrain®)	Braun, Melsungen, Germany
Dimethylsulfoxide (DMSO)	Carl Roth, Karlsruhe, Germany
DNase	Roche Diagnostics GmbH, Mannheim, Germany
ECM Gel (Extracellular matrix)	Sigma-Aldrich Chemie GmbH, Taufkirchen, Germany
EDTA (Ethylenediaminetetraacetic acid)	Carl Roth, Karlsruhe, Germany
EGF (Epidermal growth factor)	ImmunoTools GmbH, Friesoythe, Germany
Ethanol 100%	Sigma-Aldrich Chemie GmbH, Taufkirchen, Germany

FBS (Fetal bovine serum)	PAA Laboratories, Pasching, Austria
FGF (Fibroblast growth factor)	ImmunoTools GmbH, Friesoythe, Germany
Glycerol	Carl Roth, Karlsruhe, Germany
Glycin	Merck KGaA, Darmstadt, Germany
HBSS (Hanks' Balanced Salt Solution)	PAN-Biotech GmbH, Aidenbach, Germany
High Molecular weight Poly I:C (HMW)	InvivoGen, San Diego, USA
Horse Serum	Gibco, Invitrogen, Carlsbad, USA
HyClone Trypsin Protease - Trypsin cell detachment solution	GE Healthcare Life Sciences, Pittsburgh, USA
Recombinant Human Interferon-γ (IFN-γ)	Gibco, Invitrogen, Carlsbad, USA
Isopropanol	Merck KGaA, Darmstadt, Germany
Liberase TH	Roche Diagnostics GmbH, Mannheim, Germany
Low Molecular weight Poly I:C (LMW)	InvivoGen, San Diego, USA
MEM-HEPES (Minimum Essential Medium- (4-(2-hydroxyethyl)-1-piperazineethanesulfonic acid)	Thermo Fisher Scientific, Darmstadt, Germany
Methanol	Merck KGaA, Darmstadt, Germany
2-Mercaptoethanol	Sigma-Aldrich Chemie GmbH, Taufkirchen, Germany
Myo-inositol (20mM)	Sigma-Aldrich Chemie GmbH, Taufkirchen, Germany
NorthernMax-Gly sample loading dye	Thermo Fisher, Darmstadt, Germany
Papain	Worthington Biochemical Corporation, Lakewood, NJ, USA
10x PBS for cell culture (DPBS)	Lonza, Köln, Germany
Poly-D-Lysine (PDL) (mol. wt. 70,000-150,000)	Sigma-Aldrich Chemie GmbH, Taufkirchen, Germany
ProLine™ Universal Calibration Beads	Bio-Rad, CA, USA
2-Propanol	Sigma-Aldrich Chemie GmbH, Taufkirchen, Germany
Pen Strep	Gibco, Invitrogen, Carlsbad, USA
Propidium iodide staining solution (50 µg/ml)	BD Biosciences, San Jose, CA, US
Recombinant Human IL-2 (carrier-free)	BioLegend, San Diego, CA, USA
rh GDNF (Glial cell line-derived neurotrophic factor)	ImmunoTools GmbH, Friesoythe, Germany
RNase free water	Millipore corporation, MA, USA

Sodium azide (NaN3)	Merck KGaA, Darmstadt, Germany
Sodium pyruvate solution (100mM)	Sigma-Aldrich Chemie GmbH, Taufkirchen, Germany
Tergazyme enzyme detergent	Sigma-Aldrich Chemie GmbH, Taufkirchen, Germany
TLR3/dsRNA Complex Inhibitor - Calbiochem	Merck, Darmstadt, Germany
Trypan blue	Carl Roth, Karlsruhe, Germany
Tris acetate-EDTA buffer (TAE) 10X	Carl Roth, Karlsruhe, Germany
Tris borate-EDTA buffer (TBE) 10X	Carl Roth, Karlsruhe, Germany
Triton X-100	Carl Roth GmbH + Co. KG, Karlsruhe, Germany
Trypsin (2.5 g/l)	Gibco, Invitrogen, Carlsbad, USA
Trypsin-Inhibitor	Sigma-Aldrich Chemie GmbH, Taufkirchen, Germany

3.1.2. Laboratory Consumables

Consumables	Company
Amersham Hyperfilm ECL (18 × 24 cm)	GE Healthcare Life Sciences, Pittsburgh, USA
CELLSTAR® 6 well and 24 well cell culture plate	Greiner Bio-One, Frickenhausen, Germany
CELLSTAR® plastic pipettes (5 ml, 10 ml, 25ml)	Greiner Bio-One, Frickenhausen, Germany
CELLSTAR® U-shape with lid, TC-Plate, 96 well, sterile	Greiner Bio-One, Frickenhausen, Germany
CELLSTAR® Flat bottom with lid, TC-Plate, 96 well, sterile	Greiner Bio-One, Frickenhausen, Germany
CELLSTAR® 25 cm^2 Cell culture flasks	Greiner Bio-One, Frickenhausen, Germany
CELLSTAR® 75 cm^2 Cell culture flasks	Greiner Bio-One, Frickenhausen, Germany
CELLSTAR® 125 cm^2 Cell culture flasks	Greiner Bio-One, Frickenhausen, Germany
Cell scrapper	Greiner Bio-One, Frickenhausen, Germany
Cryobox 136x136x130 mm	Ratiolab GmbH, Dreieich, Germany
Cryo Tube™ vials (1,8 mL; 4,5 mL)	Sarstedt AG & Co, Nümbrecht, Germany

Eppendorf tubes 1.5 ml, 2 ml	Eppendorf Vertrieb Deutschland GmbH, Wesseling-Berzdorf, Germany
Eppendorf tubes1.5ml, 2ml (PCR clean-pyrogen & DNase free)	Nerbe Plus GmbH, Winsen (Luhe), Germany
FACS tubes 0,5 mL 38 x 6,5 mm PS	Sarstedt AG & Co, Nümbrecht, Germany
FACS tubes, 5 ml, round bottom	BD Biosciences, San Jose, CA, US
Falcon 5 ml polystyrene round bottom tube	Becton Dickinson, Heidelberg, Germany
Falcon® plastic pipettes 25 ml, 10 ml, 5 ml	Becton Dickinson, Heidelberg, Germany
Falcon tubes (15 ml, 50 ml)	Becton Dickinson, Heidelberg, Germany
Glass Pasteur pipettes 150 mm	Brand, Wertheim, Germany
Glassware (different sorts)	Fisherbrand; IDL; Schott & Gen; Simax
Grid inserts for Cryobox	Ratiolab GmbH, Dreieich, Germany
Ministart single use filter (0,2 µm, 0,45 µm)	Sartorius Stedim Biotech GmbH, Göttingen, Germany
Nitra-Tex® powder free gloves	B. Braun Melsungen AG, Germany
Nylon blotting membrane (Hybond-N+)	GE Healthcare Life Sciences, Pittsburgh, USA
Parafilm	Pechiney Plastic packaging, Menasha, WI
PCR Cap-strips	Applied Biosystems, Darmstadt, Germany
PCR Tube-strips	Applied Biosystems, Darmstadt, Germany
Petri dishes of various sizes	Greiner Bio-One, Frickenhausen, Germany
Pipette tips without filter (10 µl, 100 µl, 200µl, 1000 µl)	Sarstedt AG & Co, Nümbrecht, Germany
Protein-G HiTrap column	GE Healthcare, Pittsburgh, USA
Sterican cannula 23G/27G	B. Braun, Melsungen, Germany
Sterile PCR- clean pyrogen & DNase free with filter (10, 100, 200, 1000 µl)	Nerbe Plus GmbH, Winsen (Luhe), Germany
Thick blot filter paper (7.5 × 10 cm or 15 × 20 cm)	Bio-Rad, CA, USA
Tissue culture dishes sterile 35,0 / 10 mm	Greiner Bio-One, Frickenhausen, Germany
UV-Spectroscopic cuvettes	Bio-Rad, CA, USA

3.1.3. Laboratory Instruments

Instruments	Company
Arpege 75, Liquid nitrogen tank	Air Liquide Medical GmbH, Düsseldorf, Germany
Attune™ Acoustic Focusing Cytometer	Applied Biosystems, Darmstadt, Germany
BEP 2000 Advance (ELISA-Reader)	Dade Behring Marburg GmbH, Marburg, Germany
BIO-LINK Crosslinker BLX-254	Witec AG, Sursee, Switzerland
BIOWIZARD SterilBank	KOJAIR, Finland
Binocular	Motic China Group Co., Ltd.
Centrifuge type 2-6 Easia shaker Medgenix diagnostics	Sigma-Aldrich Chemie GmbH, Taufkirchen, Germany
Centrifuge Universal 32 R (cell culture)	Hettich GmbH, Kirchlengen, Germany
Centrifuge 5804	Eppendorf, Hamburg, Germany
ECL CHEMOCAM Imager	INTAS, Science Imaging Instruments GmbH, Göttingen, Germany
Electrophoresis chamber	Bio-Rad, CA, USA
ELISA-Reader Multiscan EX	Thermo electron corporation, Langenselbold, Germany
Hettich centrifuge (cooling)	Hettich GmbH, Kirchlengen, Germany
Light Microscope for cell culture	Carl Zeiss Microscopy GmbH, Oberkochen Germany
Magnetic stirrer	IKA® Werke GmbH, Staufen, Germany
MEA Setup (MEA Station)	Multi-Channel Systems, MCS, Reutlingen, Germany
Mini-Centrifuge	Labnet International, Inc. Global, Edison, NJ, USA
MS2 Minishaker IKA	IKA, Staufen, Germany
Nalgene™ Cryo 1°C Freezing container	Nalgene®, Germany
Nanophotometer	Implen GmbH, München, Germany
Nephelometer	ThermoFisher Scientific, Darmstadt, Germany
Neubauer improved Haemocytometer	Brand, Wertheim, Germany
Nuaire™ Biological Safety Cabinets Class II type A/B3 (Sterilbank)	INTEGRA Biosciences GmbH, Fernwald, Germany
pH-Meter	Mettler Toledo GmbH, Giessen, Germany
Olympus CKX41 Microscope	Olympus, Hamburg, Germany

Pipette boy	INTEGRA Biosciences GmbH, Fernwald, Germany
Refrigerators and freezers	Different companies
RH Basic IKA	IKA, Staufen, Germany
Rotamax 120 (Shaker)	Heidolph Instruments GmbH & Co. KG, Schwabach, Germany
S3 Cell Sorter	Bio-Rad, CA, USA
Sanyo Incu-safe incubator for cell culture	Ewald InnovationstechnikGmbH, Bad Nenndorf, Germany
SmartSpec^{TM} Plus Spectrophotometer	BioRad, München, Germany
StepOne® Real-Time PCR system	Applied Biosystems, Darmstadt, Germany
Surgical instruments	Various companies
Swivel platform	Peqlab Biotechnologie GmbH, Erlangen, Germany
Tabletop centrifuge EBA 20	Hettich GmbH, Kirchlengen, Germany
Tabletop centrifuge micro 120	Hettich GmbH, Kirchlengen, Germany
Thermomixer comfort	Eppendorf Vertrieb Deutschland GmbH, Wesseling-Berzdorf, Germany
Trans-Blot® SD Semi-dry transfer cell	Bio-Rad, CA, USA
Vortexer vortex-Genie2	Heidolph Instruments GmbH & Co. KG, Schwabach, Germany
Water bath	Memmert GmbH + Co.KG, Germany
Weighing balance	Sartorius Stedim Biotech GmbH, Göttingen, Germany
X-ray film processor CURIX 60	AGFA, Mortsel, Belgium

3.1.4. Buffers

Buffers	Components	Volume
20X SSC washing buffer (1 Liter)	3M NaCl 300 mM sodium citrate pH	175.32 g 77.41 g 7.0
2X SSC (1 Liter)	20X SSC H_2O	100 ml 900 ml
0.5X SSC (1 Liter)	20X SSC H_2O	25 ml 975 ml

10X MOPS (1 Liter)	200 mM 3-(N-morpholino) propanesulfonic acid (MOPS) 50 mM sodium acetate 10 mM EDTA (pH 8.0) pH	41.85 g 4.10 g 2.92 g 7.0
1X MOPS (1 Liter)	10X MOPS H_2O	100 ml 900 ml
10X PBS (1 Liter)	137mM NaCl 2 mM KH_2PO_4 2.7 mM KCl 10 mM Na_2HPO_4 H_2O pH	80 g 2.4 g 2 g 14.4 g 1000 ml 7.4
1X TBE (500 ml)	10X TBE H_2O	50 ml 450 ml
4% Paraformaldehyde (250 ml)	Paraformaldehyde	4 g
DIG blocking solution (40 ml)	2% (w/v) blocking reagent (Roche) Maleic acid buffer (100 mM), pH 7.5	4 ml 36 ml
DIG-detection buffer (500 ml)	100 mM Tris 100 mM NaCl pH	6.05 g 2.92 g 9.5
FACS Buffer (500 ml)	10X PBS 10% FBS 10% NaN_3 H_20	50 ml 5 ml 5 ml 500 ml
Maleic acid (500 ml)	1M pH	58.05 g 7.5
1X Perm/Wash buffer	10X Perm/Wash buffer dH_2O	10 ml 90 ml
1X Trypsin EDTA	10X Trypsin ddH_2O	5 ml 45 ml
0.1% Saponin	1% Saponin PBS	100 ml 900 ml

3.1.5. Molecular Biology KITS and Assay Reagents

Kits	Manufacturer	Article No.	Method
DIG Northern Starter Kit	Roche, Mannheim, Germany	12 039 672 910	Northern blotting

peqGOLD Total RNA Isolation Kit	Peqlab Biotechnologie GmbH, Erlangen, Germany	12-6834-02	RNA Isolation
QIA Quick spin Gel extraction Kit	Qiagen GmbH, Hilden, Germany	28704	Gel extraction
QuantiTect® Reverse Transcription Kit	Qiagen GmbH, Hilden, Germany	205314	Reverse Transcription
Quanti Fast™ SYBR ® Green PCR Kit	Qiagen GmbH, Hilden, Germany	204156	Polymerase Chain Reaction (PCR)
iTaq™ Universal SYBR ® Green qPCR Master Mix	Bio-Rad, CA, USA	172-5124	Polymerase Chain Reaction (PCR)
Cell Proliferation reagent WST-1	Roche Diagnostics GmbH, Mannheim, Germany	11644807001	Proliferation Assay
Cytotoxicity Detection Kit (LDH)	Roche Diagnostics GmbH, Mannheim, Germany	11644793001	Cytotoxicity Assay
Cytofix/Cytoperm™ Fixation/Permeabilization Kit	BD Biosciences, San Jose, CA, USA	554714	Fixation/Permeabilization of cells for intracellular staining
RosetteSep™ Human NK Cell Enrichment Cocktail	STEMCELL Technologies, Vancouver, Canada	15025	Human NK cell enrichment

3.1.6. Antibodies

Name	Reactivity	Method	Cat. No.	Company
FITC anti-human HLA-A, B, C Antibody	Human, Af Gr, Ba, Cat, C, Chim, Cyn, Rh	Flow Cytometry	311404 / 100 tests	BioLegend, San Diego, CA, USA

CD283 (TLR3) PE, human	Human, rhesus monkey	Flow Cytometry	130-100-304	Miltenyi Biotec, Bergisch Gladbach, Germany
FITC Mouse Anti-Mouse H-2K[d] Clone SF1-1.1 (RUO)	Mouse	Flow Cytometry	562003	BD Biosciences, San Jose, CA, US
PE Mouse Anti-Mouse CD283 (TLR3) Clone PaT3 (RUO)	Mouse	Flow Cytometry	565984	BD Biosciences, San Jose, CA, US

3.1.7. Softwares

Software	Company
GraphPad Prism version 7.00	GraphPad Software, SanDiego, California, USA
Microsoft word, PowerPoint, Excel 2016	Microsoft corporation
StepOne™ Software v2.1	Applied Biosystems™ by Life technologies™, Darmstadt, Germany
Primer 3.0 online tool	http://primer3.ut.ee
Primer Blast NCBI online tool	http://www.ncbi.nlm.nih.gov/tools/primerblast/
Attune™ Cytometric Software	Applied Biosystems™ by Life technologies™, Darmstadt, Germany
Ascent software for Multiskan	Thermo Electron corporation, Vantaa, Finland
Motic Image Plus 2.0	Motic China Group Co., Ltd.
ProSort Software Version 1.6	Bio-Rad Laboratories, Inc., CA, USA
FlowJo, LLC_V10	BD, Ashland, Oregon, USA
MC-Rack	Multi-Channel Systems, MCS, Reutlingen, Germany

3.1.8. Primer Sequences

Primer name	Primer sequence	
Hu TLR-3	Forward	5´- CCCTTTGTCAAGCAGAAGAA -3´
	Reverse	5´- GATTTTCCAGCTGAACCTGA -3´
Hu MHC I	Forward	5´- CAGGACACTGAGCTTGTGGA -3´
	Reverse	5´- TCTTCTCCAGAAGGCACCAC -3´

Hu GAPDH	Forward	5´- AATCCCATCACCATCTTCCA -3´
	Reverse	5´- TGGACTCCACGACGTACTCA -3´

3.1.9. Primer Sequences for northern blotting

Primer name	Primer sequence
Hu TLR-3	Forward 5´- TCC CTT TGT CAA GCA GAA GA -3´
	Reverse 5´- TAA TAC GAC TCA CTA TAG GGT CTT CCA ATT GCG TGA AAA C-3´
Hu MHC I	Forward 5´- GCT CCC ACT CCA TGA GGT AT -3´
	Reverse 5´- TAA TAC GAC TCA CTA TAG GGG TCC ACT CGG TCA GTC TGT G -3´
Hu GAPDH	Forward 5´- ATC CCT CCA AAA TCA AGT GG -3´
	Reverse 5´- TAA TAC GAC TCA CTA TAG GGT GAG TCC TTC CAC GAT ACC A -3´

3.1.10. Cell culture medium and solutions

Cell line	Medium composition	Volume	Company
SH-SY5Y	EMEM With L-Glutamine Sterile filtered	250 ml	ATCC, Virginia, United States
	F-12K Nut Mix (1X) Nutrient Mixture Kaighn's Modification [+] L-Glutamine	250 ml	Gibco, Invitrogen, Carlsbad, USA
	10% fetal bovine serum (FBS)	50 ml	PAA Laboratories, Pasching, Austria
	1% Penicillin/Streptomycin	5 ml	Gibco, Invitrogen, Carlsbad, USA
SK-N-AS	DMEM(1X) + GlutaMAX™ Dulbecco's Modified Eagle Medium [+]4.5g/L D-Glucose [+] Pyruvate	500 ml	Gibco, Invitrogen, Carlsbad, USA
	10% fetal bovine serum (FBS)	50 ml	PAA Laboratories, Pasching, Austria

	1% Penicillin/Streptomycin	5 ml	Gibco, Invitrogen, Carlsbad, USA
NK-92	MEM Alpha Medium (1X) + GlutaMAX™ –I Minimum Essential Medium [-] Ribonucleosides [-] Deoxyribonucleosides	500 ml	Gibco, Invitrogen, Carlsbad, USA
	12.5% fetal bovine serum (FBS) (heat inactivated)	65 ml	PAA Laboratories, Pasching, Austria
	12.5% horse serum (heat inactivated)	65 ml	Gibco, Invitrogen, Carlsbad, USA
	1% Penicillin/Streptomycin	5 ml	Gibco, Invitrogen, Carlsbad, USA
	Sodium pyruvate solution (100mM)	5 ml	Sigma-Aldrich Chemie GmbH, Taufkirchen, Germany
	2-Merceptoethanol (50mM)	10 ml (5mM)	Gibco, Invitrogen, Carlsbad, USA
	Myo-inositol	5 ml (20mM)	Sigma-Aldrich Chemie GmbH, Taufkirchen, Germany
HEK-293	Eagle's Minimum Essential Medium	500 ml	ATCC, Virginia, United States
	10% fetal bovine serum (FBS)	50 ml	PAA Laboratories, Pasching, Austria
	1% Penicillin/Streptomycin	5 ml	Gibco, Invitrogen, Carlsbad, USA
Human NK cells	RPMI 1640	500 ml	Thermo Fisher Scientific Inc., Darmstadt, Germany
	10% fetal bovine serum (FBS)	50 ml	PAA Laboratories, Pasching, Austria

	1% Penicillin/Streptomycin	5 ml	Gibco, Invitrogen, Carlsbad, USA
Proliferation Medium for Primary culture	DMEM/F12 + Glutamax	25 ml	Thermo Fisher Scientific Inc., Darmstadt, Germany
	1% Penicillin/Streptomycin	250 µl	Gibco, Invitrogen, Carlsbad, USA
	B27 supplement without retinoic acid	500 µl	Thermo Fisher Scientific, Darmstadt, Germany
	BSA 35%	250 µl	Sigma-Aldrich Chemie GmbH, Taufkirchen, Germany
	ß-Merceptoethanol	0.1% (25 µl)	Thermo Fisher Scientific, Darmstadt, Germany
	EGF	1 µl/ml	ImmunoTools GmbH, Friesoythe, Germany
	FGF	2 µl/ml	ImmunoTools GmbH, Friesoythe, Germany
Differentiation Medium for Primary culture	DMEM/F12 + Glutamax	25 ml	Thermo Fisher Scientific Inc., Darmstadt, Germany
	1% Penicillin/Streptomycin	250 µl	Gibco, Invitrogen, Carlsbad, USA
	B27 supplement	500 µl	Thermo Fisher Scientific, Darmstadt, Germany
	BSA 35%	250 µl	Sigma-Aldrich Chemie GmbH, Taufkirchen, Germany
	ß-Merceptoethanol	0.1% (25 µl)	Thermo Fisher Scientific, Darmstadt, Germany

	rhGDNF	1 µl/ml	ImmunoTools GmbH, Friesoythe, Germany

3.1.11. Cell lines

Cell line name	Tissue	Disease	Source
SHSY5Y (ATCC® CRL2266™)	Bone marrow	Neuroblastoma	ATCC, Virginia, United States
SKNAS (ATCC® CRL2137™)	Brain; derived from metastatic site: bone marrow	Neuroblastoma	ATCC, Virginia, United States
NK-92 (AC 488)	Peripheral blood	Malignant non-Hodgkin's lymphoma	Leibniz-Institut DSMZ-Deutsche Sammlung von Mikroorganismen und Zellkulturen GmbH, Braunschweig Germany
HEK-293 (ATCC® CRL-1573™)	Embryonic kidney		ATCC, Virginia, United States

3.2 Methods

3.2.1. Exp. Set 1: Determination of the effect of extracellular RNA on neuroblastoma cells

3.2.1.1. Cell culture methods

SHSY5Y (ATCC® CRL2266™) cells were cultured in 1:1 mixture of Eagle's Minimum Essential Medium (EMEM) (with L-Glutamine Sterile filtered) and F-12K Nut Mix (1X) Nutrient Mixture Kaighn's Modification ([+] L-Glutamine). The medium was additionally supplemented with 10% FBS and 1% Penicillin/Streptomycin.

SKNAS (ATCC® CRL2137™) cells were grown in DMEM (1X) + GlutaMAX™ Dulbecco's Modified Eagle Medium ([+] 4.5g/L D-Glucose [+] Pyruvate) and supplemented with 10% FBS and 1% Penicillin/Streptomycin.

HEK-293 (ATCC® CRL-1573™) cells were grown in Eagle's Minimum Essential Medium and supplemented with 10% FBS and 1% Penicillin/Streptomycin.

3.2.1.2. RNA Isolation

SHSY5Y and SKNAS cells were individually plated in T-25 flasks at a concentration of $1.5x10^6$ cells/ml. Cells were then incubated for 6 and 24 hours with IFN-γ, Poly(I:C)-LMW, Poly(I:C)-HMW, Total RNA (1µg/ml) and Total RNA (10µg/ml) and maintained in culture. After the respective timepoints were completed, cells were lysed using RNA lysis buffer T provided in the peqGOLD Total RNA kit (VWR International GmbH, Erlangen, Germany). The lysates were transferred to DNA removing columns placed in a 2.0 ml collection tube and centrifuged at 14,000 rpm for 1 min at room temperature. Equal volumes of 70% ethanol were added to the lysates and mixed thoroughly by vortexing. Lysates were added to the PerfectBind RNA columns in a new 2.0 ml collection tube and centrifuged at 14,000 rpm for 1 min; the flow-throw was discarded. 500µl Wash buffer I was added to PerfectBind RNA column and placed in a new 2.0 ml collection tube, centrifuged at 14,000 rpm for 1 min. The flow-throw was discarded and the same step was repeated with 400ul Wash buffer I. 600µl Wash buffer II was added and centrifuged at 14,000 rpm for 1 min. This step was repeated and flow-throw was discarded. The centrifugation was repeated to dry the column without adding any more buffers. The column was placed in a new 1.5 ml tube and 25-30µl of sterile dH_20 was added directly to the binding matrix and incubated for 5 mins at room temperature. The column was centrifuged for 2 mins at 14,000 rpm to elute the RNA. Quality of samples (A260/A280 ratio) was controlled using Nanophotometer (Implen) and quantification was done using the same.

3.2.1.3. cDNA synthesis

cDNA synthesis was done using the QuantiTect® Reverse Transcription Kit (Qiagen GmbH, Hilden, Germany) from 1 µg/ml of total RNA. 1 µg/ml of total RNA was diluted in 20 µl of water, to this 2 µl genomic DNA wipeout buffer was added and incubated at 42°C

for 2 minutes. Then 4 µl 5X Quantitect RT buffer, 1 µl RT Primer mix, 1 µl Quantitect RTase was added followed by incubation at 42°C for 30 minutes and 95°C for 3 minutes. The synthesized cDNA was stored at -20°C for further use.

3.2.1.4. Real-Time PCR

Relative quantification of gene expression for the SHSY5Y and SKNAS lysates was measured using iTaq™ Universal SYBR® Green qPCR Master Mix (Bio-Rad, CA, USA) with 5 ng of cDNA and 40 cycles at an annealing temperature specific for individual primers in the StepOne® Real-Time PCR system (Applied Biosystems, Darmstadt, Germany). Primers were designed by NCBI nucleotide primer designing tool and were synthesized in Eurofins-Genomics (Eurofins MWG Synthesis Gmbh, Ebersberg, Germany). The quantification of target genes was done using the listed primers (Table 3.1.6) and the PCR reaction mixture of 10 µl Mastermix (iTaq™ Universal SYBR® Green), 1 µl forward primer and reverse primer each, 7 µl H_2O and 1 µl of cDNA. GAPDH was used as the internal control gene and the comparative ΔΔCT method (ΔCT= target gene - housekeeping gene; $\Delta\Delta CT = 2^{\wedge -\Delta CT}$) was used to evaluate the relative quantification of gene expression.

3.2.1.5. Preparation of northern probe

For preparation of a DIG-labeled probe, 1µg total RNA from SHSY5Y cells was reverse transcribed using the QuantiTect® Reverse Transcription Kit (Qiagen GmbH, Hilden, Germany) according to manufacturer's instructions and subsequently PCR was performed using iTaq™ Universal SYBR® Green qPCR Master Mix (Bio-Rad, CA, USA), using primers designed as mentioned in (Table 3.1.7). 5µl volume was run on the gel to check the quality of RNA. Rest of the volume from PCR (45µl) was run on agarose gel and purified with QIA quick spin Gel Extraction Kit (Qiagen GmbH, Hilden, Germany). This purified product (with T7 promoter) was used as template for DIG labeling according to manufacturer's instructions by invitro transcription utilizing DIG Northern Starter Kit (Roche, Mannheim, Germany). The concentration was measured by nanophotometer

(Implen GmbH, München, Germany), and the quality was checked by electrophoresis and stored at -80°C.

3.2.1.6. Northern blotting

Denatured total RNA samples from neuroblastoma cells (SHSY5Y, SKNAS) and non-neuronal cells (HEK293) along with NorthernMax-Gly sample loading dye (Thermo Fisher, Darmstadt, Germany) in 1:1 ratio were loaded onto agarose gel and DIG-labeled DNA Molecular Weight Marker VII (0.35-8.5 kb) (Roche, Mannheim, Germany). Electrophoresis was performed for 1-2 hr at 100V. After the run was complete, gel was imaged on ECL CHEMOCAM Imager (INTAS, Science Imaging Instruments GmbH, Göttingen, Germany) by UV documentation of ethidium bromide staining. Ribosomal RNAs and marker was visible. The gel was then equilibrated in 1X TBE blotting buffer for 20 mins. The blotting paper and nylon membrane were soaked in 1X TBE blotting buffer for 5 mins. The transfer sandwich was assembled, starting with blotting paper, nylon membrane, gel and soaked blotting paper. The air bubbles were removed, and the semi-dry electrophoresis transfer assembly (Trans-Blot® SD Semi-dry transfer cell, Bio-Rad, CA, USA) was run for 1 hr at 15V (3 mA/cm^2). After blotting, the transfer sandwich was disassembled, and the membranes were marked at one corner for orientation and the nucleic acids were cross-linked to the membranes by placing them in a cross-linker (BIO-LINK Crosslinker BLX-254, Witec AG, Sursee, Switzerland) at 120 mJ/cm^2 at 254 nm. Following cross-linking, membranes were placed in glass falcons and 5 ml NorthernMax hybridization buffer (Thermo Fisher, Darmstadt, Germany) was added and kept on shaking for 1 hr at 68°C with constant rotation in a hybridization oven. The DIG-labeled riboprobe was denatured for 2 mins at 95°C and added into the hybridization buffer used for pre-hybridization (final concentration 25ng/ml). the probe was hybridized overnight at 68°C with constant rotation. The following day, the hybridization buffer containing riboprobe was removed (stored in -20°C freezer) and 25 ml of 2X SSC washing buffer was added twice to the membranes and washed with constant rotation at 65°C for 15 mins each. The washing steps were repeated with 25 ml of 0.5X SSC washing buffer at 65°C for 15 mins each. The SSC washing buffer was discarded and the membranes were

kept for blocking in a plastic tray containing 2% DIG-blocking solution (DIG Northern Starter Kit, Roche, Mannheim, Germany) in Maleic acid buffer and incubated for 1 hr at room temperature with constant shaking. Afterwards, the anti-Fab fragment (DIG Northern Starter Kit, Roche, Mannheim, Germany) was added to a final dilution of 1:10,000 to the DIG-blocking solution and continued the incubation at room temperature for 1 hr while shaking. When the incubation was over, the unbound antibody was removed by washing the membranes in DIG-washing buffer, three times, for 10 mins, shaking at room temperature. The membranes were then equilibrated in DIG-detection buffer for 2 mins. Afterwards, for detection of luminescence signals, the membranes were transferred onto a plastic sheet on top of a photo cassette and 1ml of 0.5% CPD-star substrate solution (DIG Northern Starter Kit, Roche, Mannheim, Germany) in DIG-detection solution was poured over the membranes and incubated for 5 mins in the dark. The membranes were covered with x-ray film (in the dark), exposed to different time points and developed with a processing machine (X-ray film processor CURIX 60, AGFA, Mortsel, Belgium).

3.2.1.7. Expression of proteins by flow cytometry

SHSY5Y and SKNAS cells were seeded in 24 well plates in the concentration of $1x10^6$/ml. Once the cells adhere to the surface, the cells were incubated with IFN-γ (10ng/ml), Poly(I:C)-LMW (10µg/ml), Poly(I:C)-HMW (10µg/ml), Total RNA (1µg/ml) and Total RNA (10µg/ml) for 24 hours. Once the incubation is complete, cells were detached with 500 µl 1X trypsin, followed by centrifugation at 1200 rpm for 4 mins at room temperature. The supernatant was discarded and the pellet was washed with ice-cold PBS. The cells were then resuspended in FACS buffer and added in 96 well plate for staining. The cells were stained with 5 µl FITC anti-human HLA-A,B,C antibody for 30 minutes, at 4°C in the dark. After completion of incubation, the cells were washed twice with 100µl FACS buffer and later resuspended in 100µl FACS buffer for analysis of expression of MHC I in neuroblastoma cells by flow cytometry (Attune Acoustic Focusing Flow Cytometer, ThermoFisher Scientific, Darmstadt, Germany) using Attune Cytometric software.

For TLR-3 staining, post 24 hours treatment the cells were then resuspended in FACS buffer and added in 96 well plate for intracellular staining. For this purpose, BD

Cytofix/Cytoperm Fixation/Permeabilization kit (BD, San Jose, CA, US) was used. The cells were incubated with 100µl Fixation/Permeabilization solution per well for 20 mins in the dark at 4°C. Once the incubation is complete, the plate was washed twice with 100µl 1X perm/wash buffer per well and centrifuged at 1200 rpm for 4 mins at room temperature. The supernatant was discarded and the cells were stained with 5 µl CD283 (TLR3) PE, human antibody for 30 minutes at 4°C in the dark in 100µl 1X perm/wash buffer. The washing and analyzing steps were same as mentioned for anti-human HLA-A,B,C antibody staining.

3.2.1.8. Cytotoxicity (Lactate Dehydrogenase, LDH) assay

Possible cytotoxic effects of stimulants (3.2.1.2) on SHSY5Y and SKNAS cells were measured using cytotoxicity assay according to the manufacturer's instructions (Roche applied science, Indianapolis, IN). Cells were seeded in optically clear flat-bottomed 96 well plates in the concentration of $1x10^5$ cells/ml. 100 µl of this suspension is filled in the 96 well plates. Then, old medium was discarded and 200 µl medium containing stimulants such as IFN-γ (10ng/ml), Poly(I:C)-LMW (10µg/ml), Poly(I:C)-HMW (10µg/ml), Total RNA (1µg/ml) and Total RNA (10µg/ml) was added and incubated for 6 and 24 hours at standard cell culture conditions. Assay medium was used as background control, 100 µl cell suspension and 100 µl assay medium as low control. To determine the maximum amount of LDH enzyme activity, 2% Triton-X 100 was used as high control. After 6 and 24 hours, the respective plates were centrifuged at 250 x g for 10 mins. From this, 100 µl supernatant was transferred into new 96-well plates and 100 µl assay reagent was added and incubated for 30 mins at room temperature in dark. The amount of color produced due to the release of LDH enzyme was read at 490 nm in an ELISA reader. All the assays were carried out in triplicates, average absorbance values of the triplicates were calculated and background control subtracted. Cytotoxicity (%) was calculated as follows:

$$\% \text{ Cytotoxicity} = [(\text{Experimental value} - \text{low control value}) / (\text{High control value} - \text{low control value})] \times 100$$

3.2.1.9. Proliferation (WST-1) assay

SHSY5Y and SKNAS cells were seeded in 96 well plates in a final volume of 100 µl/well ($1x10^5$ cells/ml), maintained in culture until the cells adhere to the bottom of the plates. Then the old medium was removed and the cells were incubated for 24 hours with fresh medium containing IFN-γ (10ng/ml), Poly(I:C)-LMW (10µg/ml), Poly(I:C)-HMW (10µg/ml), Total RNA (1µg/ml) and Total RNA (10µg/ml). Then 10 µl of WST-1 reagent (Cell proliferation reagent WST-1, Roche applied science, Indianapolis, IN) was added in each well and the assay was carried out as mentioned in the instructions provided by the manufacturer. Plates were shaken thoroughly for 1 min on a shaker and incubated for 4 hours at standard cell culture conditions. The color developed from the soluble formazan dye cleaved from the tetrazolium salt WST-1 was measured at an absorbance of 420-480 nm in an ELISA reader. 100 µl of assay medium was taken as blank control for measuring the background absorbance. All experiments were carried out in triplicates. To calculate proliferation, mean absorbance was calculated and background absorbance (medium alone) subtracted from each value. The percentage of specific proliferation was quantified using the following calculation:

% Proliferation = (experimental release / spontaneous release) x 100

3.2.2. Exp. Set 2: Determination of the effect of NK-92 cells on neuroblastoma cells by co-culture method

3.2.2.1. Cell culture methods

SHSY5Y and SKNAS cell lines were cultured as mentioned in 3.2.1.1.

NK-92 (AC 488) cells were cultured using MEM Alpha Medium (1X) + GlutaMAX™ - I Minimum Essential Medium ([-] Ribonucleosides [-] Deoxyribonucleosides). The media was additionally supplemented with 12.5% FBS (heat inactivated), 12.5% horse serum (heat inactivated), 1% Penicillin/Streptomycin, 5 ml of 100mM Sodium pyruvate solution, 10 ml of 5mM 2-Merceptoethanol and 5 ml from 20mM Myo-inositol. All cells were grown under standard cell culture conditions (37°C, 5% CO_2).

Human NK-cells were isolated from healthy volunteers. Fresh whole blood was collected into EDTA-covered vials. To enrich NK-cells from whole blood, commercially available NK-cell enrichment kit (RosetteSep® human NK Cell Enrichment Cocktail; StemCell Technologies, Vancouver, Canada) was utilized according to the manufacturer´s instructions. After enrichment, NK-cells were counted, diluted in RPMI 1640 media to a final concentration of $5x10^5$ cells/ml, and immediately used for experiments.

3.2.2.2. Co-culture of neuroblastoma and NK-92 cell lines

To investigate the effect of natural killer cells on neuroblastoma cells, co-culture of the aforementioned cell lines was performed. SHSY5Y cell line was seeded in 96 well plate in a final volume of 100 µl/well (10,000 cells/well). The cells were allowed to adhere to the plate. Next day, the utilized media was removed and fresh medium containing IFN-γ (10ng/ml), Poly(I:C)-LMW (10µg/ml), Poly(I:C)-HMW (10µg/ml) and Total RNA (1 µg/ml, 10 µg/ml, 25 µg/ml and 50µg/ml) was added to the cells. The stimulants were incubated with the SHSY5Y cells for 24 hours. After completion of incubation, the used medium was removed and NK-92 cells (20,000 cells/well) in a final volume of 100 µl/well were added on top of SHSY5Y cells in a (1:2 ratio). Both the cell lines were co-cultured for 4 hours.

The same procedure was utilized to perform co-culture with SKNAS and NK-92 cell line.

3.2.2.3. LDH assay of co-cultured neuroblastoma and NK-92 cell line

SHSY5Y and NK-92 cell lines were co-cultured in a (1:2 ratio) for four hours. After the completion of 4 hours, LDH assay was performed as mentioned in 3.2.1.8.

The same procedure was followed for LDH assay for co-culture of SKNAS and NK-92 cell lines.

3.2.2.4. Co-culture of neuroblastoma and NK-92 cell lines post treatment with TLR3/dsRNA complex inhibitor

Co-culture of neuroblastoma cells with NK-92 cells was performed. SHSY5Y cell line was seeded in 96 well plate in a final volume of 100 µl/well (10,000 cells/well). The cells were allowed to adhere to the plate. Next day, the utilized media is removed and fresh medium containing TLR3/dsRNA complex inhibitor (200µM) was added for 3 hours. After completion of the incubation, the used medium was removed and fresh medium containing IFN-γ (10ng/ml), Poly(I:C)-LMW (10µg/ml), Poly(I:C)-HMW (10µg/ml), Total RNA (1 µg/ml and 10µg/ml), IFN-γ (10ng/ml) + Poly(I:C)-LMW (10µg/ml), IFN-γ (10ng/ml) + Poly(I:C)-HMW (10µg/ml), IFN-γ (10ng/ml) + Total RNA (1µg/ml) and IFN-γ (10ng/ml) + Total RNA (10µg/ml) was added to the cells for 24 hours. After completion of incubation, the used medium was removed and NK-92 cells (20,000 cells/well) in a final volume of 100 µl/well were added on top of SHSY5Y cells in a (1:2 ratio). Both the cell lines were co-cultured for 4 hours.

The same procedure was followed to perform co-culture with SKNAS and NK-92 cell line.

3.2.2.5. LDH assay of co-cultured neuroblastoma and NK-92 cell line post treatment with TLR3/dsRNA complex inhibitor

SHSY5Y and NK-92 cell lines were co-cultured in a (1:2 ratio) for four hours. After the completion of 4 hours, LDH assay was performed as mentioned in 3.2.1.8.

The same procedure was followed for LDH assay for co-culture of SKNAS and NK-92 cell lines.

3.2.2.6. Patients

We analyzed sera from nine patients with OMS, nine patients with neuroblastoma alone (NB) and seven healthy controls (HC). The age of the OMS-patients (five females, four males) was between 18 and 44 months with a mean age of 28.3 ± 9.4 months. Mean age of neuroblastoma-patients was 17.2 ± 11.3 months (two females, seven males). Tumor stages in the neuroblastoma group were 1 (n=3), 2 (n=5) and 3 (n=1). The mean age of the controls was 35.6 ± 14.9 months (three females, four males) (for OMS patient data see Table 1). Samples were obtained before treatment and written consent was obtained

from the patients or their parents. All samples were aliquoted and stored at -20°C until tested. This study was approved from the local ethical review board.

3.2.2.7. IgG isolation

IgG-isolation was performed using a protein-G trap column (HiTrap, Pharmacia, GE Healthcare, Pittsburgh, USA). The IgG-concentration was determined by nephelometry, and IgG-fractions were diluted in PBS to a final concentration of 6 g/l and stored at -20°C until used.

3.2.2.8. Surface binding of autoantibodies to neuroblastoma cell lines

Cells ($1x10^5$ cells/well) were plated onto 96-well plates and sera, diluted 1/50 in FACS-buffer, were added to the cells at a concentration of 100 µl/well and incubated for 30 minutes at 4° C. After washing twice with FACS-buffer, FITC-conjugated anti-human-IgG (1/75 in FACS-buffer, DAKO) was added for another 30 minutes. Cells were washed again in FACS-buffer and then analyzed on Attune Acoustic Focusing Flow Cytometer, ThermoFisher Scientific, Darmstadt, Germany, using Attune Cytometric software. Surface binding was considered positive if mean fluorescence intensity was higher than the mean plus 2.5 times standard deviation of healthy controls.

3.2.2.9. NK-cell-mediated tumor cell lysis

ADCC induced by incubation of neuroblastoma-cells with patients' IgG and human NK-cells (or NK92 cell line) was measured by LDH-release as per the manufacturer's instructions (Roche Diagnostics GmbH, Mannheim, Germany). Cells were seeded onto 96 well-plates at $1x10^4$ cells/well and left overnight. The cells were incubated in either IgG (0.2 µg/ml), assay-medium containing Triton-X (1%, to give maximum release possible), medium alone (background absorbance), target cells alone (spontaneous release), or NK-cells alone (effector control). NK-cells were added to the respective wells at an

effector: target ratio of 5:1 and incubated for 20 hours at 37°C and then centrifuged at 900x g for 10 minutes. LDH assay was performed as mentioned in 3.2.1.8.

3.2.3. Exp. Set 3: Investigating the effect of extracellular RNA on primary cultures of murine subventricular zone (SVZ) and enteric nervous system (ENS)

3.2.3.1. Animals

Balb/c wild-type mice of both sexes aged 2-5 days were used.

Animal preparations were conducted according to the animal protection laws in Rhineland-Palatinate, Germany. All experiments were carried out in AG Enterisches Nervensystem, Hochschule Kaiserslautern, Campus Zweibrücken, Zweibrücken, Germany.

3.2.3.2. Isolation of high-purity myenteric plexus (MP) from postnatal mouse gastrointestinal tract and subventricular zone (SVZ) from postnatal mouse brain

The gastrointestinal tract was dissected from postnatal balb/c mice using a binocular microscope (Motic China Group Co., Ltd.). The mesenteries were completely removed. After a brief washing in MEM-Hepes with 1% P/S to remove the remaining luminal content, the muscle layer was dissected completely under a binocular microscope using forceps and was stored in MEM-Hepes with 1% P/S on ice.

The muscle layers were cut into pieces and placed in a 1.5 ml tube containing neutral 830 µl HBSS + 1% P/S, 150 µl Liberase TH (Roche Diagnostics GmbH) from stock solution and 20 µl DNase (Roche Diagnostics GmbH). The tissue was allowed to digest for 2.5 hours at 37°C and was then mechanically disrupted by vortexing for ten seconds, inorder to separate the MP networks with anatomical integrity from the surrounding smooth-muscle cells. The suspension containing the MP networks was placed in a 35 mm petri dish and fresh MEM-Hepes with 1% P/S was added to improve the visibility of the isolated MP networks within the overall cell suspension. The supernatant containing mainly

muscle cells was discarded when the MP networks were sedimented on the bottom of the petri dish. The sedimented MP networks were harvested with a pipette and transferred to fresh MEM-Hepes, until all the networks were collected. The MP networks were kept on ice until further use.

For neural stem cells isolation, the heads of postnatal mice were removed after quick decapitation and stored on ice in a 35 mm petri dish. Using small scissors, a longitudinal incision at the base of the head was made and continued until the nose. Using pointed forceps, skull of one of the hemispheres was peeled off and likewise done for the second hemisphere. Once the brain was visible, it was excised out of the head and kept in a 35 mm petri dish containing ice cold MEM-Hepes with 1% P/S. An incision was made starting from bottom of one hemisphere until the top. Once the incision was completed, the hemisphere was peeled away from its surface, thus making the SVZ visible. By using sharp forceps, the SVZ area was cut and kept in ice cold MEM-Hepes with 1% P/S on ice until the SVZ of second hemisphere was excised out as well. The subventricular zones were dissected from both hemispheres under microscopical control.

3.2.3.3. Cultivation of high-purity myenteric plexus from postnatal mouse gastrointestinal tract and subventricular zone (SVZ) from postnatal mouse brain

Once the myenteric plexus networks were collected, they were centrifuged at 100xg for 5 mins and cultured in 6 well plate (MP networks from 2 postnatal balb/c mice per well seeded) in proliferation media ((DMEM/F12 + GlutaMAX) + 1% P/S + B27 supplement without retinoic acid + 35% BSA + β-Merceptoethanol). Growth factors such as EGF (1 µl/ml) and FGF (2 µl/ml) were added to the proliferation medium.

After collecting the SVZ from wild-type balb/c mice, it was transferred to a 1.5 ml eppendorf containing 1 ml accutase solution for 20 minutes at 37°C. Once the incubation was finished, the tissue pieces were triturated using consecutively 23 and 27 gauge needles (three times each). To avoid shear stress, aspiration of the tissues was performed very gently. After the dissociation, the cells were centrifuged at 100xg for 5 mins and supernatant was discarded. The pellet was resuspended in proliferation medium and seeded in 1X T-25 flask.

All primary cultures were cultivated under standard cell culture conditions (37°C, 5% CO_2). The media was changed every third day. Neurospheres appeared within 2-4 days. For individual experiments, the neurospheres had to be cultivated for 5 days to produce sufficient number of cells.

3.2.3.4. Flow cytometric analysis of extracellular and intracellular proteins in differentiated fetal neurospheres of murine subventricular zone (SVZ)

The SVZ cells were kept in proliferation culture for five days and then put into differentiation. For this purpose, extracellular matrix (ECM) was used for coating 6 well plate. ECM was prepared as 1:100 in differentiation media and wells were coated 600 µl/well and allowed to sit in incubator for 1-1.5 hours.

Meanwhile, for dissociation of neurospheres in T-25 flask in proliferation medium, it was centrifuged at 100xg for 5 mins. The supernatant was discarded and 1 ml accutase was added for 20 mins to the pellet and kept in incubator at 37°C. After the incubation was finished, the tissue cells were triturated using consecutively 23 and 27 gauge needles (three times each). To avoid shear stress, aspiration of the tissues was performed very gently. Centrifugation was done at 100xg for 5 mins, supernatant discarded and 1 ml differentiation medium ((DMEM/F12 + GlutaMAX) + 1% P/S + B27 supplement + 35% BSA + β-Merceptoethanol) was added to the pellet and resuspended. The dissociated cells were counted and dead cells excluded by Trypan blue assay.

Once the ECM was set after 1-1.5 hours in incubator, half of its volume was removed and 700,000 cells/well in differentiation medium were seeded and allowed to sit in incubator to adhere to the ECM coated plate. After allowing the cells to sit in the incubator for 1-1.5 hours, differentiation medium was added on top of the cells and kept in incubator to differentiate.

After 18 hours in differentiation medium, the cells were treated with Poly(I:C)-LMW (10µg/ml), Poly(I:C)-HMW (10µg/ml), Total RNA (1µg/ml) and Total RNA (10µg/ml) for 24 hours. As control, cells were cultured in differentiation medium alone. Once the 24 hour incubation was complete, the cells were prepared for flow cytometry. For this purpose,

the medium was removed from the cells and Papain (Worthington Biochemical Corporation) solution was prepared (Papain + α-Cysteine), added to the cells for 30 mins, and kept in the incubator at 37°C to detach and dissociate the cells. Once the incubation was finished, stop solution (Trypsin-Inhibitor + DNase) was added to halt the reaction and cells were collected in 1.5 ml eppendorf and very gently pipetted 10-15 times with 1000 µl pipette until cells were completely dissociated. Centrifugation was done at 100xg for 5 mins and supernatant was discarded. The cells were resuspended in FACS buffer. Live/dead staining was performed by using propidium iodide (PI staining 50 µg/ml) and Calcein AM. Calcein was incubated with the cells for 20 mins at 37°C in the incubator, followed by PI addition and running of sample on the flow cytometer (S3 Cell Sorter, Bio-Rad Laboratories, Inc.). After live/dead assay showed atleast 60-70% cells to be alive, cells were stained with FITC Mouse Anti-Mouse H-2K[d] (Clone SF1-1.1) antibody (1 µl/100,000 cells) in 100 µl FACS buffer for 40 mins at 4°C in the dark. For TLR-3 staining, cells were resuspended in FACS buffer containing 0.1% saponin for intracellular staining. PE Mouse Anti-Mouse CD283 (TLR3) Clone PaT3 (BD Biosciences) was used (1 µl/100,000 cells) in 100 µl FACS buffer + 0.1% saponin for staining cells for 40 mins at 4°C in the dark.

After both the staining of MHC-1 and TLR-3 were completed, cells were washed once with FACS buffer and resuspended in 100 µl FACS buffer and run on flow cytometer (S3 Cell Sorter, Bio-Rad Laboratories, Inc.) with ProSort™ Software.

3.2.3.5. Cytotoxicity (Lactate Dehydrogenase, LDH) assay of SVZ culture

SVZ cells after being in proliferation culture for five days were dissociated with 1 ml accutase solution for 20 minutes at 37°C and seeded in optically clear flat-bottomed 96 well plates in the concentration of 50,000 cells/ml in proliferation media containing growth factors such as EGF (1 µl/ml) and FGF (2 µl/ml). 100 µl of this suspension is filled in the 96 well plates. Then, old medium was discarded and 200 µl medium containing stimulants such as Poly(I:C)-LMW (10µg/ml), Poly(I:C)-HMW (10µg/ml) and Total RNA (1, 10 and 25µg/ml) in proliferation media without growth factors was added and incubated for 24

hours at standard cell culture conditions. After the completion of 24 hours, LDH assay was performed as mentioned in 3.2.1.8.

3.2.3.6. Proliferation (WST-1) assay of SVZ culture

SVZ culture was dissociated with 1 ml accutase solution for 20 minutes at 37°C and cells were seeded in 96 well plates in a final volume of 100 µl/well (50,000 cells/ml) in proliferation media containing growth factors such as EGF (1 µl/ml) and FGF (2 µl/ml). Then the old medium was removed and the cells were incubated for 24 hours with fresh medium containing Poly(I:C)-LMW (10µg/ml), Poly(I:C)-HMW (10µg/ml) and Total RNA (1, 10 and 25µg/ml) in proliferation media without growth factors. After the completion of 24 hours, WST-1 assay was performed as mentioned in 3.2.1.9.

3.2.3.7. Multi-electrode array measurements of enteric neurospheres from postnatal mouse gut

Commercially available MEA setup from Multi Channel Systems (MCS, Reutlingen, Germany) together with the provided software for data recording and analyses (MC-Rack) was utilized for electrophysiological investigations. Standard microelectrode arrays with an internal reference electrode were used. The electrode grid was 8 x 8 with 60 electrodes and an electrode spacing of 200 mm with an electrode diameter of 30 mm. The center of the MEA was used for cell culturing.

The surface of MEA was coated with 1 ml of 10 µg/ml poly-D-lysine (Sigma, mol wt. 70,000-150,000) (PDL) and kept in incubator for 1-2 hours. After the coating was done, the PDL was removed and the surface was washed thrice with dH_2O and kept for drying under the laminar flow hood for 1-1.5 hours. Once the PDL coating on the MEA surface was dried, extracellular matrix (ECM-Gel) (Sigma) coating was done (1:50) in the center of the MEA-chip and kept in incubator for 1-1.5 hours at 37°C.

Enteric neurospheres from wild type balb/c postnatal mice gut were cultivated for 5 days before dissociating them with papain solution (Worthington Biochemical Corporation) (Papain + α-Cysteine) for 30 mins at 37°C, followed by addition of stop solution (Trypsin-

Inhibitor + DNase). The dissociated neurospheres were centrifuged at 100xg for 5 mins and pipetted 10-15 times very gently with a 1000 µl pipette tip for dissociation. Counting was done with trypan blue and 100,000 cells/MEA were seeded in differentiation medium after removing the previously done ECM coating. The cells were kept in incubator for 1-1.5 hours to settle down, followed by addition of 1 ml differentiation medium along with rhGDNF (Recombinant Human Glial-derived Neurotrophic Factor) 1 µl/ml on top of the cells and kept in incubator for differentiation.

After being in culture for 10-12 days and formation of neurospheres and glial cells over the PDL and ECM coating, the MEAs were taken for measurements to the MEA workstation. The recordings started with a baseline of approximately 100 seconds followed by the stimulation of Poly(I:C)-LMW (10, 25, 50, 100 µg/ml), Poly(I:C)-HMW (10, 25, 50, 100 µg/ml) and Total RNA (1, 10, 25, 50 µg/ml). The MEA workstation allowed us data recording and analyzing from up to 60 MEA electrodes. The amplifier platform was mounted on a shock isolated stereo optic microscope, which was placed in a Faraday's cage. Inside the cage, a gravity driven batch application system was installed.

3.3 Statistical Analysis

Statistical analysis between different groups were assessed using one-way ANOVA and post-test analysis. T-Test was used for comparisons between two groups. Statistical analysis was performed using GraphPad Prism version 7.00 for Windows (GraphPad Software, San Diego, California, USA). Graphs were prepared using GraphPad Prism version 7.00 for Windows (GraphPad Software, San Diego, California, USA). Histogram overlays for FACS data were prepared using FlowJo version 10 (FlowJo v10, BD, Ashland, Oregon, USA). All data are presented as mean ± standard error of mean. $p < 0.05$ was considered statistically significant. (* $p < 0.05$; ** $p < 0.01$; *** $p < 0.001$; **** $p < 0.0001$).

4. RESULTS

4.1 Exp. Set 1: Expression of immune system molecules on neuroblastoma and non-neuronal control cell line HEK293

4.1.1 Basal gene expression of MHC I and TLR-3 in neuroblastoma and non-neuronal control cell line HEK293

Basal level expression of MHC I and TLR-3 in neuroblastoma cells and non-neuronal control cell line HEK293 cells was detected via northern blot assay. The qualitative analysis showed that all the cell lines expressed MHC I and none of them showed TLR-3 expression without being treated with IFN-γ (Fig. 8). After stimulation with IFN-γ, SHSY5Y and SKNAS showed an increase in MHC I and TLR-3 expression in comparison to the basal expression. No effect on the HEK293 cell line was seen.

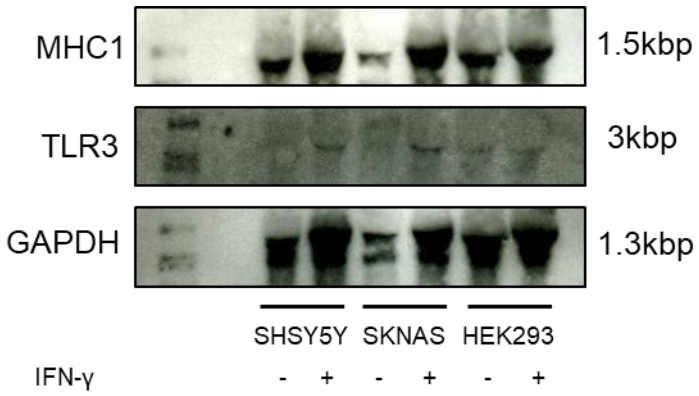

Figure 8. Northern blotting - The basal and IFN-γ stimulated expression of MHC I and TLR-3 in neuroblastoma and non-neuronal HEK293 cells – Detection of MHC I and TLR-3 by northern blotting post treatment with IFN-γ (10ng/ml) for 24 hours. GAPDH served as housekeeping control. IFN-γ - Interferon gamma.

4.1.2 Change in gene expression of MHC I in neuroblastoma and non-neuronal control cell line HEK293

We quantified the change in expression of MHC I in neuroblastoma and non-neuronal cell line HEK293 using real time PCR after stimulating with IFN-γ for 24 hours, in order to compare it with the untreated cells.

In SHSY5Y cells, treatment with IFN-γ resulted in a ~10-fold increase in MHC I expression ($p < 0.0001$, Fig. 9A). Moreover, in SKNAS cells, a ~6-fold increase is observed ($p < 0.01$, Fig. 9B). In both the cell lines the basal expression is negligible and stimulation with IFN-γ results in significant increase in MHC I expression. In HEK293 cells no significant effect was observed in IFN-γ treated cells in comparison to untreated cells ($p > 0.05$, n.s., Fig. 9C).

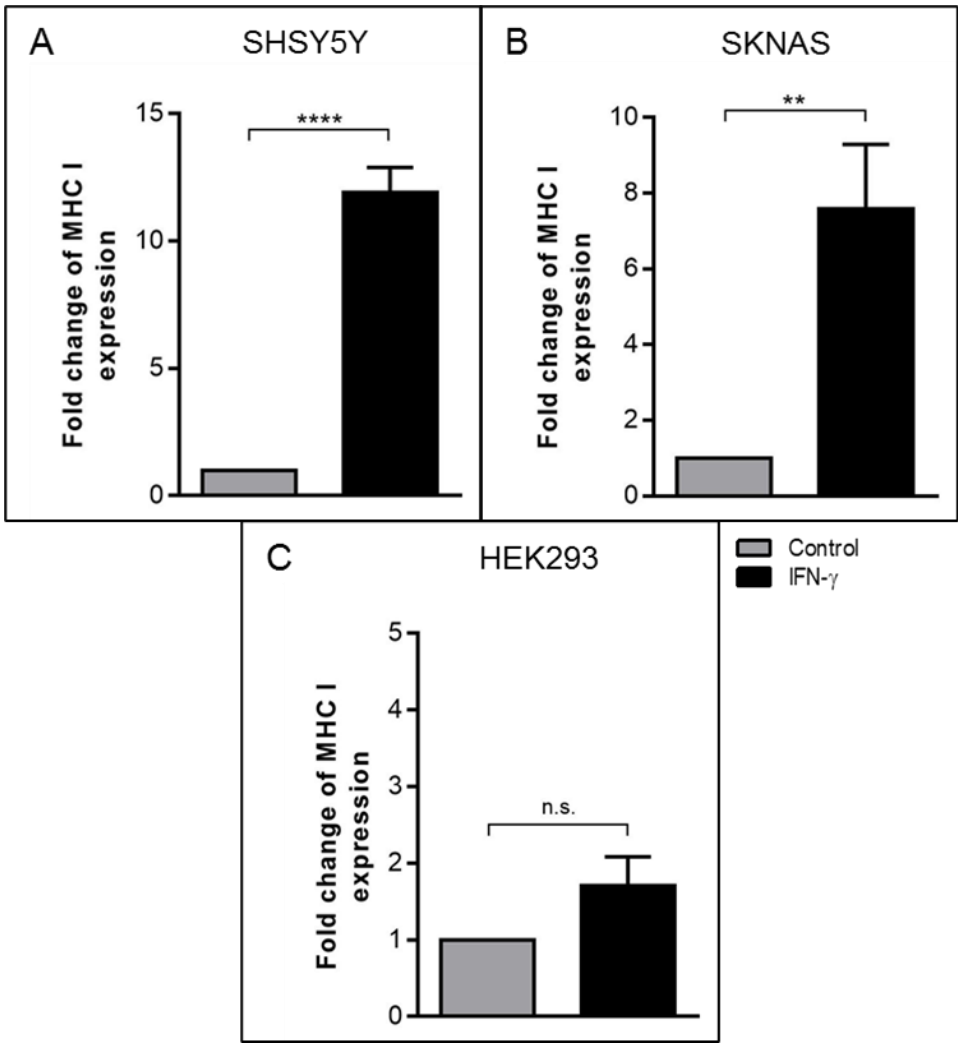

Figure 9. Change in basal and IFN-γ stimulated gene expression of MHC I in neuroblastoma and HEK cells – $1.5x10^6$ cells/well were kept untreated (control) or incubated with IFN-γ (10ng/ml) for 24 hours. **(A)** Neuroblastoma cell lines SHSY5Y **(A)** SKNAS **(B)** showed a significant increase in MHC I expression , whereas HEK293 cells **(C)** did not (SHSY5Y **** $p < 0.0001$; SKNAS, ** $p < 0.01$; HEK293 n.s. (not significant)). Values are expressed as mean ± standard error of mean. Data was normalized with GAPDH as housekeeping gene and presented as mean ± SEM of three independent experiments.

4.1.3 Change in gene expression of TLR-3 in neuroblastoma and non-neuronal control cell line HEK293

The neuroblastoma cells treated with IFN-γ for 24 hours showed a significant increase in expression of TLR-3. SHSY5Y ($p < 0.01$, Fig. 10A) and SKNAS cells ($p < 0.0001$, Fig. 10B) showed a 6- and 3-fold increase in TLR-3 expression respectively. However, the HEK293 cells used as a control cell line showed no significant effect after treatment with IFN-γ ($p > 0.05$, n.s., Fig. 10C).

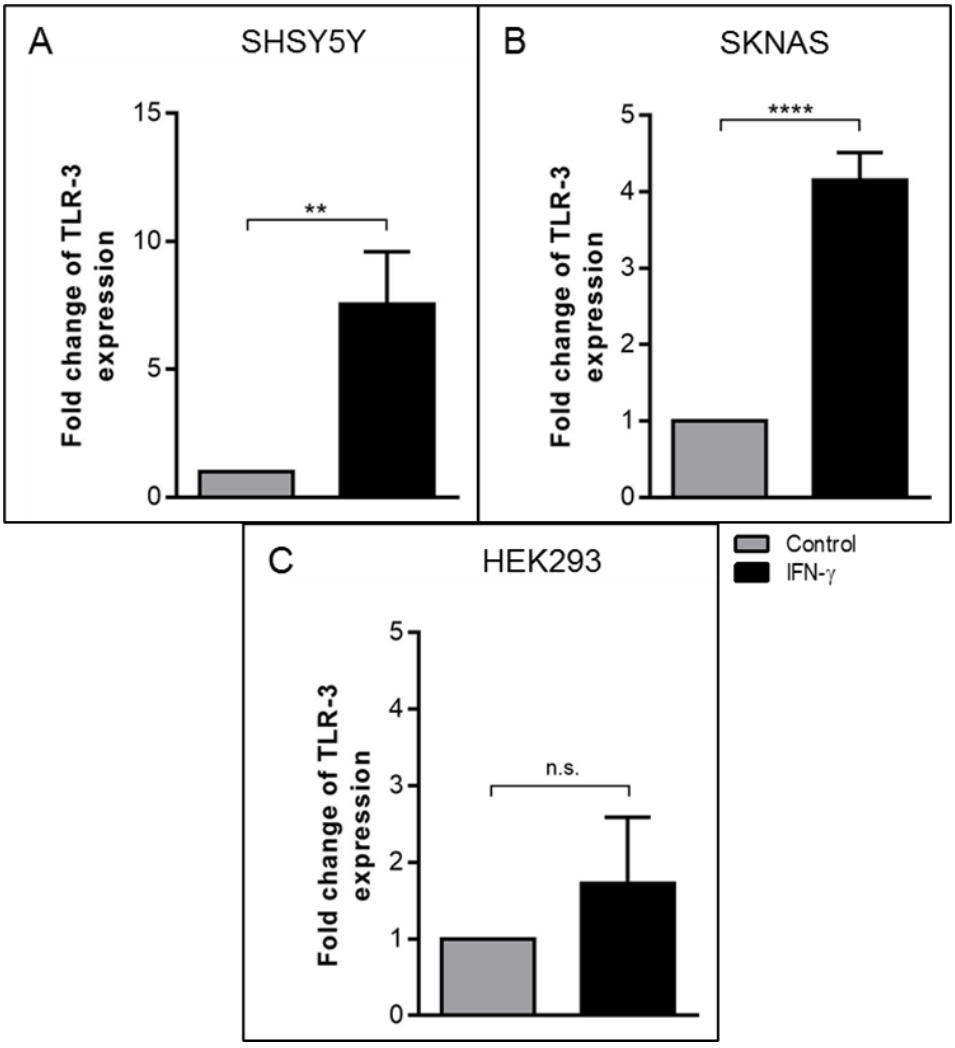

Figure 10. Change in basal and IFN-γ stimulated gene expression of TLR-3 in neuroblastoma and HEK cells – $1.5x10^6$ cells/well were kept untreated (control) or incubated with IFN-γ (10ng/ml) for 24 hours. **(A)** Neuroblastoma cell lines SHSY5Y **(A)** SKNAS **(B)** showed a significant increase in TLR-3 expression , whereas HEK293 cells **(C)** did not (SHSY5Y ** $p < 0.01$; SKNAS, **** $p < 0.0001$; HEK293 n.s. (not significant)). Values are expressed as mean ± standard error of mean. Data was normalized with GAPDH as housekeeping gene and presented as mean ± SEM of three independent experiments.

4.1.4 Change in protein expression of MHC I in neuroblastoma and non-neuronal control cell line HEK293

The flow cytometric analysis of MHC I expression in SHSY5Y cells showed, that on protein level there is almost no basal expression of MHC I. However, IFN-γ treatment significantly increased the expression of MHC I in SHSH5Y cells ($p < 0.001$, Fig. 11A). Similar effect was observed with increase in expression of MHC I post treatment with IFN-γ in SKNAS cells ($p < 0.0001$, Fig. 11B). No significant effect was observed in IFN-γ treated cells in comparison to untreated cells for HEK293 cells ($p > 0.05$, n.s., Fig. 11C).

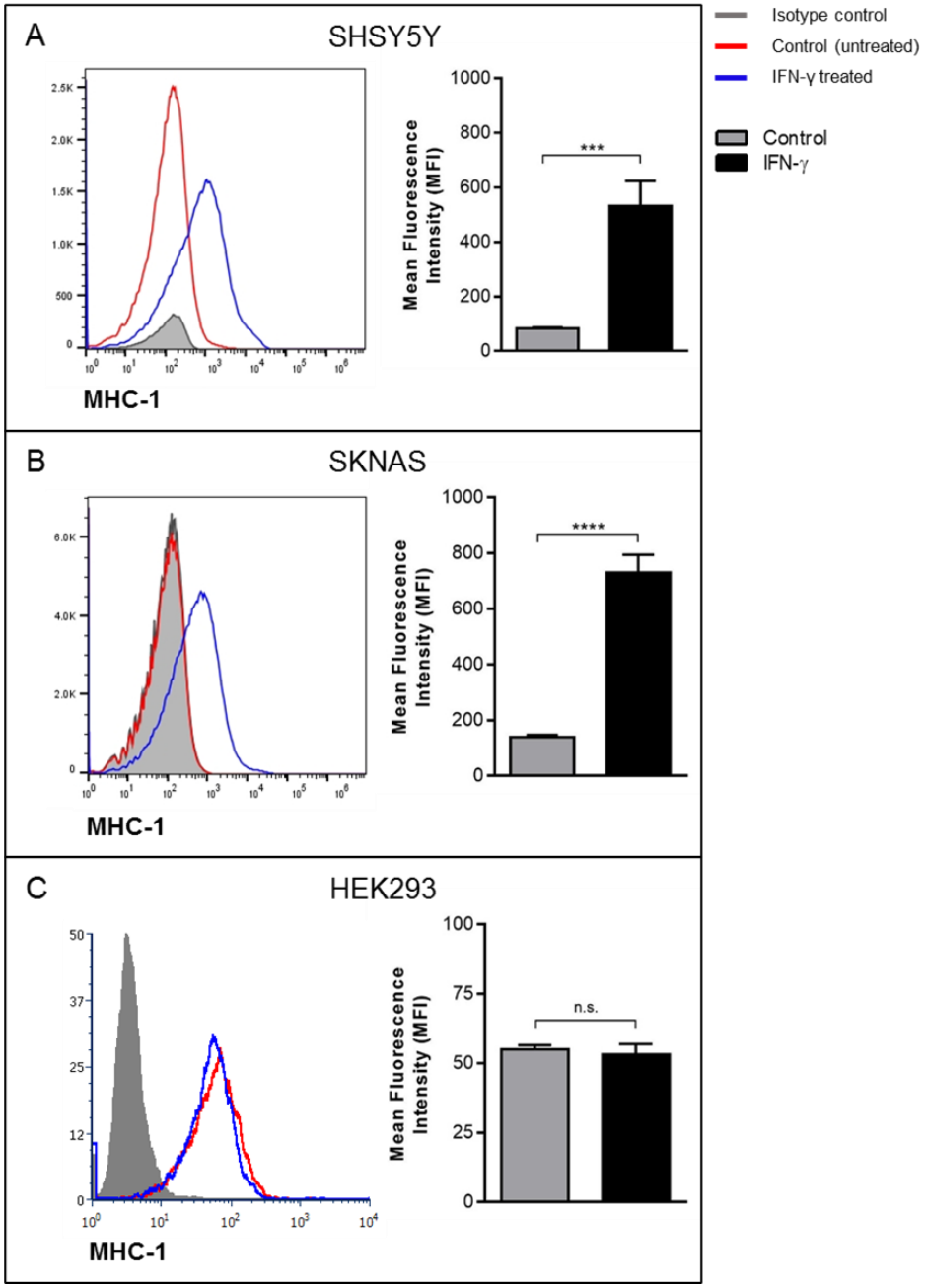

Figure 11. Change in basal and IFN-γ stimulated protein expression of MHC I in neuroblastoma and HEK293 cells – 1x10^6 cells/well were kept untreated or incubated with IFN-γ (10ng/ml) for 24 hours. **(A)** SHSY5Y **(B)** SKNAS **(C)** HEK293 cell lines. MHC I was upregulated by IFN- **γ** in SHSY5Y (*** $p < 0.001$) and SKNAS (**** $p < 0.0001$), but not in HEK293. Values are expressed as mean ± standard error of mean. Data was analyzed on FlowJo, V10 software, BD, USA and presented as mean ± SEM of three independent experiments.

4.1.5 Change in protein expression of TLR-3 in neuroblastoma and non-neuronal control cell line HEK293

For TLR-3, protein expression on basal level was observed to be negligible. However, after IFN- γ treatment, an increased TLR-3 expression was observed in SHSY5Y cells ($p < 0.05$, Fig. 12A). Comparable results were seen post IFN- γ treatment in SKNAS cells ($p < 0.001$, Fig. 12B) with significant increase in TLR-3 expression. In HEK293 cells, no significant effect was observed in IFN-γ treated cells in comparison to untreated cells. HEK293 ($p > 0.05$, n.s., Fig. 12C).

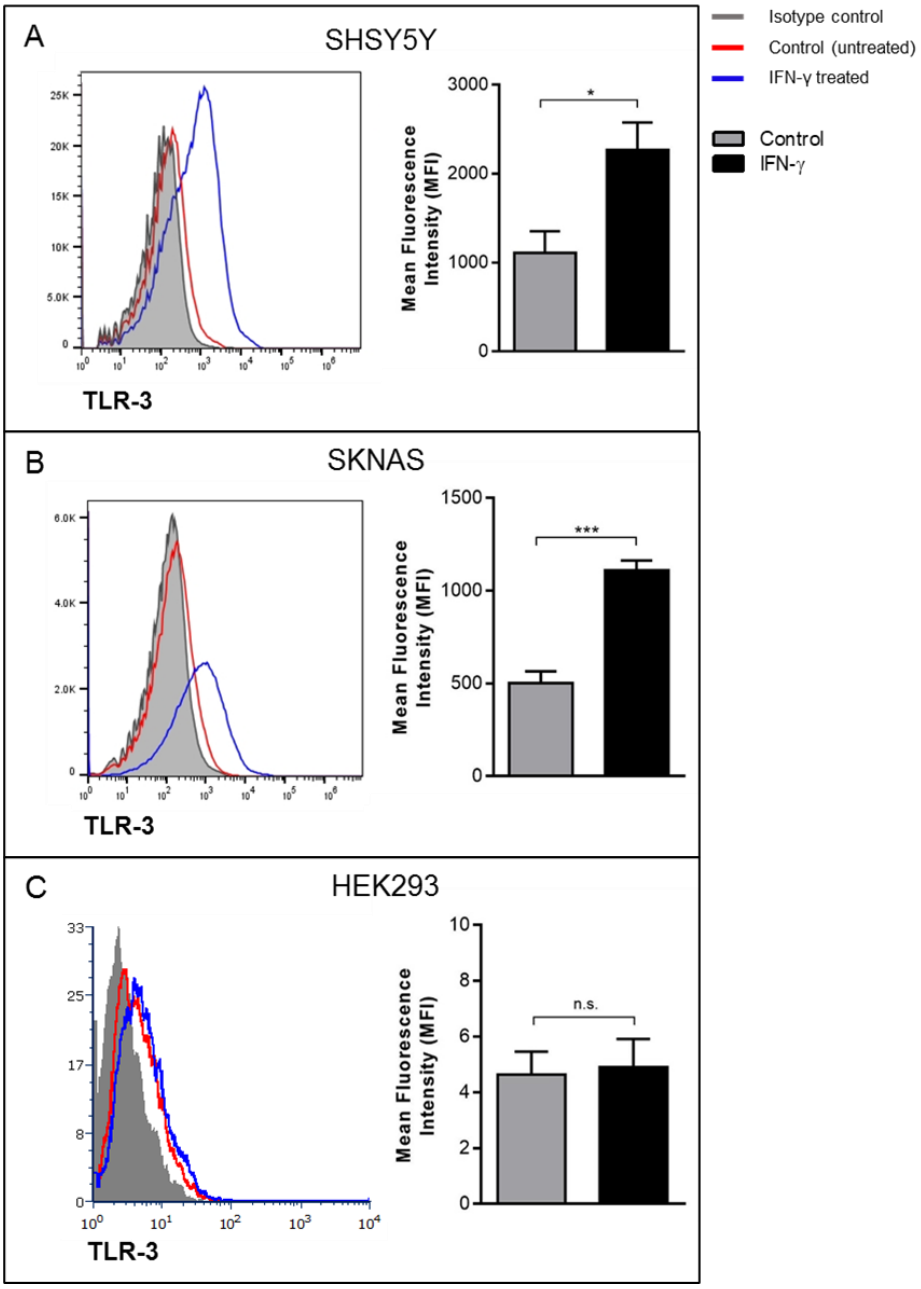

Figure 12. Change in basal and IFN-γ stimulated protein expression of TLR-3 in neuroblastoma and HEK293 cells – $1x10^6$ cells/well were kept untreated or incubated with IFN-γ (10ng/ml) for 24 hours. **(A)** SHSY5Y **(B)** SKNAS **(C)** HEK293 cell lines. TLR-3 was upregulated by IFN- **γ** in SHSY5Y (* $p < 0.05$) and SKNAS (*** $p < 0.001$), but not in HEK293. Values are expressed as mean ± standard error of mean. Data was analyzed on FlowJo, V10 software, BD, USA and presented as mean ± SEM of three independent experiments.

4.2 Exp. Set 2: Influence of immune stimulants and RNA on the immunological phenotype of neuroblastoma cells

4.2.1 Change in gene expression of MHC I in neuroblastoma cells at various time intervals

In order to determine the timepoint at which gene expression of MHC I is the highest, both the neuroblastoma cell lines were seeded and treated with IFN-γ, Poly(I:C)-LMW , Poly(I:C)-HMW and Total RNA for 6, 12, 24, 48 and 72 hours. At 24 hours, the stimulants induce the highest expression of MHC I amongst all timepoints in SHSY5Y and SKNAS cells. Based on the results, the 24 hour timepoint was decided to be used in upcoming experiments as incubation time for stimulants.

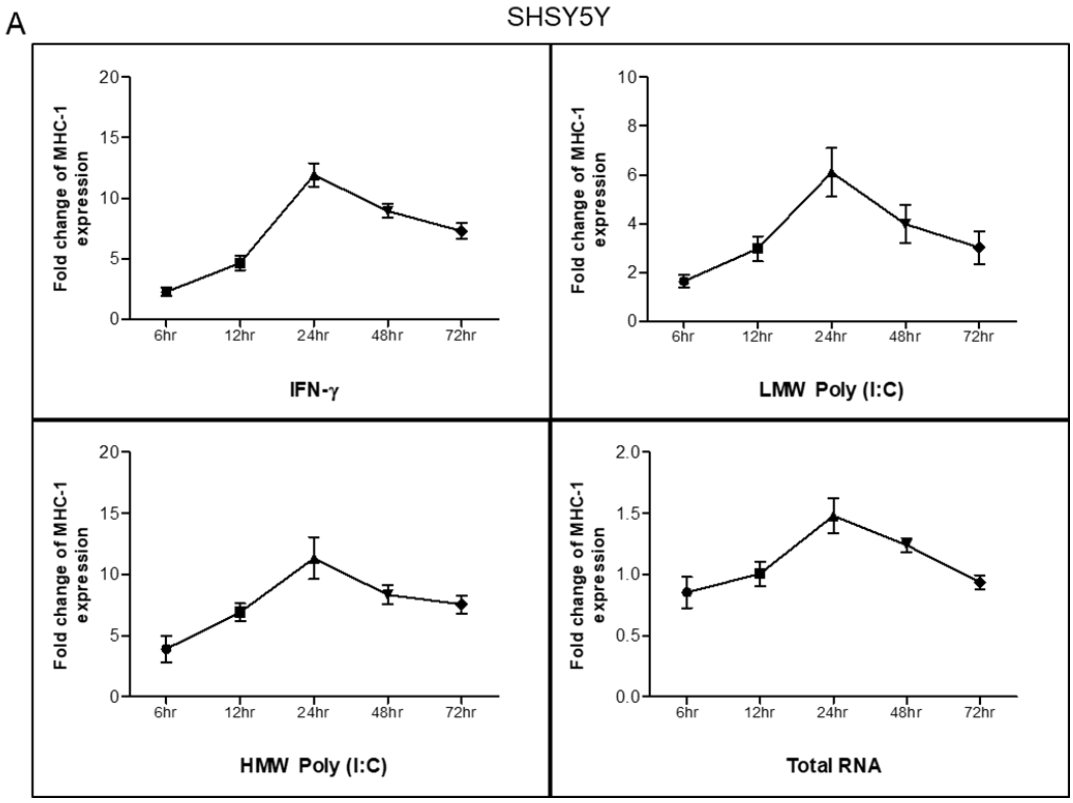

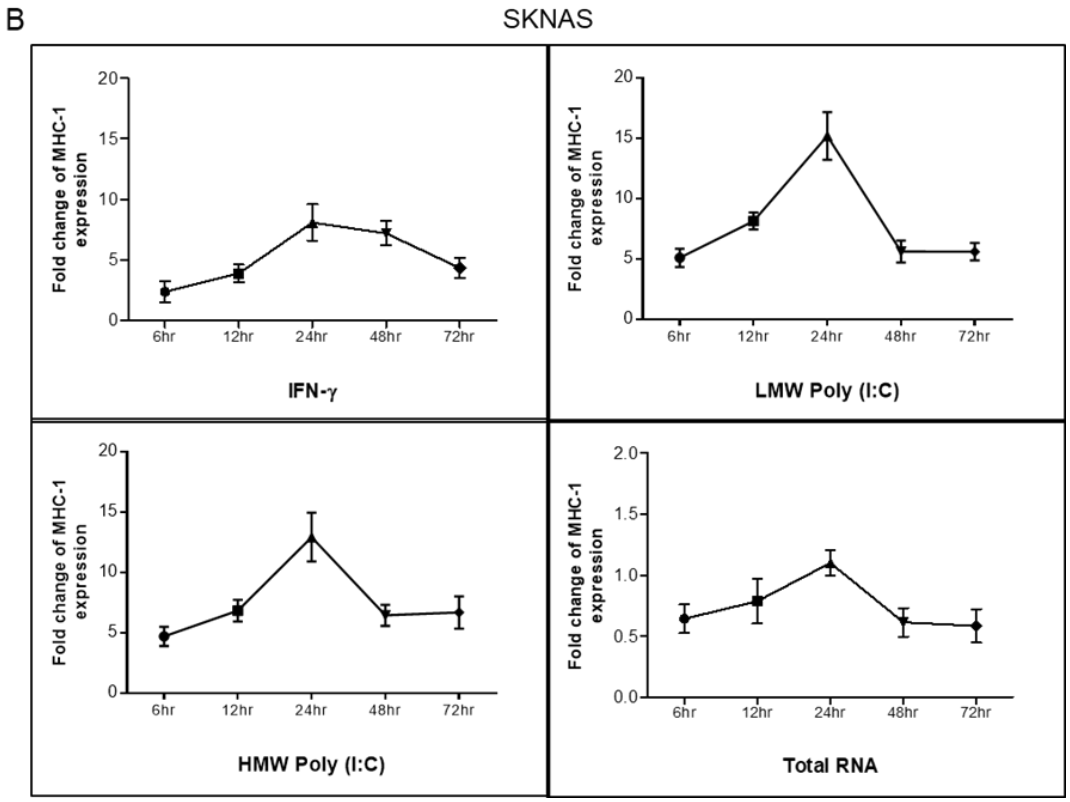

Figure 13. Change in gene expression of MHC I over various timepoints in neuroblastoma cells – 1.5x10^6 cells/well were incubated with IFN-γ (10ng/ml), Poly(I:C)-LMW (10µg/ml), Poly(I:C)-HMW (10µg/ml) and Total RNA (10µg/ml) for 6, 12, 24, 48 and 72 hours. **(A)** SHSY5Y **(B)** SKNAS gene expression. Data was normalized with GAPDH as housekeeping gene and presented as mean ± SEM of three independent experiments.

4.2.2 Influence of RNA on the expression of MHC I in neuroblastoma cells

To investigate the influence of RNA on gene expression of MHC I, neuroblastoma cells were stimulated for 24 hours followed by real time PCR. In SHSY5Y cells, expression of MHC I increased □10-folds when treated with IFN-γ ($p < 0.05$). Furthermore, there was an increase in MHC I expression in combination treatments of IFN-γ with LMW Poly (I:C) ($p < 0.001$), HMW Poly (I:C) ($p < 0.0001$) and total RNA ($p < 0.01$, Fig. 14A).

A similar pattern was observed in SKNAS cells, with increased expression of MHC I when treated with IFN-γ ($p < 0.05$), LMW Poly (I:C) ($p < 0.0001$), HMW Poly (I:C) ($p < 0.0001$) and IFN-γ in combination with LMW poly (I:C) ($p < 0.0001$) and HMW poly (I:C) ($p < 0.0001$, Fig. 14B).

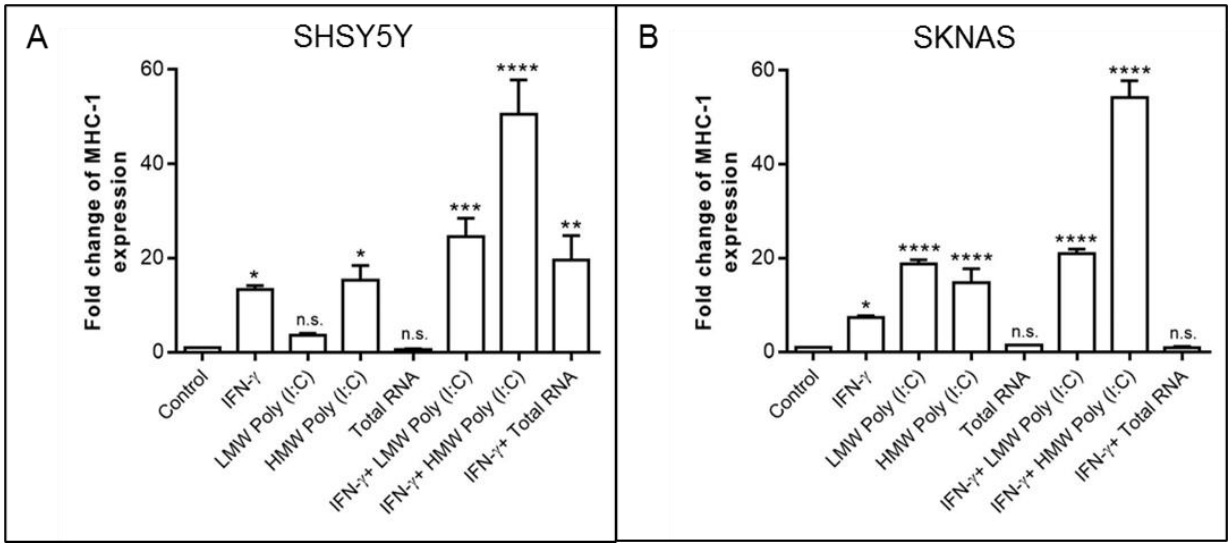

Figure 14. Gene expression of MHC I in neuroblastoma cells – $1.5x10^6$ cells/well were incubated with IFN-γ (10ng/ml), Poly(I:C)-LMW (10µg/ml), Poly(I:C)-HMW (10µg/ml), Total RNA (10µg/ml), IFN-γ (10ng/ml)+Poly(I:C)-LMW (10µg/ml), IFN-γ (10ng/ml)+Poly(I:C)-HMW (10µg/ml) and IFN-γ (10ng/ml)+Total RNA (10µg/ml) for 24 hours. **(A)** SHSY5Y **(B)** SKNAS cell lines. P values of * $p < 0.05$, ** $p < 0.01$, *** $p < 0.001$, **** $p < 0.0001$ were considered as significant. Values are expressed as mean ± standard error of mean. Data was normalized with GAPDH as housekeeping gene and presented as mean ± SEM of three independent experiments. n.s. = not significant.

4.2.3 Influence of RNA on the expression of TLR-3 in neuroblastoma cells

For TLR-3 expression, SHSY5Y cells were stimulated for 24 hours, resulting in significant increase when treated with IFN-γ ($p < 0.0001$) and IFN-γ in combination with LMW poly (I:C) ($p < 0.0001$) and HMW poly (I:C) ($p < 0.0001$). No difference was seen in IFN-γ + total RNA ($p > 0.05$, n.s., Fig. 15A). For SKNAS cells, no difference was observed post

treatment with IFN-γ ($p > 0.05$, n.s.). However, LMW Poly (I:C) ($p < 0.01$) and HMW Poly (I:C) ($p < 0.01$) showed increased TLR-3 expression. A significantly increased expression was observed in IFN-γ+LMW Poly(I:C) ($p < 0.0001$) and IFN-γ+HMW Poly(I:C) ($p < 0.0001$, Fig. 15B).

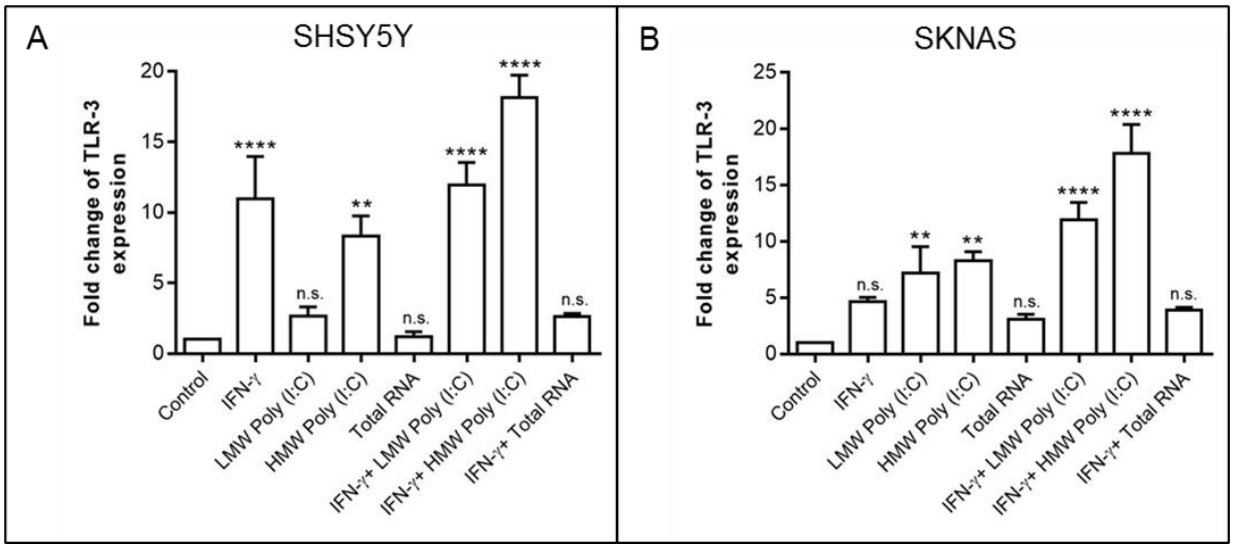

Figure 15. Gene expression of TLR-3 in neuroblastoma cells – $1.5x10^6$ cells/well were incubated with IFN-γ (10ng/ml), Poly(I:C)-LMW (10µg/ml), Poly(I:C)-HMW (10µg/ml), Total RNA (10µg/ml), IFN-γ (10ng/ml)+Poly(I:C)-LMW (10µg/ml), IFN-γ (10ng/ml)+Poly(I:C)-HMW (10µg/ml) and IFN-γ (10ng/ml)+Total RNA (10µg/ml) for 24 hours. **(A)** SHSY5Y **(B)** SKNAS cell lines. P values of * $p < 0.05$, ** $p < 0.01$, *** $p < 0.001$, **** $p < 0.0001$ were considered as significant. Values are expressed as mean ± standard error of mean. Data was normalized with GAPDH as housekeeping gene and presented as mean ± SEM of three independent experiments. n.s. = not significant.

4.2.4 Influence of RNA on the protein expression of MHC I in neuroblastoma cells

In order to investigate the effect of RNA on neuroblastoma cells, flow cytometric analysis was performed for the expression of MHC I. A significant increase in expression of MHC I was observed upon stimulation with IFN-γ ($p < 0.001$) and IFN-γ in combination with

both LMW poly (I:C) ($p < 0.0001$), HMW poly (I:C) ($p < 0.0001$) and total RNA ($p < 0.0001$, Fig. 16A) at 24 hours in SHSY5Y cells. Moreover, SKNAS cells showed a significant increase in MHC I expression upon stimulation with IFN-γ ($p < 0.01$), LMW Poly (I:C) ($p < 0.0001$), HMW Poly (I:C) ($p < 0.0001$) and IFN-γ in combination with LMW Poly (I:C) ($p < 0.0001$), HMW Poly (I:C) ($p < 0.0001$), total RNA ($p < 0.05$, Fig. 16B) at 24 hour timepoint.

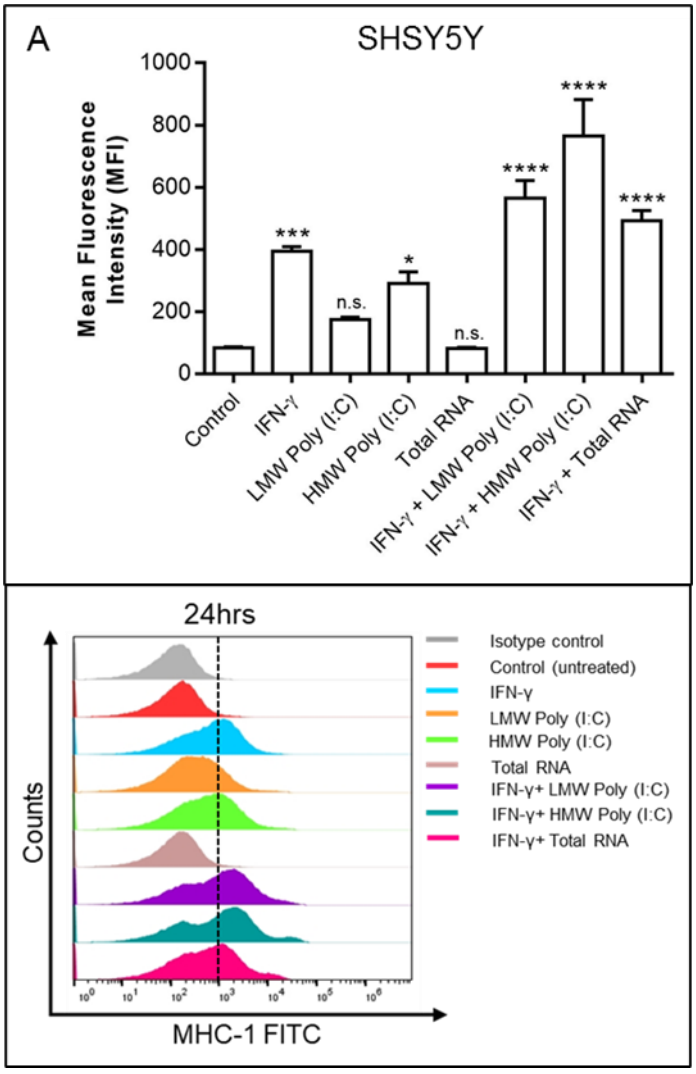

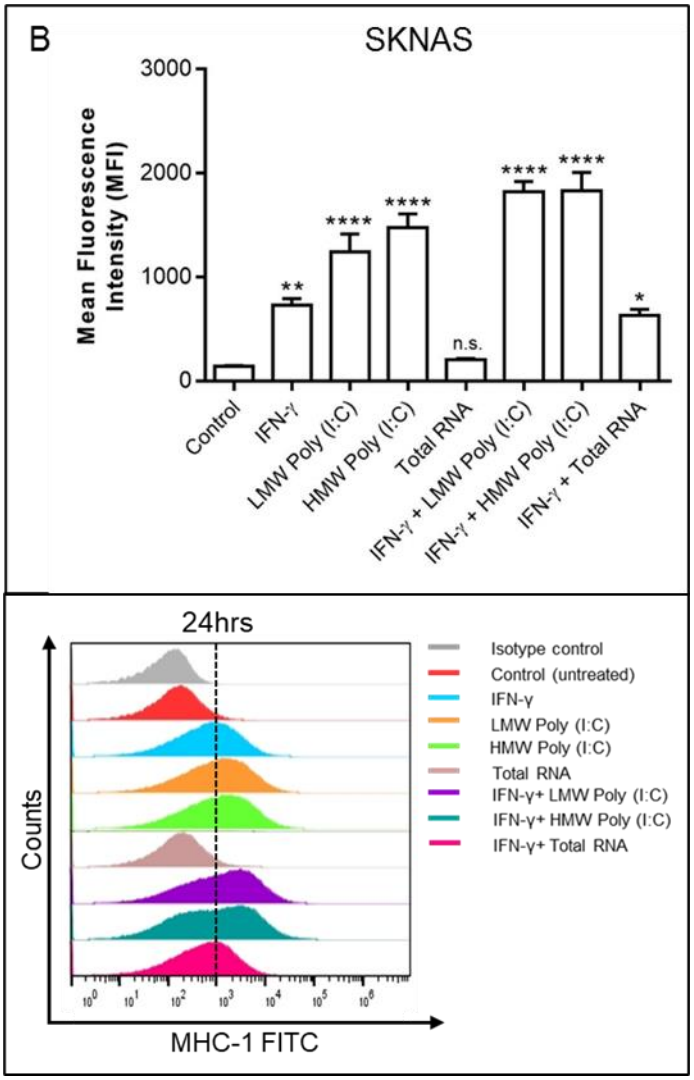

Figure 16. Flow cytometric analysis of MHC I in neuroblastoma cells – $1.5x10^6$ cells/well were incubated with IFN-γ (10ng/ml), Poly(I:C)-LMW (10µg/ml), Poly(I:C)-HMW (10µg/ml), Total RNA (10µg/ml), IFN-γ (10ng/ml)+Poly(I:C)-LMW (10µg/ml), IFN-γ (10ng/ml)+Poly(I:C)-HMW (10µg/ml) and IFN-γ (10ng/ml)+Total RNA (10µg/ml) for 24 hours. **(A)** SHSY5Y **(B)** SKNAS cell lines. P values of * $p < 0.05$, ** $p < 0.01$, *** $p < 0.001$, **** $p < 0.0001$ were considered as significant. Values are expressed as mean ± standard error of mean. Data was analyzed on FlowJo, V10 software, BD, USA and presented as mean ± SEM of three independent experiments. n.s. = not significant.

4.2.5 Influence of RNA on the protein expression of TLR-3 in neuroblastoma cells

For TLR-3, same stimulants were given, and an increased expression was observed post 24 hour treatment with IFN-γ ($p < 0.05$) in SHSY5Y cells. No statistically significant effect was observed in both Poly (I:C) and total RNA ($p > 0.05$, n.s.) but a statistically significant increase was observed in IFN-γ+LMW Poly(I:C) ($p < 0.01$), IFN-γ+HMW Poly(I:C) ($p < 0.0001$) and IFN-γ+total RNA ($p < 0.01$, Fig. 17A). Likewise, TLR-3 expression was significantly increased in SKNAS cells 24 hours post treatment with IFN-γ ($p < 0.01$). Individual treatments with LMW Poly (I:C) ($p > 0.05$, n.s.) and HMW Poly (I:C) ($p > 0.05$, n.s.) had no significant difference. However, the expression was observed to be increased further in combination treatments with IFN-γ in comparison to stimulants given alone IFN-γ+LMW Poly(I:C) ($p < 0.0001$), IFN-γ+HMW Poly(I:C) ($p < 0.0001$, Fig. 17B).

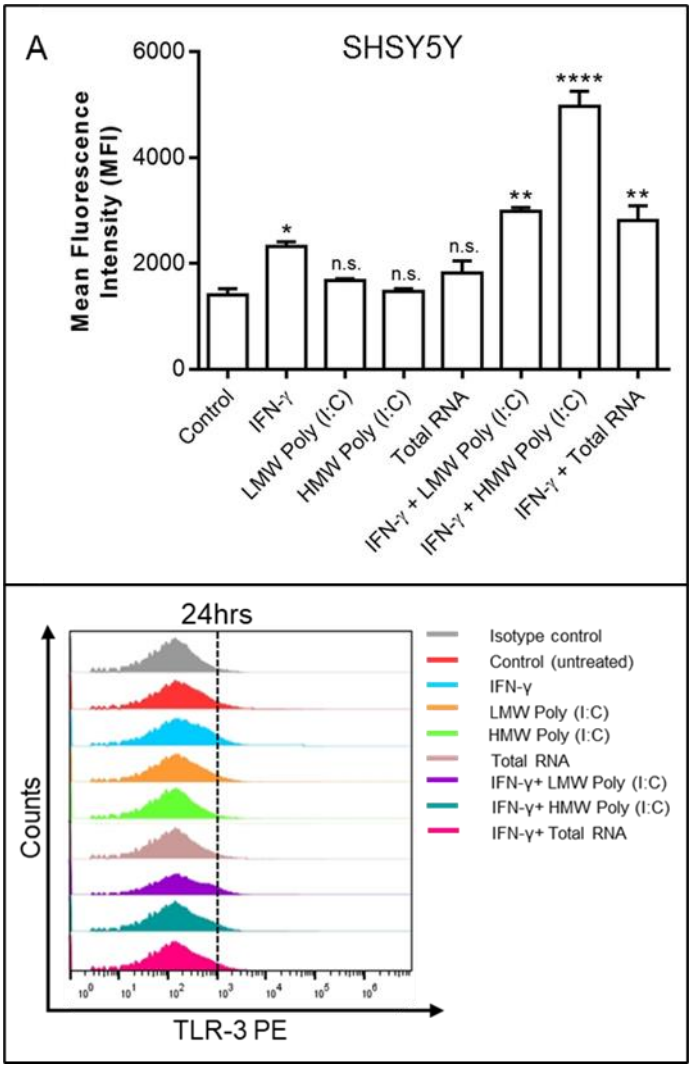

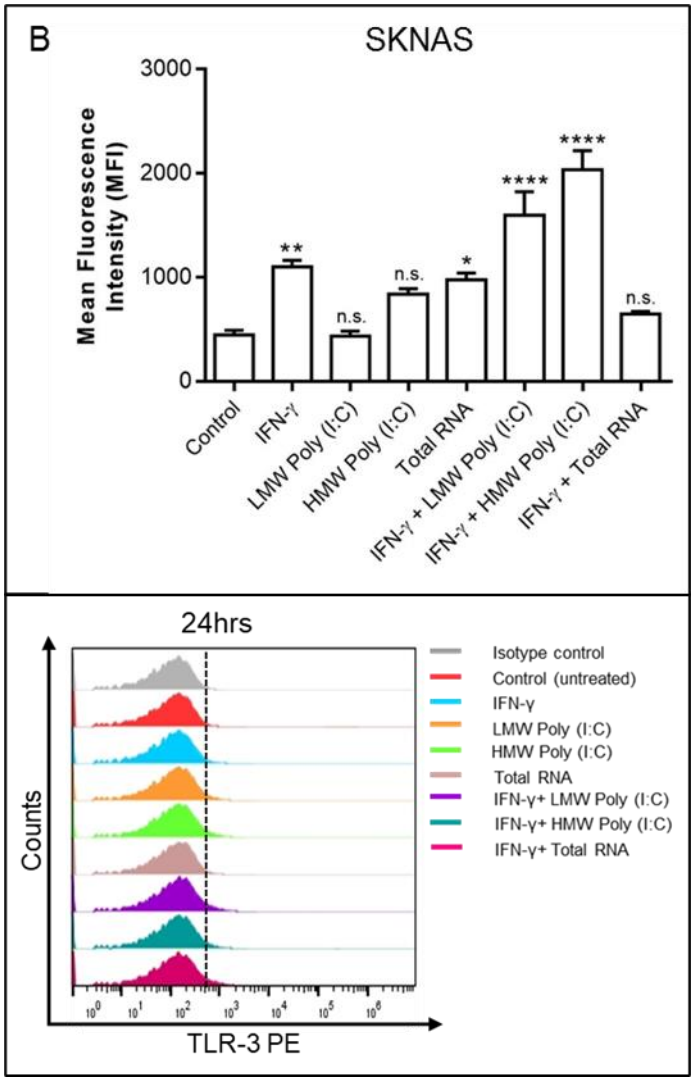

Figure 17. Flow cytometric analysis of TLR-3 in neuroblastoma cells – $1.5x10^6$ cells/well were incubated with IFN-γ (10ng/ml), Poly(I:C)-LMW (10µg/ml), Poly(I:C)-HMW (10µg/ml), Total RNA (10µg/ml), IFN-γ (10ng/ml)+Poly(I:C)-LMW (10µg/ml), IFN-γ (10ng/ml)+Poly(I:C)-HMW (10µg/ml) and IFN-γ (10ng/ml)+Total RNA (10µg/ml) for 24 hours. **(A)** SHSY5Y **(B)** SKNAS cell lines. P values of * $p < 0.05$, ** $p < 0.01$, *** $p < 0.001$, **** $p < 0.0001$ were considered as significant. Values are expressed as mean ± standard error of mean. Data was analyzed on FlowJo, V10 software, BD, USA and presented as mean ± SEM of three independent experiments. n.s. = not significant.

4.2.6 Flow cytometric analysis for MHC I expression post treatment with TLR3/dsRNA complex inhibitor

With the focus on determining the effect of TLR3/dsRNA complex inhibitor on the expression of MHC I, neuroblastoma cells were seeded and treated with the aforementioned inhibitor for 3 hours, followed by treatment with IFN-γ, LMW/HMW poly (I:C), total RNA and both poly (I:C), total RNA in combination with IFN- γ for 24 hours. Flow cytometric analysis was performed to look for the change in expression of MHC I post treatment with inhibitor.

Treatment with both LMW ($p < 0.05$) and HMW poly (I:C) ($p < 0.05$) significantly decreased MHC I expression in inhibitor treated cells in comparison to untreated SHSY5Y cells. Moreover, IFN-γ+LMW Poly(I:C) ($p < 0.05$), IFN-γ+HMW Poly(I:C) ($p < 0.05$) also showed significant decrease in MHC I expression post 24 hours inhibitor treatment. IFN-γ ($p > 0.05$, n.s.), total RNA ($p > 0.05$, n.s.) and IFN-γ+total RNA ($p > 0.05$, n.s., Fig. 18A) showed no effect post treatment with TLR3/dsRNA complex inhibitor.

A similar pattern was observed in SKNAS cells with no significant effect in IFN-γ ($p > 0.05$, n.s.), total RNA ($p > 0.05$, n.s.) and IFN-γ+total RNA ($p > 0.05$, n.s.). However, LMW ($p < 0.05$) and HMW poly (I:C) ($p < 0.05$) showed significant decrease in MHC I expression along with IFN-γ+LMW Poly(I:C) ($p < 0.05$), IFN-γ+HMW Poly(I:C) ($p < 0.05$, Fig. 18B) also showing similar pattern of decreased MHC I expression in cells treated with TLR3/dsRNA complex inhibitor in comparison to untreated cells.

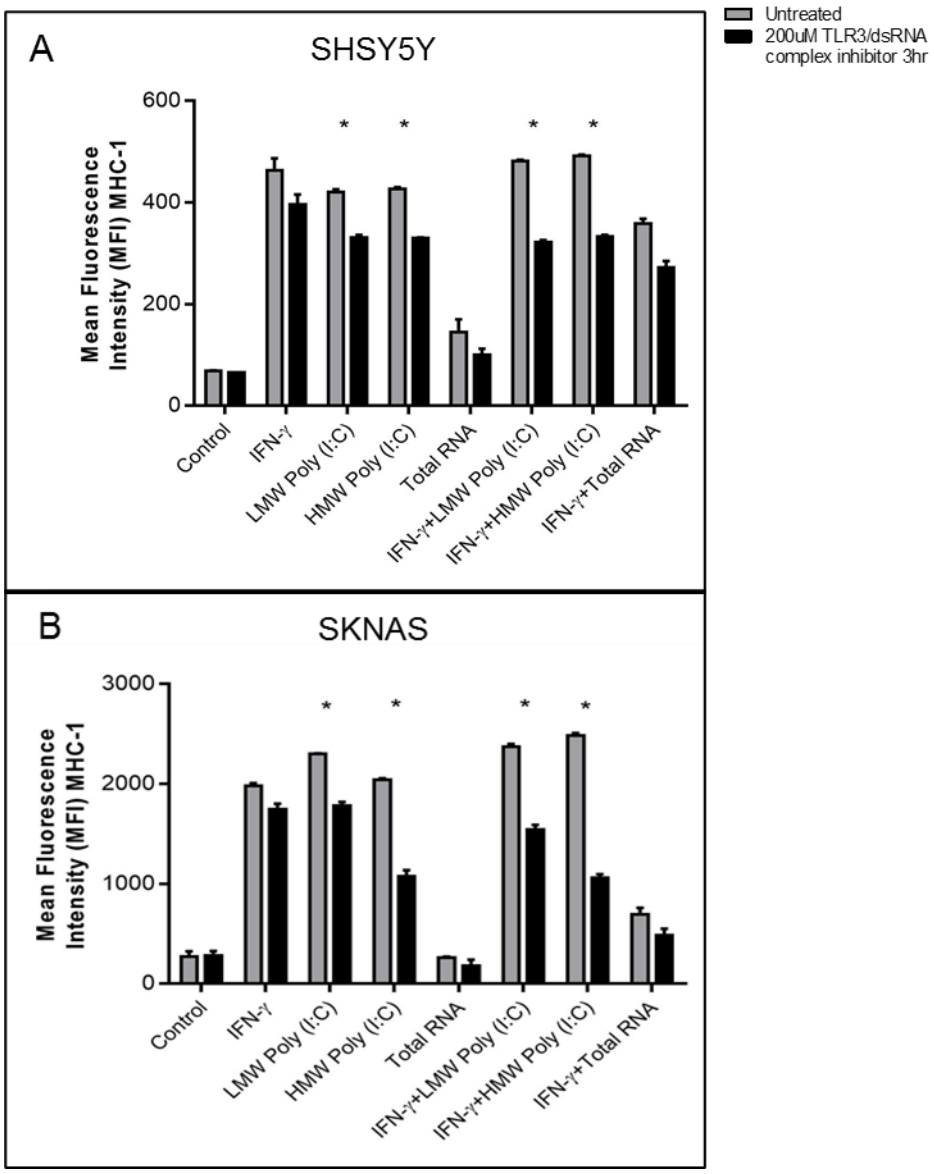

Figure 18. Effect of TLR3/dsRNA complex inhibitor treatment on the expression of MHC I in neuroblastoma cells – 1x10^6 cells/well were incubated with 200μM TLR3/dsRNA complex inhibitor for 3 hours, followed by treatment with IFN-γ (10ng/ml), Poly(I:C)-LMW (10μg/ml), Poly(I:C)-HMW (10μg/ml), IFN-γ (10ng/ml) + Poly(I:C)-LMW (10μg/ml) and IFN-γ (10ng/ml) + Poly(I:C)-HMW (10μg/ml) for 24 hours. **(A)** SHSY5Y **(B)** SKNAS. P values of * $p < 0.05$, ** $p < 0.01$, *** $p < 0.001$, **** $p < 0.0001$ were considered as significant. Values are expressed as mean ± standard error of mean. Data was presented as mean ± SEM of three independent experiments. n.s. = not significant.

4.2.7 Proliferation assay in neuroblastoma cells

SHSY5Y cells were stimulated with IFN-γ, LMW, HMW Poly (I:C), total RNA, IFN-γ in combination with LMW Poly (I:C), HMW Poly (I:C) and total RNA for 24 hours. Incubation with WST-1 proliferation reagent revealed that SHSY5Y cells stimulated with IFN-γ, LMW/HMW Poly (I:C) and total RNA showed no significant increase in proliferation. However, combination of IFN-γ+LMW Poly (I:C) ($p < 0.05$), IFN-γ+HMW Poly (I:C) ($p < 0.05$) and IFN-γ+total RNA ($p < 0.05$, Fig. 19A) increased the proliferation with more than ~7-folds increase when compared with untreated cells.

Similar effects were seen in SKNAS cells; however, the proliferation was observed to be higher in comparison to SHSY5Y cells. There was a □20-fold increase using IFN-γ ($p < 0.01$) or total RNA ($p < 0.01$) in comparison to untreated cells. This effect was even stronger, when treated in combination, IFN-γ+LMW Poly (I:C) ($p < 0.001$), IFN-γ+HMW Poly (I:C) ($p < 0.0001$) and IFN-γ+total RNA ($p < 0.0001$, Fig. 19B).

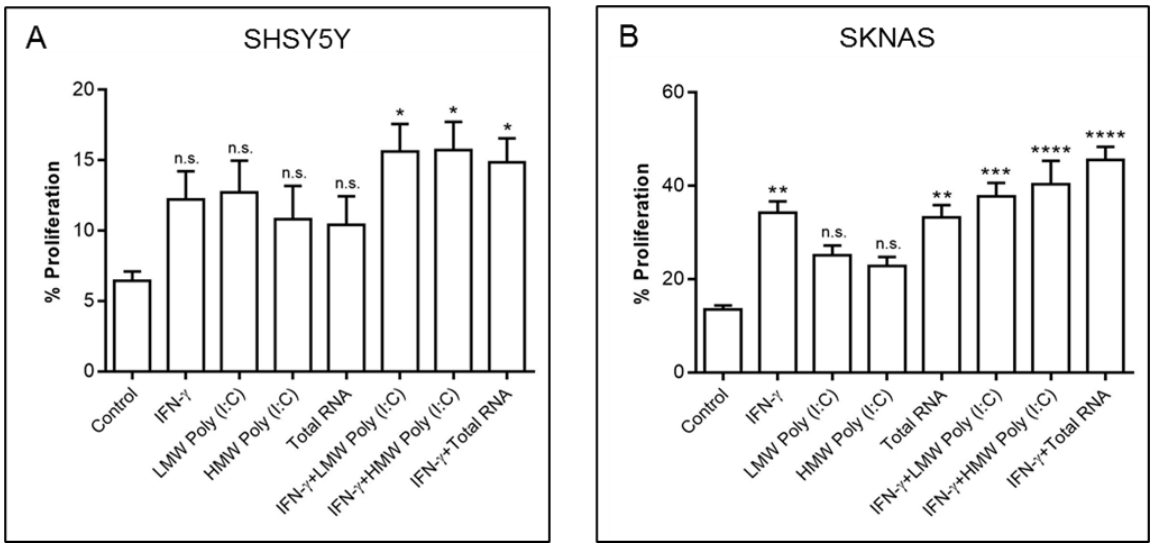

Figure 19. RNA influenced proliferation effects in neuroblastoma cells – $1x10^5$ cells/ml were incubated with IFN-γ (10ng/ml), Poly(I:C)-LMW (10µg/ml), Poly(I:C)-HMW (10µg/ml), Total RNA (10µg/ml), IFN-γ (10ng/ml)+Poly(I:C)-LMW (10µg/ml), IFN-γ (10ng/ml)+Poly(I:C)-HMW (10µg/ml) and IFN-γ (10ng/ml)+Total RNA (10µg/ml) for 24

hours. **(A)** SHSY5Y **(B)** SKNAS proliferation. P values of * $p < 0.05$, ** $p < 0.01$, *** $p < 0.001$, **** $p < 0.0001$ were considered as significant. Each bar represents mean ± SEM of 3 independent experiments performed in duplicate. n.s. = not significant.

4.2.8 Cytotoxicity assay in neuroblastoma cells

The cytotoxic effects of both poly (I:C) and total RNA were analyzed in neuroblastoma cells. Incubation of SHSY5Y cells with aforementioned stimulants showed the cytotoxicity to be decreased by ~10-12 folds when compared to untreated cells. IFN-γ ($p < 0.0001$), LMW Poly (I:C) ($p < 0.001$), HMW Poly (I:C) ($p < 0.0001$) and total RNA ($p < 0.0001$) showed significant decrease in cytotoxicity. Moreover, IFN-γ+LMW Poly(I:C) ($p < 0.001$), IFN-γ+HMW Poly(I:C) ($p < 0.001$) and IFN-γ+total RNA ($p < 0.001$, Fig. 20A) also showed reduced cytotoxicity in comparison to untreated cells.

Similar pattern of reduced cytotoxicity was seen in SKNAS cells with IFN-γ ($p < 0.0001$), LMW Poly (I:C) ($p < 0.0001$), HMW Poly (I:C) ($p < 0.0001$), total RNA ($p < 0.0001$) and combination treatments of IFN-γ+LMW Poly(I:C) ($p < 0.0001$), IFN-γ+HMW Poly(I:C) ($p < 0.0001$) and IFN-γ+total RNA ($p < 0.0001$, Fig. 20B). Slightly higher cytotoxicity was observed in untreated SKNAS cells when compared to SHSY5Y cells; however, upon treatment with stimulants the cytotoxicity is reduced by ~20-folds.

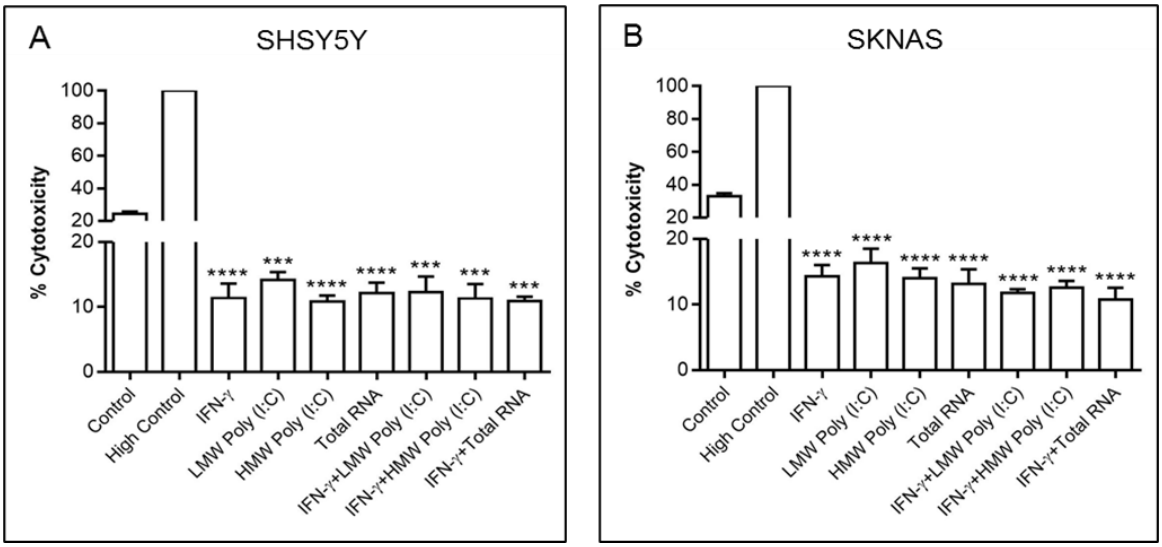

Figure 20. RNA influenced cytotoxic effects in neuroblastoma cells – $1x10^5$ cells/ml were incubated with IFN-γ (10ng/ml), Poly(I:C)-LMW (10µg/ml), Poly(I:C)-HMW (10µg/ml), Total RNA (10µg/ml), IFN-γ (10ng/ml)+Poly(I:C)-LMW (10µg/ml), IFN-γ (10ng/ml)+Poly(I:C)-HMW (10µg/ml) and IFN-γ (10ng/ml)+Total RNA (10µg/ml) for 24 hours. **(A)** SHSY5Y **(B)** SKNAS cytotoxicity. P values of * $p < 0.05$, ** $p < 0.01$, *** $p < 0.001$, **** $p < 0.0001$ were considered as significant. Each bar represents mean ± SEM of 3 independent experiments performed in duplicate. n.s. = not significant.

4.2.9 Cytotoxicity assay post treatment with TLR3/dsRNA complex inhibitor

As shown in earlier experiments TLR-3 expression increases when treated with IFN-γ and IFN-γ in combination with poly (I:C) and total RNA. Moreover, it was also observed that the aforementioned stimulants decrease the cytotoxicity in neuroblastoma cells. In order to determine the effect of TLR-3 on the NK cell induced cytotoxicity on neuroblastoma cells; NB cells were seeded and treated with TLR3/dsRNA complex inhibitor (200µM) for 3 hours, followed by 24 hours incubation with the above-mentioned stimulants. After the incubation, NK cells were added in a ratio of 1:2 and co-cultured for 4 hours.

It was observed that upon NB and NK cell co-culture cytotoxicity was seen; however, upon addition of IFN- γ and other stimulants the cytotoxicity was decreased, especially with the stimulants in combination with IFN-γ. Due to the addition of the TLR-3 inhibitor, the cytotoxicity was increased in comparison to the without inhibitor wells, however not significantly. These results demonstrate the effect of TLR-3 in decreasing the cytotoxicity in neuroblastoma cells. IFN-γ, both Poly(I:C), total RNA and combination treatments ($p > 0.05$, n.s.,21A) all showed an increased in cytotoxicity in treated cells, however not significant.

A similar pattern was observed in SKNAS cells upon inhibition of TLR-3, the cytotoxicity was not increased significantly in IFN-γ, both Poly(I:C), total RNA and combination treatments ($p > 0.05$, n.s.,21B).

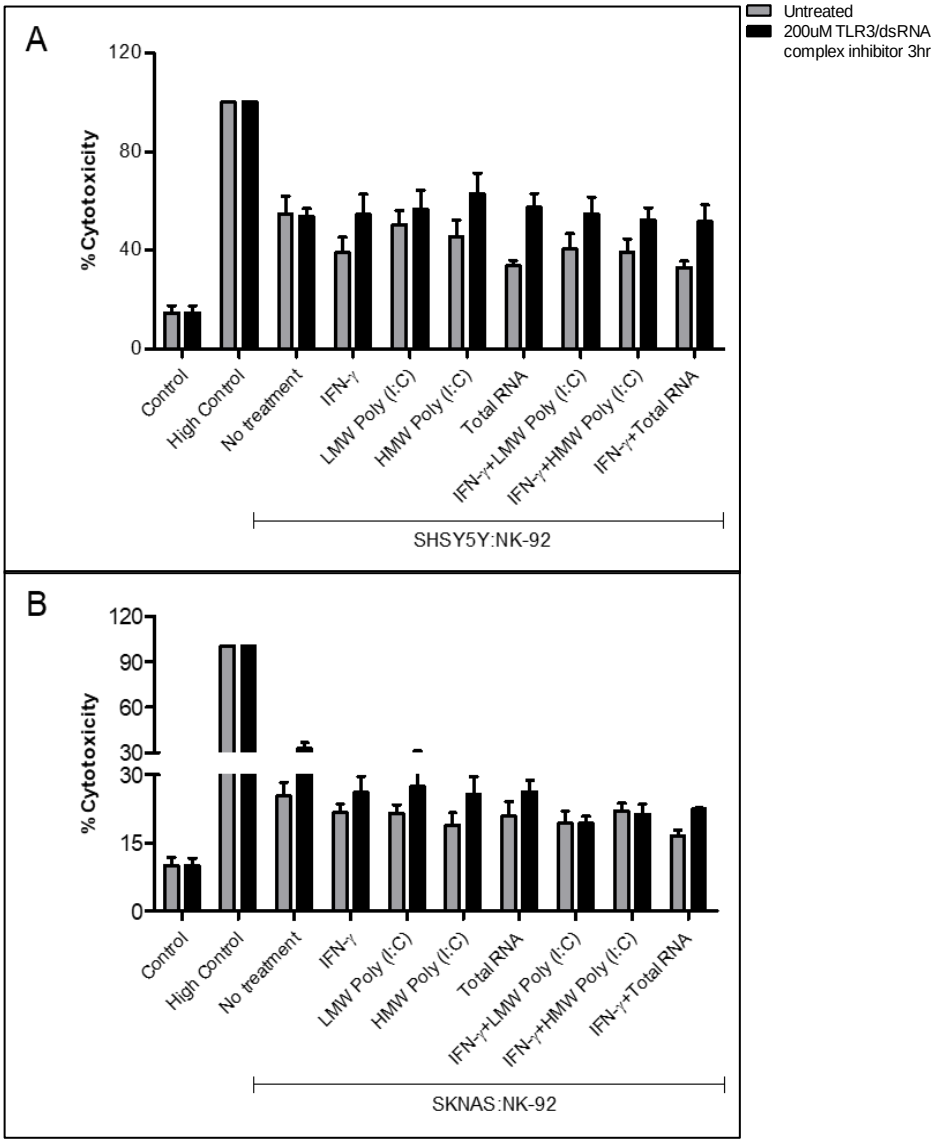

Figure 21. Cytotoxicity assay - effect of RNA on NB:NK co-culture post treatment with TLR3/dsRNA complex inhibitor in neuroblastoma cells – 10,000 NB cells/well were incubated with 200μM TLR3/dsRNA complex inhibitor for 3 hours, followed by treatment with IFN-γ (10ng/ml), Poly(I:C)-LMW (10μg/ml), Poly(I:C)-HMW (10μg/ml), Total RNA (10μg/ml), IFN-γ (10ng/ml) + Poly(I:C)-LMW (10μg/ml), IFN-γ (10ng/ml) + Poly(I:C)-HMW (10μg/ml) and IFN-γ (10ng/ml) + Total RNA (10μg/ml) for 24 hours, followed by addition of 20,000 NK-92 cells/well over NB cells. The cells were co-cultured for 4 hours. **(A)** SHSY5Y and NK-92 co-culture **(B)** SKNAS and NK-92 co-culture. Each bar represents mean ± SEM of 3 independent experiments performed in duplicate. n.s. = not significant.

4.3 Exp. Set 3: Influence of RNA on NK-cell mediated cytotoxicity of neuroblastoma cells

4.3.1 Different effector to target ratios

Inorder to establish the effector to target ratio of neuroblastoma cells and NK-92 cells, different number of neuroblastoma cells were seeded with NK-92 cells and co-cultured for 4 hours. Triton x-100 (2%) was used a high control. The cytotoxicity assay showed the effector to target ratio of 1:2 to be the least cytotoxic in comparison to 1:5 and 1:10 and thus the effect of stimulants could be observed clearly. Therefore, the ratio of 1:2 (10,000 SHSY5Y: 20,000 NK-92 cells) was finalized to be used in forthcoming experiments (Fig. 22A).

SKNAS showed similar pattern of cytotoxicity as SHSY5Y cells, hence same effector: target ratio was decided for it as well (Fig. 22B).

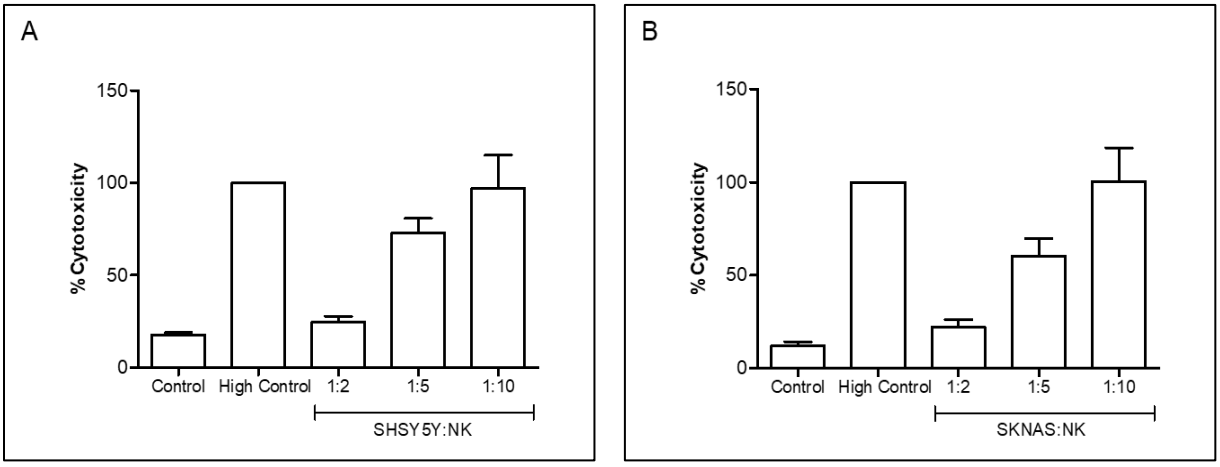

Figure 22. Various effector to target ratios – 10,000 cells/well of neuroblastoma cells were seeded, followed by addition of 20,000, 50,000 and 100,000 cells/well NK-92 cells on top of neuroblastoma cells in (1:2, 1:5 and 1:10) effector to target ratios and co-cultured for 4 hours. **(A)** SHSY5Y and NK-92 co-culture **(B)** SKNAS and NK-92 co-culture. Each bar represents mean ± SEM of 3 independent experiments performed in duplicate.

4.3.2 Cytotoxicity assay post treatment with RNA

To determine the effect of RNA on the co-cultured neuroblastoma cells with NK-92 cells, SHSY5Y cells were seeded and treated with the aforementioned stimulants for 24 hours, followed by addition of NK-92 cells on top of the already treated NB cells. The untreated cells (control) shows cytotoxicity, however upon addition of IFN-γ ($p < 0.0001$), the cytotoxicity is reduced and same is observed by addition of both poly (I:C) ($p < 0.0001$) and total RNA ($p < 0.0001$). The most reduction in cytotoxicity is observed when the aforementioned treatments were given in combination. IFN-γ+LMW ($p < 0.0001$), IFN-γ+HMW ($p < 0.0001$) and IFN-γ+total RNA ($p < 0.0001$, Fig. 23A).

For SKNAS cells, the same results were observed. However, upon treatment with IFN- γ in combination with both poly (I:C) and total RNA decreased the cytotoxicity to the maximum when compare to stimulants alone. IFN-γ ($p < 0.0001$), LMW/HMW Poly (I:C) ($p < 0.0001$), total RNA ($p < 0.0001$), IFN-γ+LMW ($p < 0.0001$), IFN-γ+HMW ($p < 0.0001$) and IFN-γ+total RNA ($p < 0.0001$, Fig. 23B).

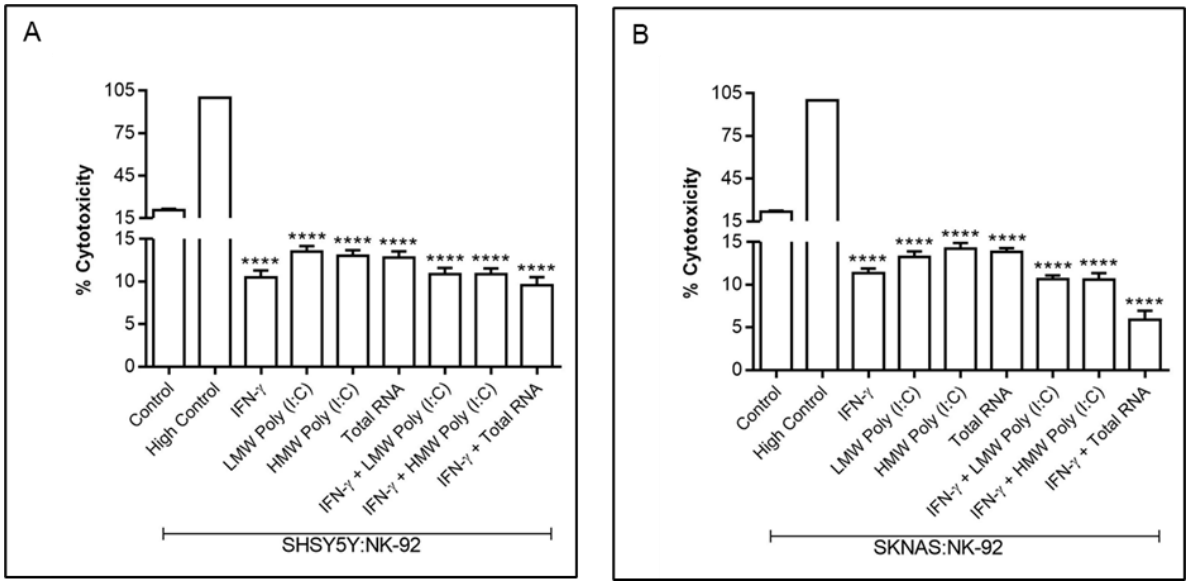

Figure 23. Cytotoxicity assay post treatment with RNA – 10,000 cells/well of neuroblastoma cells were seeded, followed by treatment with IFN-γ (10ng/ml), Poly(I:C)-LMW (10µg/ml), Poly(I:C)-HMW (10µg/ml), Total RNA (10µg/ml), IFN-γ (10ng/ml) + Poly(I:C)-LMW (10µg/ml), IFN-γ (10ng/ml) + Poly(I:C)-HMW (10µg/ml) and IFN-γ

(10ng/ml) + Total RNA (10µg/ml) for 24 hours, followed by addition of 20,000 cells/well NK-92 cells on top of neuroblastoma cells (1:2) effector to target ratio and co-cultured for 4 hours. **(A)** SHSY5Y and NK-92 co-culture **(B)** SKNAS and NK-92 co-culture. P values of * $p < 0.05$, ** $p < 0.01$, *** $p < 0.001$, **** $p < 0.0001$ were considered as significant. Each bar represents mean ± SEM of 3 independent experiments performed in duplicate. n.s. = not significant.

4.3.3 Surface binding to neuroblastoma cells post treatment with OMS - IgG

Children with a so-called opsoclonus-myoclonus syndrome (OMS) have earlier been shown to have surface-binding and functionally active autoantibodies cross-reactive between cerebellar and neuroblastoma antigens. Using flow cytometry (FACS), IgG from patients with paediatric OMS (n=9), NB (n=9) and HC (n=7) were analysed for surface-binding autoantibodies against neuroblastoma cells.

FACS analysis revealed higher IgG surface binding to SHSY5Y and SKNAS cells (expressed as geo mean fluorescence intensity - gMFI) in paediatric OMS compared to healthy controls (HC) and neuroblastoma patients without OMS (NB) patients (SHSY5Y: OMS 23.1 ± 15.0; NB 7.9 ± 3.4; HC 6.3 ± 4.2; OMS vs. NB $p<0.05$, OMS vs. HC $p <0.01$; SKNAS: OMS 18.3 ± 8.1; NB 11.0 ± 3.1; HC 10.8 ± 2.2; OMS vs. NB and OMS vs. HC $p<0.05$ each. Fig. 24A-C). No difference could be found between OMS with (OMS-NB) and without (OMS-no tumor) concomitant neuroblastoma (SHSY5Y: OMS-NB 18.6 ± 8.1 vs. OMS-no tumor 28.7 ± 20.9; SKNAS: OMS-NB 19.0 ± 9.1 vs. OMS-no tumor 17.4 ± 7.9, each n.s.).

Table 4. Clinical and demographic characteristics of patients with paediatric opsoclonus-myoclonus-syndrome (OMS)

Patient	Age [Month] / sex	Diagnosis	Tumor stage
1	24 /f	OMS-NB	III
2	18 / f	OMS-NB	I
3	18 / f	OMS-NB	III
4	23 / m	OMS-NB	I
5	28 / m	OMS-NB	II
6	24 / f	OMS	no tumor
7	44 / m	OMS	no tumor
8	36 / m	OMS	no tumor
9	40 / f	OMS	no tumor

A

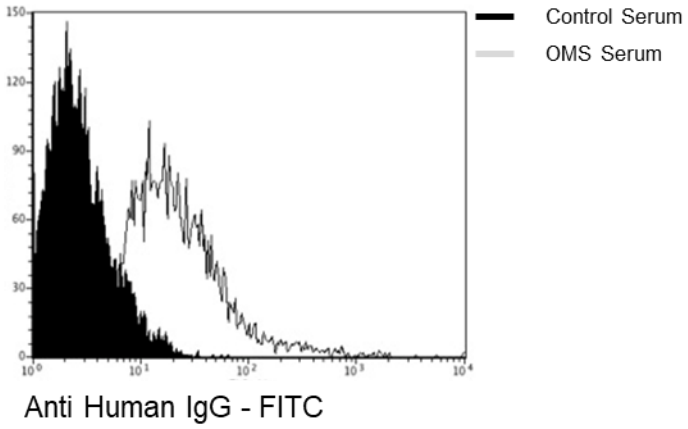

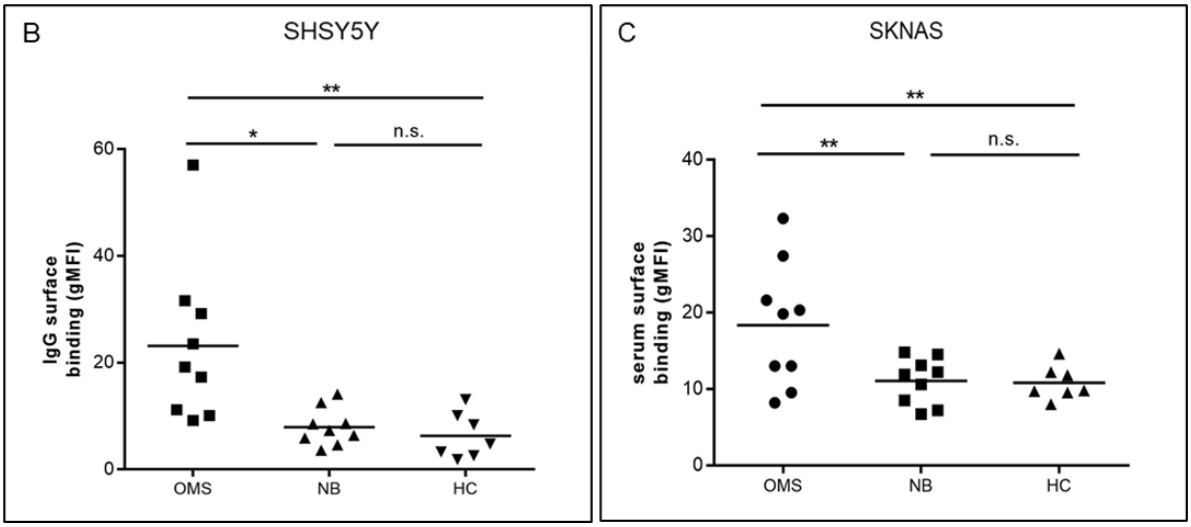

Figure 24. Surface binding of sera from patients with opsoclonus-myoclonus syndrome (OMS), neuroblastoma (NB) or healthy controls (HC) to the neuroblastoma cell lines (B) SHSY5Y and (C) SKNAS – (A): shows a typical binding of a control serum (filled graph) and an OMS serum (line graph) to SHSY5Y neuroblastoma cells. B, C: OMS showed significantly higher binding to both cell lines, compared to neuroblastoma patients without OMS (NB) and healthy controls (HC) ($p < 0.05$ each and $p < 0.01$ for OMS vs. HC in SHSY5Y). P values of * $p < 0.05$, ** $p < 0.01$, *** $p < 0.001$, **** $p < 0.0001$ were considered as significant. n.s. = not significant.

4.3.4 Cytotoxicity of NK-92 cells to neuroblastoma cells post treatment with OMS - IgG

In a first set of experiments, we co-cultured the neuroblastoma cell line SKNAS with the natural killer cell line NK-92 in the presence or absence of OMS-, NB-, or HC-IgG. The incubation with OMS- or control IgG alone (without NK cells) already increased the SKNAS cytotoxicity, compared to controls (OMS 33.6 ± 9.6%; NB 18.4 ± 13.0%; HC 16.8 ± 8.5%, OMS vs NB and OMS vs. HC p each <0.05, Two-way ANOVA with Tukey´s multiple comparison test, Fig. 25). However, when co-cultured with NK-92 cells, cytotoxicity in the HC and the NB group increased only slightly, whereas in the presence

of OMS-IgG, the antibody dependent NK-cell mediated cytotoxicity increased significantly (OMS 57.3 ± 13.1%; NB 23.6 ± 16.1%; HC 21.1 ± 6.8%, OMS vs NB and OMS vs. HC p each <0.01, Two-way ANOVA with Tukey´s multiple comparison test, Fig. 25).

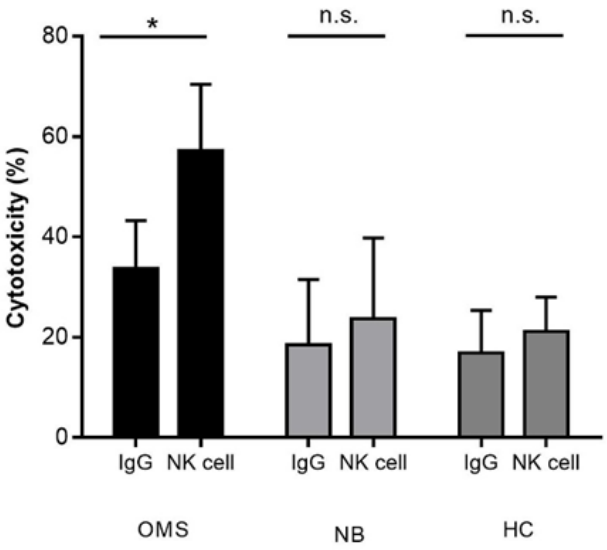

Figure 25. Incubation of the neuroblastoma cell line SKNAS with IgG from OMS, NB, or HC with or without NK-92 cells – OMS-IgG induced significantly higher cytotoxicity than NB- or HC-IgG (p each < 0.05). However, co-cultivation of IgG and NK-92 cells with the neuroblastoma cells led to a significant increase of cytotoxicity in the OMS group (p < 0.05), but only a slight increase in the other groups (n.s.). P values of * p < 0.05, ** p < 0.01, *** p < 0.001, **** p < 0.0001 were considered as significant. n.s. = not significant.

4.3.5 Cytotoxicity to human isolated NK cells post treatment with OMS - IgG

Since reactivity of immune cell lines, such as NK-92 may not always represent real NK cell reactivity, we used freshly human isolated NK cells in a co-culture experiment with both NB cell lines (SKNAS and SHSY5Y). Preincubation with OMS-IgG, but not NB- or HC-IgG induced a significant NK cell-mediated cytotoxicity of both NB cell lines (SHSY5Y:

OMS 52.5±15.2%; NB 22.3±17.0%; HC 31.1±7.8%, OMS vs NB $p<0.01$, OMS vs HC $p<0.01$, Fig. 26A SKNAS: OMS 42.4±15.1%; NB 19.9±10.2%; HC 18.2±5.9%, OMS vs NB $p<0.01$, OMS vs HC $p<0.01$, Fig. 26B). There was no correlation between the absolute level of surface binding of OMS IgG to the NB cells and their ability to induce ADCC (SHSY5Y: $r^2 = 0.026$, n.s. SKNAS: $r^2 = 0.24$, n.s. No significant difference was seen between NB-associated OMS and OMS without tumor (SHSY5Y: OMS-NB 37.6 ± 10.5 vs. OMS-no tumor 28.5 ± 6.1, n.s. ; SKNAS: OMS-NB 53.0 ± 13.4 vs. OMS-no tumor 62.4 ± 12.4, n.s.)

Moreover, we preincubated the neuroblastoma cell line SHSY5Y with OMS-IgG from 2 patients in the presence or absence of RNA (LMW poly (I:C), HMW poly (I:C) and total human RNA). Preincubation of the NB cells with OMS IgG and LMW poly (I:C) or total RNA did not reduce the OMS-antibody mediated cytotoxicity, whereas HMW poly (I:C) showed a marked reduction (OMS-IgG 65.6 ± 2.6%, HC IgG 29.8 ± 1.7%, OMS-IgG/LMW poly (I:C) 58.3 ± 4.3%, OMS-IgG/HMW poly (I:C) 47.1 ± 12.7%, OMS-IgG/total RNA 56.4 ± 8.0%, statistical analysis not done because of the small number of samples, Fig. 26C).

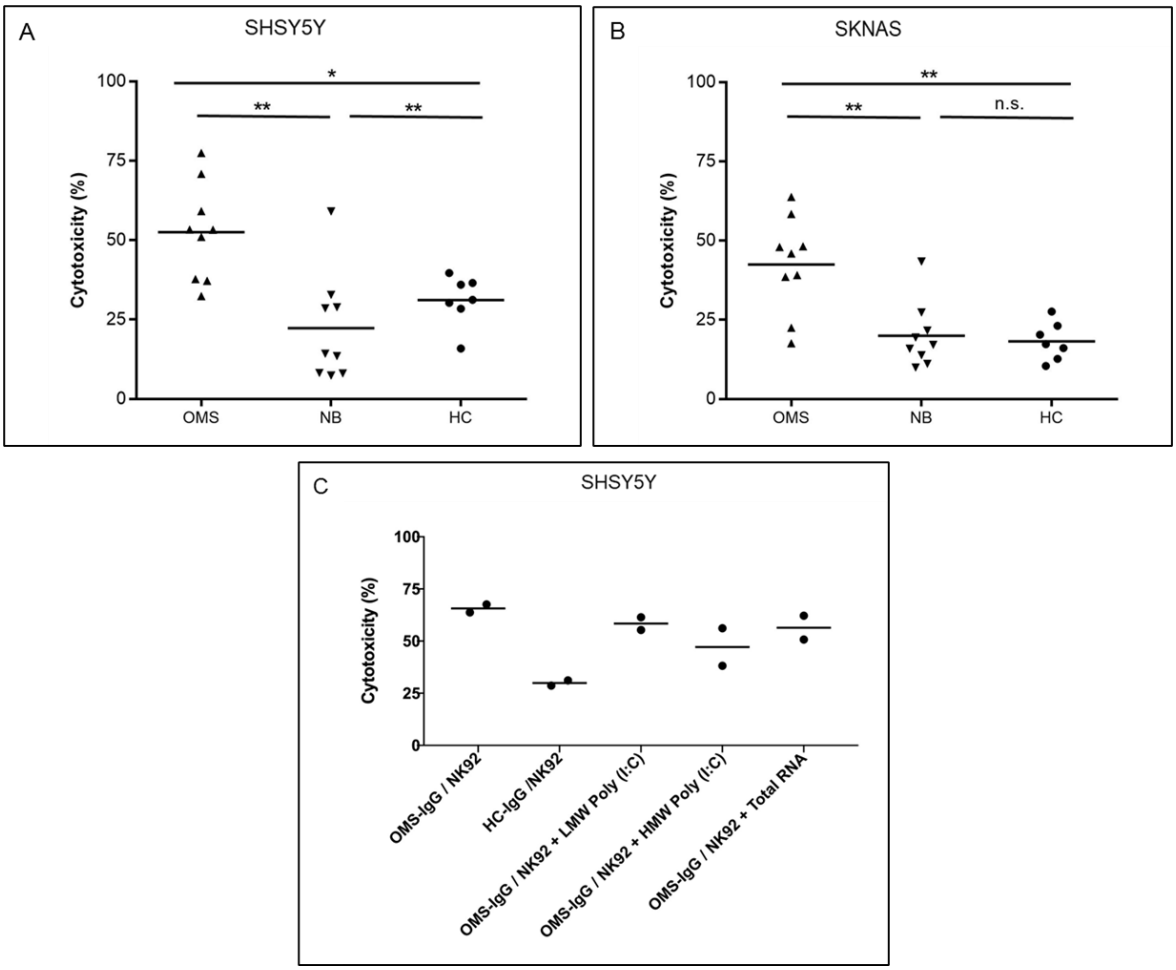

Figure 26. Incubation of the neuroblastoma cell lines (A) SHSY5Y and (B) SKNAS with IgG from OMS, NB, or HC and human isolated NK cells – Human isolated NK-cells together with IgG from OMS patients induced significant cytotoxicity to both neuroblastoma cell lines, compared to the neuroblastoma group (NB) and the healthy control group HC) ($p < 0.01$ for all, except OMS vs. HC in SKNAS with $p < 0.05$). P values of * $p < 0.05$, ** $p < 0.01$, *** $p < 0.001$, **** $p < 0.0001$ were considered as significant. n.s. = not significant. **Cytotoxicity of neuroblastoma cells (C) SHSY5Y**, when incubated with NK92 and IgG from OMS patients and healthy controls (HC) in the absence or presence of RNA (LMW poly (I:C), HMW poly (I:C) and total human RNA). HMW poly (I:C), but not LMW poly (I:C) or total RNA reduces the cytotoxic OMS antibody-mediated effect of the NK cells markedly (statistical analysis not done because of the small number of samples).

4.4 Exp. Set 4: Effect of RNA on differentiated fetal neurons

4.4.1 Influence of RNA on differentiated fetal neurons via flow cytometry

To elucidate, whether RNA has an effect on the neural stem cells from postnatal mice brain region - sub-ventricular zone, the SVZ was isolated and differentiated in differentiation medium. The cells were seeded and treated with both poly (I:C) and total RNA of varying concentrations (1, 10 and 25µg/ml) for 24 hours, followed by flow cytometric analysis for MHC I and TLR-3.

The treatment with LMW poly (I:C) ($p < 0.001$), HMW poly (I:C) ($p < 0.001$) and different concentrations of total RNA showed a significant increase in MHC I expression. Total RNA (1µg/ml) ($p < 0.001$), total RNA (10µg/ml) ($p < 0.001$) and total RNA (25µg/ml) ($p < 0.001$, Fig. 27A). Furthermore, treatment with both LMW Poly (I:C) ($p < 0.001$) and HMW Poly (I:C) ($p < 0.001$) increased the TLR-3 expression, along with increasing concentrations of total RNA, 1µg/ml ($p < 0.001$), total RNA (10µg/ml) ($p < 0.001$) and total RNA (25µg/ml) ($p < 0.001$, Fig. 27B).

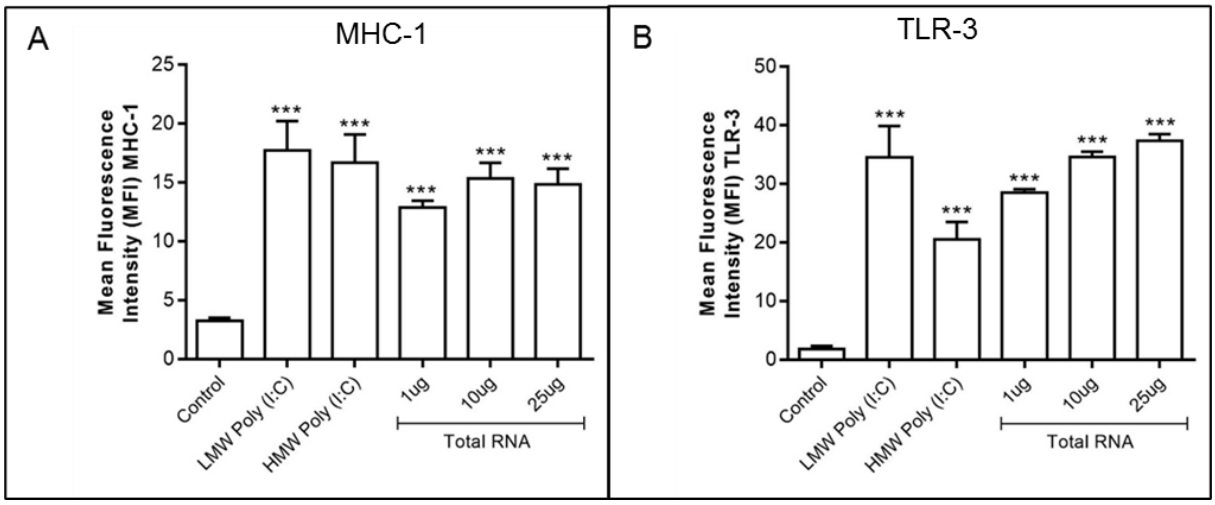

Figure 27. Flow cytometry of MHC I and TLR-3 on differentiated fetal neurons – 100,000 cells/well were incubated with Poly(I:C)-LMW (10µg/ml), Poly(I:C)-HMW (10µg/ml), Total RNA (1µg/ml), Total RNA (10µg/ml) and Total RNA (25µg/ml) for 24 hours. **(A)** MHC I **(B)** TLR-3 expression. Data was analyzed on S3 Cell Sorter, Bio-Rad

Laboratories, CA, USA using ProSort™ software. P values of * $p < 0.05$, ** $p < 0.01$, *** $p < 0.001$, **** $p < 0.0001$ were considered as significant. Each bar represents mean ± SEM of 3 independent experiments. n.s. = not significant.

4.4.2 Proliferation assay

To investigate the effect of Poly (I:C) and RNA on proliferation of fetal neurospheres, SVZ was isolated and cultivated as mentioned in 3.2.3.2 and 3.2.3.3 respectively. The cells were seeded and treated with LMW and HMW poly (I:C) and total RNA for 24 hours. Upon treatment, the proliferation was increased as compared to control. Both LMW poly (I:C) ($p < 0.05$) and HMW poly (I:C) ($p < 0.001$) showed increased proliferation and varying concentrations of total RNA increased proliferation proportionally. Total RNA (1µg/ml) ($p < 0.01$), Total RNA (10µg/ml) ($p < 0.0001$) and Total RNA (25µg/ml) ($p < 0.0001$, Fig. 28).

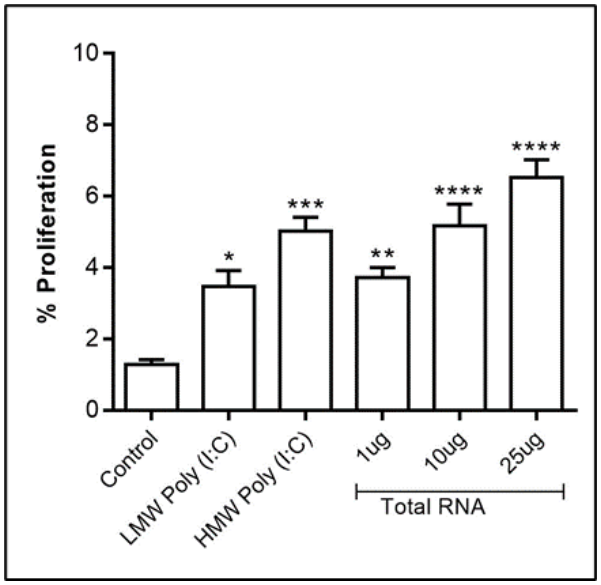

Figure 28. RNA influenced proliferation effects in fetal neurospheres of SVZ region – 50,000 cells/well were incubated with Poly(I:C)-LMW (10µg/ml), Poly(I:C)-HMW (10µg/ml), Total RNA (1µg/ml), Total RNA (10µg/ml) and Total RNA (25µg/ml) for 24 hours. P values of * $p < 0.05$, ** $p < 0.01$, *** $p < 0.001$, **** $p < 0.0001$ were considered as significant. Each bar represents mean ± SEM of 3 independent experiments. n.s. = not significant.

4.4.3 Cytotoxicity assay

The same procedure of isolation, cultivation and treatment as proliferation assay was utilized for determining the cytotoxic effect of the aforementioned stimulants on fetal neurospheres. The assay used was Lactate Dehydrogenase (LDH) release assay.

After 24 hours of treatments, the cytotoxicity of LMW ($p < 0.05$) and HMW poly (I:C) ($p < 0.0001$) treated wells was decreased and different concentrations of total RNA showed less cytotoxicity as the concentration used was increased. For example, the cytotoxicity was further decreased for 25µg/ml total RNA ($p < 0.0001$) than for 10µg/ml ($p < 0.0001$) and 1µg/ml ($p < 0.01$, Fig. 29).

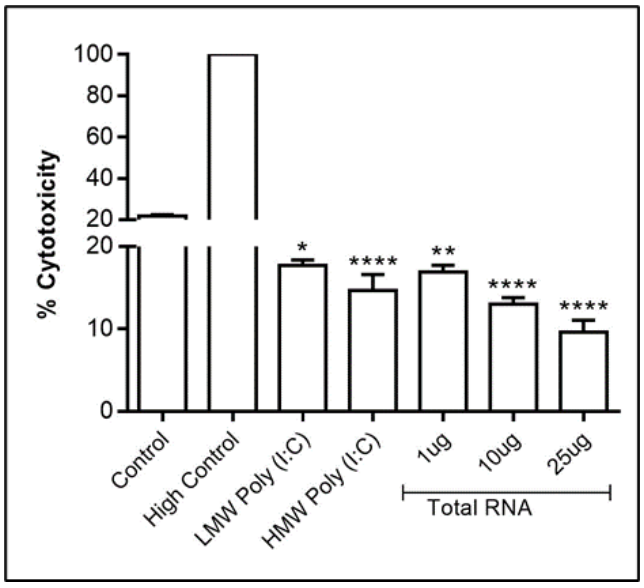

Figure 29. RNA influenced potential cytotoxic effects in fetal neurospheres of SVZ region – 50,000 cells/well were incubated with Poly(I:C)-LMW (10µg/ml), Poly(I:C)-HMW (10µg/ml), Total RNA (1µg/ml), Total RNA (10µg/ml) and Total RNA (25µg/ml) for 24 hours. Triton x-100 was used as high control. P values of * $p < 0.05$, ** $p < 0.01$, *** $p < 0.001$, **** $p < 0.0001$ were considered as significant. Each bar represents mean ± SEM of 3 independent experiments. n.s. = not significant.

4.4.4 Multi-electrode array (MEA) measurements of enteric neurospheres from postnatal murine gut

Our earlier findings suggest that RNA and both poly (I:C) have an effect on differentiated fetal neurons of murine SVZ, with increased MHC I and TLR-3 after 24 hour treatment with the said stimulants. Additionally, there was an increase and decrease in proliferation and cytotoxicity respectively post treatments. Hence, the aim further was to determine, whether RNA has an effect on differentiated enteric neurospheres from postnatal mouse gut. For this purpose, the isolation and cultivation of MP from postnatal mice gut was performed as mentioned in 3.2.3.2 and 3.2.3.3 respectively.

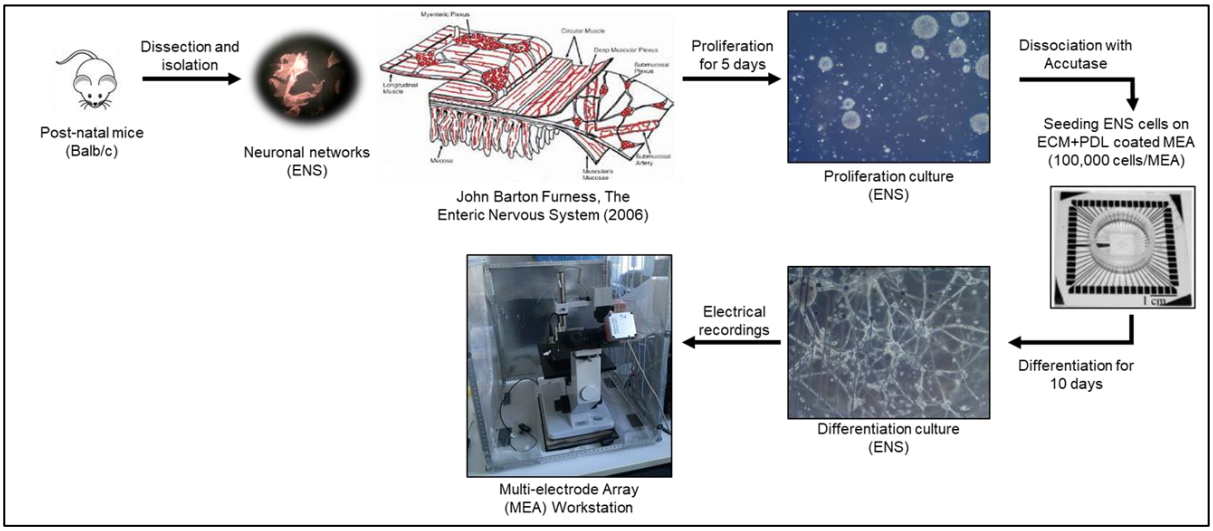

Figure 30. Workflow – Isolation and cultivation – post-natal Balb/c mice were used for dissection and isolation of myenteric plexus, followed by proliferation for 5 days, dissociation with accutase. 100,000 cells/MEA were seeded on ECM/PDL coated MEAs and differentiated for 10 days. Electrophysiological recordings were taken after addition of respective compound to be measured.

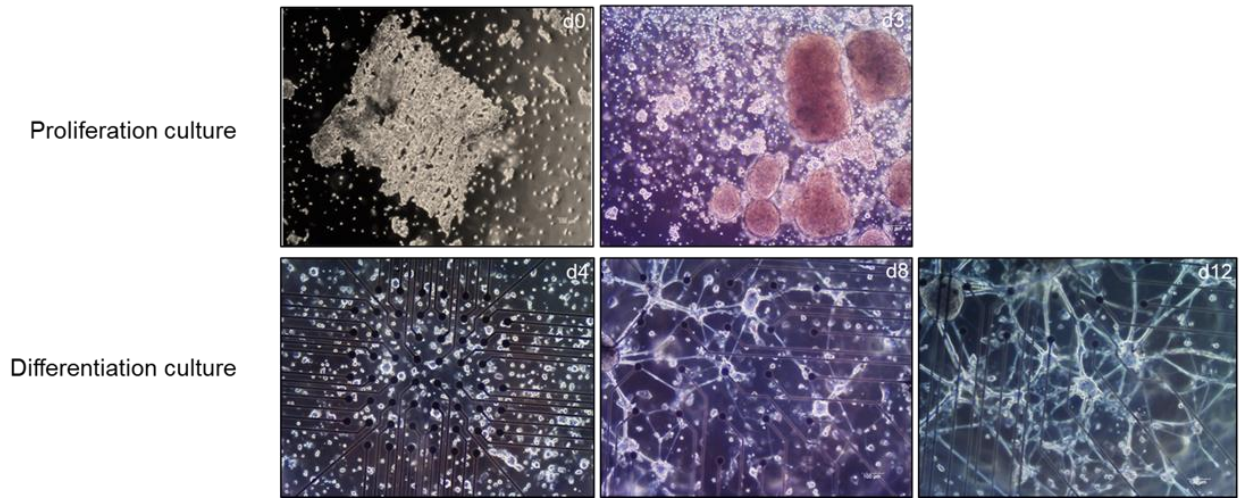

Figure 31. Proliferation and Differentiation of ENS culture (MP) – The isolated myenteric plexus was cultured in proliferation medium for 5 days, followed by differentiation on ECM/PDL coated MEAs for 10-12 days in differentiation medium.

In order to record the effect of RNA on the activity of enteric neurons, measurements were taken. The electrophysiological signals were recorded before and after applying the compound of interest on the neuronal network on the MEA.

The amplitude was measured after application of compound of interest. LMW poly (I:C) showed an increase in amplitude with increasing concentrations proportionally, 50µg/ml LMW ($p < 0.05$) and 100µg/ml LMW ($p < 0.01$). Whereas 10µg/ml ($p > 0.05$, n.s.) and 25µg/ml LMW ($p > 0.05$, n.s., Fig. 32A) showed no significant effect. For HMW Poly (I:C), an increase was observed with increasing concentration of HMW Poly (I:C). 10µg/ml ($p < 0.05$), 25µg/ml HMW ($p < 0.05$), 50µg/ml HMW ($p < 0.01$) and 100µg/ml HMW ($p < 0.0001$, Fig. 32B). Likewise, total RNA showed a significant increase in amplitude after addition to the enteric neurons on the MEA. 1µg/ml ($p < 0.01$), 10µg/ml total RNA ($p < 0.01$), 25µg/ml total RNA ($p < 0.001$) and 50µg/ml total RNA ($p < 0.001$, Fig. 32C), signifying that both poly (I:C) and total RNA have an effect on the activity of enteric neurons, as suggested by increase in amplitude.

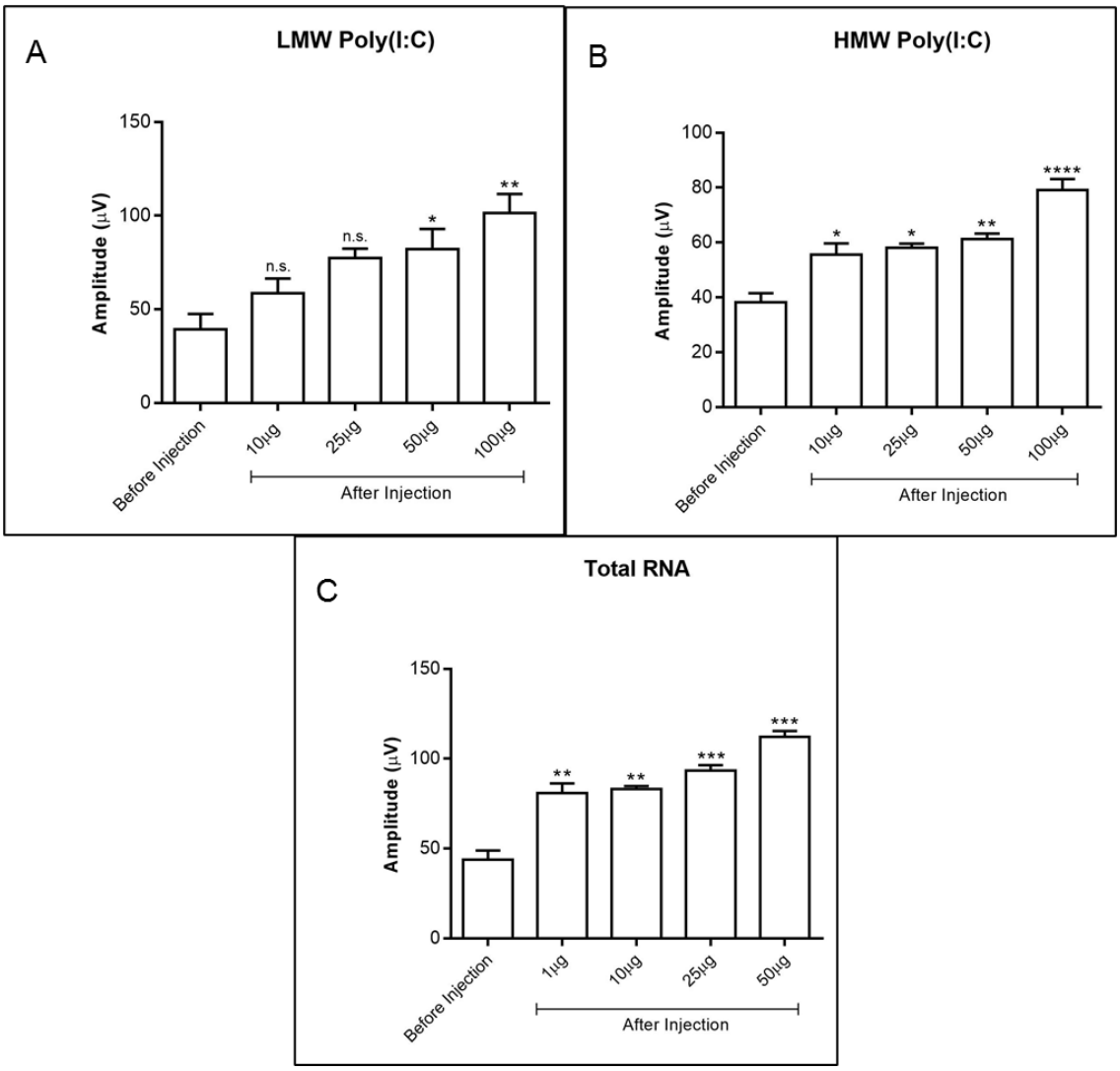

Figure 32. RNA induced electrophysiological activity of enteric neurospheres from postnatal murine gut – 100,000 cells/MEA were measured before and after addition of **(A)** Poly(I:C)-LMW (10, 25, 50 and 100μg/ml), **(B)** Poly(I:C)-HMW (10, 25, 50 and 100μg/ml) and **(C)** Total RNA (1, 10, 25 and 50μg/ml). P values of * $p < 0.05$, ** $p < 0.01$, *** $p < 0.001$, **** $p < 0.0001$ were considered as significant. Each bar represents mean ± SEM of 3 independent experiments. n.s. = not significant.

5. DISCUSSION

Neuroblastoma (NB), is the most common extracranial solid childhood tumor derived from primitive neural crest cells in the sympathetic nervous system. In this thesis, I have studied the interaction between tumor cells/neuroblastoma and immune system and the role of exRNA on the susceptibility of neuroblastoma cells to immune cell killing by NK cells. Furthermore, this study provides an approach to pursue the idea that immune reaction in NB-associated OMS can contribute to an anti-tumor immune response in neuroblastoma associated OMS and the pathogenic role of surface binding antibodies in OMS.

5.1. Effects of RNA on neuroblastoma cells

Neuroblastoma (NB) is a pediatric solid tumor characterized by its wide range of clinical manifestations and poor outcome for those with high-risk clinical phenotypes, despite significant advance in the treatment in the last 10 years (Maris et al., 2007 and Haupt et al., 1979). Antibody-based immunotherapy of neuroblastoma has greatly improved the prognosis of the affected children during the last 20 years (Yu et al., 2010). It has become the limelight for the treatment of children with aggressive and high-risk NB to improve survival and reducing relapse rate (Yu et al., 2010 and Seeger, 2011). A new therapeutic approach is nevertheless warranted in patients whose disease cannot be cured by further increasing the intensity of conventional chemotherapy (Boes et al., 2015). Innate immune cells such as monocytes/macrophages and neutrophils can create an inflammatory environment in neuroblastoma tumors, which affects tumor progression and metastasis (Borriello, 2016). We chose to focus on IFN-γ and the TLR3 ligand poly(I:C) as stimuli to influence TLR-3 expression because they mimic processes relevant for neuroblastoma immune biology: local inflammation in the case of IFN-γ and total RNA and systemic viral infection in the case of poly(I:C).

Toll-like receptors (TLRs) are initiators of the innate immune response to pathogens. One of the TLR family members - TLR3 has been confirmed to be differentially expressed in NB and predict a favorable prognosis with a high expression in tumor tissues and NB patients (Chuang et al., 2011 and Hsu et al., 2013). TLR3, which is localized in endosomes or on cell surfaces in conventional dendritic cells, serves as a sensor of viral infection to recognize double stranded RNA and triggers antiviral signal transduction in innate immunity (Sen et al., 2005). TLR3 agonist polyinosinic-polycytidylic acid [poly(I:C)] could induce apoptosis in TLR3 expressing NB cells, preferentially through mitochondrial pathway (Chuang et al., 2012). It has been used as a cancer vaccine adjuvant in several types of cancers, such as prostate cancer, lymphoma, lung cancer, melanoma, and hepatocellular carcinoma (Matsumoto et al., 2008 and Ammi et al., 2015).

In our study, the neuroblastoma cells do not express TLR-3. However, after stimulation with LMW/HMW Poly (I:C) and total RNA for 24 hours, both neuroblastoma cell lines expressed TLR-3 on gene and protein level, whereas non-neuronal HEK293 cells showed no TLR-3 stimulation. TLR3 plays an important role in the innate responses to viral infections, as it recognizes double stranded dsRNA, a common intermediate of viral replication (Alexopoulou et al., 2001). In response to dsRNA, TLR3 is activated, initiating the expression of antiviral genes, including type I and type III IFNs (Zhou et al., 2013). Because of the importance of TLR3 in host innate immune responses to viral infections, great attention is now given to the use of effective TLR3 ligands for the treatment of viral diseases, including HCV and HIV (Kanzler et al., 2007). Additionally, we observed that HMW-poly I:C is more efficient in activating TLR3 than LMW-poly (I:C) in terms of IFN induction. Addition of IFN-γ along with LMW and HMW Poly (I:C) showed higher expression of TLR-3 in comparison to poly (I:C) alone. Although the mechanisms for the effectiveness of poly (I:C) on TLR3 remains to be determined, it is likely that the activation efficiency of poly (I:C) could be influenced by the size of its molecule and duplex structure that contributes to the binding affinity of poly (I:C) to TLR3 (Zhou et al., 2013). In addition to neuroblastoma, several other tumors have occurrence of free RNA. For example, in breast cancer, measurement of serum metastasin mRNA has been proposed as a screening tool, predicting poor survival and distant metastases (El-Abd et al., 2008). In

lung cancer, serum hTERT mRNA together with EGFR mRNA was proposed as a good biomarker for diagnosis and clinical stage assessment (Miura et al., 2006). In prostate cancer, serum PCA3 mRNA detection (Neves et al., 2008), HIF-1alpha mRNA quantitative RT-PCR (Pipinikas et al., 2008), and serum E2F3 mRNA measurement (Pipinikas et al., 2007), are proposed for the diagnosis of the disease. In thyroid cancer, peripheral thyrotropin hormone receptor (TSHR) mRNA has been proposed for cancer detection in patients with thyroid nodules (Chinnappa et al., 2004).

Since MHC class I expression is a prerequisite for a cytotoxic anti-tumor T-cell response, we next inquired if MHC class I could be influenced by TLR3 or IFN-γ receptor triggering. Neuroblastoma typically presents with extremely low levels of MHC class 1 (MHC I), especially in stage 4 patients (Wolfl et al., 2005), preventing recognition and lysis of neuroblastoma cells by cytotoxic T lymphocytes (CTL) (Spel et al., 2018). The level of MHC I in neuroblastoma cells was observed to be low. In our study, IFN-γ, LMW/HMW poly (I:C) and total RNA increased the expression both on RNA and protein level. Interestingly, IFN-γ potentiates the effect of poly (I:C) and total RNA on MHC I expression. Among the cytokines, IFN-γ appears to be of particular interest due to its ability to upregulate surface expression of HLA class I molecules in human NB cells (Lampson et al., 1983, Ponzoni et al., 1993 and Corrias et al., 2001) and to activate cytotoxic T lymphocyte-mediated anti-tumor responses in a murine model (Watanabe et al., 1989). IFN-γ is a member of the IFN family of multifunctional cytokines with immune modulatory, antiproliferative, differentiation-promoting, and proapoptotic effects (Stark et al., 1998, Platanias et al., 1999 and Boehm et al., 1997). Various studies have indicated the potential usefulness of IFN-γ in the treatment of cancer, including neuroblastoma; however, these studies were performed under a single or few experimental conditions (Tekautz et al., 2006). Furthermore, although it has been established that IFN-γ influences the expression of numerous genes (Stark et al., 1998 and Platanias et al., 1999) many of which inhibition of cell growth and/or stimulation of cell differentiation, the effects of IFN-γ on gene expression in NB have not been characterized in detail (Boehm et al., 1997). Several tumors have shown effect of poly (I:C), the tumor antigen, Muc1, with poly (I:C) successfully produce potent protective effects, which polarize immune

responses towards Th1, and elicit antitumor immunity to inhibit the progression of pituitary tumors. Muc1 + poly (I:C) stimulated the expression of costimulatory molecules and promoted the secretion of inflammatory cytokines, IL-6, TNF-α, I L-1β, by human PBMC-derived DCs. Therefore, it may offer potential as a useful strategy for the treatment of malignant pituitary tumors (Sui et al., 2016). It is known that poly (I:C) increases the expression of cytokines and adhesion molecules on endothelial cells (EC) illustrating its proinflammatory nature and its application in vivo also influences body temperature, locomotor activity, and blood pressure. It was found that poly (I:C) increased circulating D-dimer levels indicating that both coagulation and fibrinolysis were stimulated. Fibrin deposition in kidney and liver was also elevated, again confirming the endogenous activation of coagulation. Moreover, poly (I:C) also induced endothelial tissue factor (TF) and repressed thrombomodulin (TM) expression in vivo thereby causing endothelial dysfunction (Shibamiya et al., 2009). However, some studies have presented the limitations of poly (I:C) by showing that upon stimulation of human monocytes and bone marrow derived macrophages (BMDM) with eRNA, no changes in macrophage Stat1 expression were found suggesting that self-eRNA may not be engaged in TLR-2 or TLR-4 signaling. Likewise, no alterations in the mRNA expression of the cytokine studied (TNF-α) were observed after poly (I:C) treatment, indicating that TLR-3 did not contribute to eRNA-mediated cytokine induction either (Cabrera-Fuentes et al., 2015).

Interfering with protein-protein interactions or protein-nucleic acid interactions have been regarded as daunting goals in drug discovery (Boger et al., 2003). Several studies have been made in the past decade developing small molecule agents to target protein-protein interactions. However, regulation of protein-RNA interactions lags behind, arguably because RNA molecules pose a particular challenge with their high flexibility (Jinek et al., 2009). RNA-binding proteins (RBPs) play important roles in post-transcriptional modifications, which, along with transcriptional regulation, is a key method of controlling gene expression during development. We used TLR3/dsRNA complex inhibitor to disrupt the dsRNA binding to TLR3 in neuroblastoma cells, resulting in decrease in MHC I expression, which otherwise increases upon stimulation with LMW/HMW poly (I:C) and in combination with IFN-γ. This observation supports our hypothesis that TLR3 inhibition

via theTLR3/dsRNA inhibitor leads to decrease in MHC I expression in neuroblastoma cells. Moreover, in our study, the proliferation of neuroblastoma cells was observed to increase when treated with IFN-γ in combination with LMW, HMW poly(I:C) and total RNA and likewise cytotoxicity decreased with the same stimulants. Diverse combination therapy targeting multiple pathways has been used for cancer treatment (Park et al., 2012). Combined with anti-cancer drugs, poly (I:C) has been used for treatment of various cancers including colon, breast, and ovary (Lacour et al., 1992, Laplanche et al., 2000 and Adams et al., 2005). In contrast, a few studies claimed that TLR3 is involved in promoting cell proliferation (Pries et al., 2008, Chin et al., 2006, Mao et al., 2004, Hopper et al., 2004 and Park et al., 2010). These findings indicate that TLR3 exhibits a dual effect on cell proliferation, which may be cell type specific (Jiang et al., 2008 and Hasan et al., 2005). Modulation of TLR3 pathways offers an attractive strategy to fight a variety of diseases. Moreover, in a study, it was found that while single knockdown of either MDA5 or RIG-I alone fails to suppress poly (I:C)-induced NB cell death, concomitant knockdown of MDA5 and TLR3 was effective to rescue poly (I:C)-induced NB cell death. These lines of evidence strongly support the potential role of targeting innate immune system in the treatment of NB. It was further found that siTLR3 could rescue NB cells from poly (I:C) induced cell death and that this rescue effect of siTLR3 could be improved by additional suppression of MDA5 (Hsu et al., 2015). In contrast, another study showed that a type I IFN response by primary human glioblastoma cells was generated by Poly (I:C), which plays an important role in antitumor immunity (Parker et al., 2016), but also the release of other cytokines was modulated. The data shows that poly (I:C) induces the release of both IFN-a and IFN-b by primary glioblastoma cells and upon addition of chloroquine, a TLR3 inhibitor (Kuznik et al., 2011), the poly (I:C)-mediated upregulation of membrane PD-L1 and PD-L2 was drastically reduced (De-Waele et al., 2017). These results are similar to our findings with NB cells, upon stimulation with poly (I:C), NB cells express TLR-3 and MHC I and addition of TLR-3 inhibitor decreases MHC I expression significantly.

5.2. Effects of RNA on tumor cell - NK cell interaction

About 1-2% of the neuroblastoma patients develop a so-called paraneoplastic syndrome, the opsoclonus-myoclonus syndrome. Vice versa, around 50% of the OMS children have an associated neuroblastoma. An autoimmune etiology of the disorder has been postulated, and autoantibodies binding to surface-structures are found in a majority of OMS patients both with and without neuroblastoma (Blaes et al., 2005 and Korfei et al., 2005). Additionally, a predominant B-cell response associated with disease activity has been reported in the cerebrospinal fluid of OMS children, supporting the pathogenic relevance of B-cells and autoantibodies (Pranzatelli et al., 2004 and Pranzatelli et al., 2004). A recent study identified the orphan receptor GluR δ2 as one major autoantigen in childhood OMS. However, the exact impact of these autoantibodies and others is not completely clear. Since neuroblastoma patients with OMS have a better prognosis of their tumor diseases, it has been hypothesized that this may be due to a functional active role of the surface-binding autoantibodies. It has been shown that these surface-binding autoantibodies have a cytotoxic effect on neuroblastoma cells *in vitro* (Korfei et al., 2005). However, the successful treatment of advanced neuroblastoma with anti-GD2 antibodies is not due to the cytotoxic effect of the anti-GD2, but the induction of antibody-dependent cellular cytotoxicity (ADCC) by NK-cells (Cheung et al., 2012). Therefore, OMS-associated, surface binding autoantibodies may influence the NK-cell mediated cytotoxicity of neuroblastoma cells by higher IgG surface binding to NB cells in paediatric OMS compared to healthy controls (HC) and NB patients without OMS. Moreover, NB cells when co-cultured with NK cells in presence of OMS-IgG showed increased antibody dependent NK cell-mediated cytotoxicity. NK-cells are a subgroup of the innate lymphoid cells, which may provide a bridge between unspecific and antigen-specific immune reactions. In my study, I looked for the effect of NK cell coculture with neuroblastoma cells for four hours. I explored the combination of NB and NK cells in various effector to target ratios and found NK cell-mediated killing of NB cells.

Natural killer (NK) cells play important roles in tumor immunity and tumor immune surveillance (Iannello et al., 2016). The antitumor functions of NK cells are tightly

regulated by the balance of activating and inhibitory signals (Long et al., 2013). The interaction of NK cell-activating receptors such as DNAX accessory molecule 1 (DNAM-1) and natural killer group 2D (NKG2D), with the irrespective ligands expressed on tumor cells, poliovirus receptor (PVR) and Nectin-2 for DNAM-1, major histocompatibility complex class I-related chain A/B(MICA/B), and UL16-binding proteins (ULBPs) for NKG2D, triggers the release of cytolytic granules by NK cells, leading to tumor cell death (Cordeau et al., 2016). Tumor cells often have low MHC class I expression on their surface, which decreases T-cell dependent anti-tumor immunity, but increases NK-cell reactivity to these cells (Cerwenka et al., 2001 and Morgado et al., 2011). In one experiment, NK cell-mediated cytotoxicity of neuroblastoma cells was decreased by LMW/HMW poly(I:C) and total RNA and even further decreased when given in combination with IFN-γ. This may be due to the MHC I upregulation by IFN-γ, poly (I:C) or a combination of them. Moreover, another experiment showed that OMS-IgG from both paraneoplastic and non-paraneoplastic OMS increased ADCC in neuroblastoma cells. This effect was not produced by IgG from either HC or from patients with NB alone. Although OMS-IgG alone induced cytotoxicity of NB cells, I could show that the NK cell-mediated cytotoxic effect on NB cells is clearly enhanced after pre-incubation with OMS-IgG. Interestingly, this effect was only slightly inhibited by preincubation of neuroblastoma cells with IFN- γ and/or poly (I:C), indicating that MHC I upregulation cannot completely inhibit the ADCC. An important factor in NK activation in the NB tumor microenvironment is the presence of NK-activating ligands on the NB cell surface. Neuroblasts downregulate MHC I allowing for NK recognition and activation. However, in NB, NKs also recognize activation signals from proteins on neuroblasts including polio-virus receptor (PVR) and NCR ligands via their DNAM-1 and NCRs (Bottino et al., 2014). Additionally, cancer stem cells (CSCs), which are often refractory to radiation and chemotherapy, express stress ligands recognizable by NKG2D with resultant NK-mediated cytotoxicity (Ames et al., 2015). Thus, for NKs in NB, the combination of downregulated MHC-I proteins and expression of NK receptor ligands provides an environment conducive to NK activation and killing of neuroblasts and CSCs. Furthermore, the influence of NK receptors on NB outcomes demonstrates the potential of NKs as therapeutic tools.

NK cells play critical roles in host immunity against cancer. In response, cancers develop mechanisms to escape NK cell attack or induce defective NK cells. Currently, NK cell-based cancer immunotherapy can aim to overcome NK cell paralysis using chemotherapeutic to activate NK cells. However, a multimodal therapy approach, such as combining chemotherapy agents with cellular immunotherapy, suffers from potential drug-mediated toxicity to immune-effector cells. Disabling such toxic effects of anticancer cellular products is a potential critical barrier to the development of combined therapeutic approaches (Kollipara et al., 2014). Our results support the hypothesis that the immune-reaction in NB associated OMS can contribute to a better anti-tumor immune response in neuroblastoma-associated OMS, and also support the pathogenic role of surface-binding autoantibodies in OMS. In conclusion, our study shows that antibody-dependent cell mediated tumor cell lysis plays a role in anti-tumor immunity of patients with neuroblastoma-associated pediatric OMS. Whether this process is also involved in the pathophysiology of the OMS itself remains yet to be elucidated.

5.3. Effects of RNA on neuronal cells

It has generally been presumed that the central nervous system (CNS) is immune privileged, and that MHC I is not expressed by neurons (Lampson, 1995). However, accumulating data have confirmed MHC I expression by subsets of neurons in both adult and developing mammalian brain (Cullheim et al., 2010). Many of these reports describe a role for neuronal MHC I in synaptic plasticity, brain development and axonal regeneration. Recent studies suggest that neuronal expression of this molecule is involved in neuroinflammatory processes and participates in immune-mediated neurodegeneration (Cebrián et al., 2014). MHC I expression analyzed via flow cytometry increased upon LMW/HMW poly (I:C) and total RNA treatments, which otherwise was observed to be negligible in the neuronal cells. Although the presence of MHC I in the mature rodent CNS was for many years thought to be confined to glial cells (Wong et al., 1984), ensuing reports demonstrate MHC I expression by some neuronal populations, both *in vitro* and *in vivo*, usually triggered by exposure to interferon gamma (IFN-γ). The initial such study showed that MHC I gene expression was induced by IFN-γ in cultured

rat hippocampal neurons (Neumann et al., 1995). Subsequently, mRNA for MHC I was identified in nuclei of neonatal and adult rodent brain including the SN, brainstem motor neurons (Lindå et al., 1999), cortex, hippocampus (Huh et al., 2000) and cerebellum (Letellier et al., 2008). Multiple groups reported expression of MHC I subunits by immunolabel in CNS regions including cingulate cortex and hippocampus (Needleman et al., 2010 and Liu et al., 2013), with expression gradually decreasing as neonatal mice reached adulthood (Liu et al., 2013). In most studies, the basal expression of MHC I in differentiated neuronal cells is very low. However, as described before, IFN- γ is able to induce MHC I in differentiated neurons. Another study showed data from human tissue that show that dopaminergic human neurons derived from human embryonic stem cells normally do not express MHC I but will do so following exposure to IFN-γ. Cultured primary catecholamine murine neurons also normally do not express MHC I, but do so upon exposure to IFN-γ, activated microglia or exposure to high levels of L-dihydroxyphenylalanine (L-DOPA), and are far more susceptible to MHC I induction than other neuronal populations tested, including cortical, striatal and thalamic neurons (Cebrián et al., 2014). These findings propose that neuronal MHC I expression and antigen display in catecholamine neurons may be triggered by microglial activation or high cytosolic dopamine, which in the presence of the appropriate antigen and CTLs could play a role in neuronal death during diseases in which CNS inflammation is robust. The mechanism, which suppresses the MHC I expression during the differentiation of neuronal cells is not completely understood. However, suppressor of cytokine signalling-1 (SOCS-1) seems to suppress basal MHC I expression and its upregulation by IFN- γ in different cell types (Chong et al. 2013). Additionally, silencing of the SOCS-1 gene in neuroblastoma cells increases both basal MHC I expression and reactivity to IFN- γ (Blaes, personal communication).

Another molecule observed in neuronal cells was TLR-3. The expression increases upon LMW/HMW poly (I:C) and total RNA treatments. LMW Poly (I:C) showed greater expression than HMW Poly (I:C) and total RNA showed increased expression of TLR-3 as the concentrations increased proportionally. The results significantly illustrate the effect of poly (I:C) and total RNA on differentiated neuronal cells and is similar to the

results obtained with neuroblastoma cells. Therefore, it can be suggested that neuronal cells respond similar to the RNA treatment as neuroblastoma cells. TLR3 is present within the central nervous system (CNS) (Alexopoulou et al., 2001). High levels of TLR3 are found in glial cells (Farina et al., 2005 and Jack et al., 2005) and neurons in disorders of the brain, neurodegenerative diseases, and viral infections (Prehaud et al., 2005 and Jackson et al., 2006). The high levels of TLR3 in the CNS suggests an important role in the response to neuronal injury and/or viral infection (Lafon et al., 2006), which may involve mechanisms other than those limited to the innate immune response. A major function of TLR3 is to sense and respond to viral infection. The presence of TLR3 in the core of NBs is an effort to inactivate TLR3 function. Sequestration of TLR3 into NBs could reduce the cellular innate immune response. The absence of TRIF adaptor of TLR3 in NB could support the hypothesis that TLR3 molecules in NB are inactive. The presence of viral RNA in NBs may reflect an interaction of TLR3 with viral components at an early stage of infection when the virus enters the cell through the TLR3 endosomal compartment. TLR3 could thus be involved in recruitment of viral nucleocapsid from the endosomal compartment before aggregation in NBs. In addition, the presence of dsRNAs in NBs may suggest that NBs can also sequester dsRNAs and thus may play a role in the innate immune response to RABV infection (Ménager et al., 2009). The presence of TLRs on immune cells and epithelial cells is well known, but their expression is not restricted to these cell types. Glial cells and neurons express TLRs in both the peripheral nervous system (PNS) and the central nervous system (CNS), allowing neurons to act as immune cells (Wadachi et al., 2006, Barajon et al., 2009, Goethals et al., 2010 and Kurt-Jones et al., 2004). Interaction between neurons and the immune system has already been reported, setting the scene for neurons acting as immune cells (van der Kleij et al., 2003, Rijnierse et al., 2009, Downes et al., 2010, Snoek et al., 2010 and Wood 2011). It has been reported that neuronal TLRs are involved in the development and homeostasis of the nervous system, and notably in several neurodegenerative diseases (Trudler et al., 2010 and Drouin-Ouellet et al., 2012). The intracellular TLRs mainly recognize microbial nucleic acid including viral double-strand RNAs (TLR3) (Kawasaki et al., 2014). TLR expression on primary neurons has been found in several species, amongst which are humans (Wadachi et al., 2006), mice (Goethals et al., 2010), and rats (Peltier et al., 2010).

Neuronal TLRs are present in both parts of the nervous system; the CNS (Jackson et al., 2006) and the PNS (Barajon et al., 2009). Expression of TLRs by neurons has been confirmed at mRNA level, and protein level (Ochoa-Cortes et al., 2010). In primary neurons, TLR3 stimulation inhibits neurite outgrowth and causes irreversible growth cone collapse, without affecting cell survival (Cameron et al., 2007). Different results were found in the high TLR3-expressing neuroblastoma cell line SK-N-AS, where exposure to a TLR3 ligand resulted in growth inhibition and apoptosis (Chuang et al., 2011). The difference in results on cell viability could be due to the use of different cell types (dorsal root ganglia, (Cameron et al., 2007) NPCs, (Lathia et al., 2008) and cell lines (Chuang et al., 2011), thus revealing the limits of cell culture as a model of biological processes. A study explained the protective effect of TLR-3 during viral infection. The infection of TLR3-/- mice with West Nile virus resulted in a higher viral burden in neurons and increased mortality compared to WT mice. The viral (Daffis et al., 2008) sensing receptors TLR3 and TLR8 can initiate a protective immune-like response in neurons upon viral challenge. Current literature shows that several neuronal TLRs are involved in the development of the nervous system and in neurodegenerative diseases. Neuronal TLRs are important for NPC proliferation, axonal growth, cell survival and in defense against viral infections (Rietdijk et al., 2016).

Various studies have shown that embryonic brain development is a complex process that includes the proliferation and differentiation of neural stem cells (NSCs) and neural progenitor cells (NPCs), neuronal migration and polarity establishment (Bradley, 1990 and Abranches et al., 2009). In the ventricular zone/subventricular zone (VZ/SVZ), NSCs/NPCs originated from neuroepithelial cells continuously proliferate and produce new neurons to form a six layered laminar structure, which is necessary for proper brain functions (McConnell, 1995 and Farkas et al., 2008). During embryonic neurogenesis, NSCs/NPCs undergo asymmetric divisions to self -renewal and generate one neuron or one intermediate progenitor cell (IPC), which subsequently divides symmetrically in the SVZ and differentiates into two neurons (Noctor et al., 2008). We observed increased proliferation in neuronal cells upon treatment with both poly (I:C) and total RNA and a decrease in cytotoxicity. Neuronal cells behave like neuroblastoma cells upon stimulation

with similar stimulants and lead to an increase and decrease in proliferation and cytotoxicity, respectively.

Additionally, the electrophysiological activity of the enteric neurospheres was detected to increase upon addition of LMW, HMW poly (I:C) and total RNA. Extracellular recording method, multielectrode array (MEA) was utilized to detect the electrical activity of complex neuronal networks. An array of single-contactable electrodes recorded the electrical field potentials induced by the ion flux across the cell membranes, therefore making MEAs an ideal tool to investigate network activities for prolonged periods. MEAs are instruments that provide a means of monitoring spontaneous electrophysiological activity within invitro neuronal cultures. The LMW/HMW poly (I:C) and total RNA was given to assess the ability of differentiated enteric neurospheres on multi electrode array (MEA) and observe electrical activity generated by complex neuronal networks. As shown in previously mentioned results, neuroblastoma cells showed increased expression of TLR-3 and MHC I upon poly (I:C) and total RNA treatment. Similar results were shown, how the network activity within cultures can be monitored using MEA recordings by assessing the changes in coordinated firing across individual neurons leading to poly (I:C) influencing the neuronal networks of enteric neurospheres. Inorder to exclude any unspecific effect, albumin/differentiation medium was utilized, and it showed no effect therefore confirming the effect observed with the stimulants to be specific. MEAs are a compelling assay platform for neuroscience combining a label-free, functional, electrophysiological read-out with the ability to multiplex experimental conditions.

5.4. Limitations of the study

In my experiments, I used total human RNA and poly (I:C) to evaluate the effects of RNA on neuroblastoma cells and their immunological features. Total human RNA alone showed less significant effects than poly (I:C), although immunogenic effects of total RNA have been described in other studies (Kannemeier et al. 2007 and Fischer et al. 2013). However, since the RNA preparation protocols are different, it may well be that this influences the RNA effects in the studies and makes them difficult to compare.

In the OMS autoantibody part, the coculture experiment with neuroblastoma and NK cells in the presence of OMS-IgG and RNA could only be done with two IgG fractions each due to the very low serum amounts taken from the (very small) OMS children. Therefore, a statistical powerful analysis from this experiment could not be done to clearly quantify the effect of RNA/poly (I:C) on the ADCC. However, since the main autoantigen (Glu delta 2) in OMS has been described during the conduction of my experiments, a polyclonal anti-Glu Delta 2 antibody could be developed and used in further experiments.

5.5. Conclusion

In conclusion, our study highlights the role of RNA in various forms (poly (I:C) / total RNA) in the tumor-immune interactions as well as their effects on neuronal cells. RNA affects the proliferation, cytotoxicity of neuroblastoma cells and induces MHC I and TLR-3, which increases the immunogenicity of these cells. Additionally, we concluded that neuronal cells exert similar effects as neuroblastoma cells upon addition of similar stimulants. We also showed that ADCC may be a mechanism in neuroblastoma patients with additional autoimmune paraneoplastic opsoclonus-myoclonus syndrome, despite the upregulation of MHC I by RNA and/or IFN- γ. TLR-3 is involved in the regulation of MHC I expression in neuroblastoma cells. An elaborate study of TLR-3 receptors and the signaling mechanism in neuroblastoma may extend our knowledge on the interaction of tumor/NB and the immune system. Moreover, work on neuroblastoma-associated pediatric OMS can be elucidated by doing a detailed study on the role of antibody dependent cell mediated tumor cell lysis.

6. SUMMARY

Neuroblastoma is a childhood tumor, resulting from uncontrolled growth of neuroblasts instead of developing into nerve cells. Since immune therapies have an increasing impact on the treatment and prognosis of neuroblastoma, this study focuses on the interaction between neuroblastoma and immune system and the role of RNA on susceptibility of neuroblastoma cells to immune cell killing of NK cells. Additionally, the role of NK-cell mediated antibody-dependent tumor cytotoxicity (by autoantibodies of children with a paraneoplastic opsoclonus-myoclonus syndrome (OMS)) has been studied.

Neuroblastoma cells treated with IFN-γ (as a proinflammatory control), poly (I:C) and total RNA induced TLR-3 and MHC I expression on gene and protein level. The effect of poly (I:C) was stronger than using total RNA and the RNA / poly (I:C) effect was potentiated by IFN-γ. Blocking the TLR-3 receptor with TLR3/dsRNA complex inhibitor decreased the expression of MHC I suggesting that TLR-3 is crucial for the regulation of MHC I expression in neuroblastoma cells. Furthermore, co-culture of NK-92 and neuroblastoma cells showed cytotoxic effects of NK cells on NB cells. Pretreatment of NB cells with poly (I:C) and RNA decreased this effect. In contrast, surface-binding IgG from OMS patients induced higher NK-cell mediated cytotoxicity in neuroblastoma cells than IgG from NB patients without OMS or IgG from healthy controls. Although OMS-IgG itself has slight cytotoxic effect on NB cells, the effect on the NB-mediated tumor cell cytotoxicity was significantly higher. To compare the effects of RNA on neuroblastoma cells with non-tumor neuronal cells, we used fetal autonomic neurons. Similar to neuroblastoma cells, increased expression of MHC I and TLR-3 could be seen in fetal autonomic neurons along with increased proliferation and decreased cytotoxicity upon treatment with poly(I:C) and RNA. Multi-electrode array (MEA) measurements showed increased electrophysiological activity upon treatment with poly(I:C) and RNA in enteric neurospheres, indicating that free RNA and/or viral RNA could influence the electric function of neuronal cells. Our findings contribute to the knowledge of the role of RNA in interplay between tumor cells and the immune system.

7. ZUSAMMENFASSUNG

Ein Neuroblastom ist ein Tumor des Kindesalters, der durch ein unkontrolliertes Wachstum von Neuroblasten entsteht, die sich nicht zu Neuronen des autonomen Nervensystems differenzieren. Da Immunvorgänge eine zunehmende Rolle beim Neuroblastom spielen, untersucht die vorliegende Studie die Rolle von freier RNA im Rahmen der Tumor-NK-Zell-Interaktion. Im Vergleich dazu wird der Einfluss von Autoantikörpern gegen Neuroblastomzellen auf die Wechselwirkung mit NK-Zellen untersucht.

Inkubation von Neuroblastomzellen (NB) mit Interferon-γ (IFN-γ, proinflammatorische Kontrolle) sowie RNA (humane RNA, poly (I:C)) führt zu einer Induktion von MHC I und Toll-like receptor (TLR) 3 auf RNA- und Proteinebene. Der Effekt von poly (I:C) war dabei deutlich stärker als der Effekt der humanen RNA und IFN-γ potenzierte den RNA_Effekt. Eine Blockade des TLR-3 reduzierte die MHC I Expression deutlich, was auf eine wichtige Rolle des Rezeptors beid er MHC I Regulation schließen lässt. Werden NB Zellen mit natürlichen Killer- (NK-) Zellen kokultiviert, lässt sich eine deutliche Zytotoxizität nachweisen, die durch Präinkubation der NB-Zellen mit RNA vermindert wird. Im Gegensatz dazu kann der zytotoxische Effekt der NK-Zellen durch Zugabe von IgG, welches aus dem Serum von Neuroblastompatienten mit einem paraneoplastischen Opsoklonus-Syndrom gewonnen wurde, deutlich gesteigert werden. Diese NK-Zell-abhängige Antikörper-vermittelte Zytotoxizität kann durch den RNA Einfluss nur wenig reduziert werden. Um den Effekt von RNA auf Neuroblastomzellen mit nicht-malignen neuronalen Zellen zu vergleichen, haben wir den Einfluss von RNA auf fetale autonome Neurone untersucht. Auch bei diesen Neuronen konnte TLR-3 und MHC I durch RNA induziert werden. Darüber hinaus verändert RNA die elektrochemischen Eigenschaften der fetalen Neurone. Zusammenfassend zeigt unsere Studie, dass RNA die Immunogenität von Neuroblastomzellen und neuronalen Zellen verändert.

8. REFERENCES

Abranches E et al. (2009). Neural differentiation of embryonic stem cells in vitro: a road map to neurogenesis in the embryo. PLoS One 4: e6286.

Adams M et al. (2005). The rationale for combined chemo/immunotherapy using a Toll-like receptor 3 (TLR3) agonist and tumour-derived exosomes in advanced ovarian cancer. Vaccine. 23:2374–8.

Alexopoulou L et al. (2001). Recognition of double-stranded RNA and activation of NF-kappaB by Toll-like receptor 3. Nature. 18;413(6857):732-8.

Al-Nedawi K et al. (2008). Intercellular transfer of the oncogenic receptor EGFRvIII by microvesicles derived from tumour cells. Nat Cell Biol. 10(5):619-24.

AL et al., (2010). Anti-GD2 antibody with GM-CSF, interleukin-2, and isotretinoin for neuroblastoma, N. Engl. J. Med. 363 1324–1334.

Ames E et al. (2015). Enhanced targeting of stem-like solid tumor cells with radiation and natural killer cells. Oncoimmunology. 4:e1036212.

Ammi R et al. (2015). Poly(I:C) as cancer vaccine adjuvant: knocking on the door of medical breakthroughs. Pharmacol Ther. 146:120–131.

Asgharzadeh S et al. (2006). Prognostic significance of gene expression profiles of metastatic neuroblastomas lacking MYCN gene amplification. J Natl Cancer Inst. 98(17):1193-203.

Baj-Krzyworzeka M et al. (2006). Tumour-derived microvesicles carry several surface determinants and mRNA of tumour cells and transfer some of these determinants to monocytes. Cancer Immunol Immunother. 55(7):808-18.

Barajon I et al. (2009). Toll-like receptors 3, 4, and 7 are expressed in the enteric nervous system and dorsal root ganglia. J Histochem Cytochem 57:1013-23.

Berridge G et al. (2018). Glutamate receptor δ2 serum antibodies in pediatric opsoclonus myoclonus ataxia syndrome. Neurology. Aug 21;91(8):e714-e723.

Biron CA et al. (1999). Natural killer cells in antiviral defense: function and regulation by innate cytokines. Annu Rev Immunol. 17:189-220.

Blaes F et al. (2005). Surface-binding autoantibodies to cerebellar neurons in opsoclonus syndrome. Ann Neurol. 58:313–317.

Bobrie A et al. (2012). Rab27a supports exosome-dependent and -independent mechanisms that modify the tumor microenvironment and can promote tumor progression. Cancer Res. 1;72(19):4920-30.

Boehm U et al. (1997). Cellular responses to interferon-gamma, Annu. Rev. Immunol. 15. 749–795.

Boes M et al. (2015). TLR3 triggering regulates PD-L1 (CD274) expression in human neuroblastoma cells. Cancer Lett. 361(1):49-56.

Boger DL et al. (2003). Solution-phase combinatorial libraries: modulating cellular signaling by targeting protein-protein or protein-DNA interactions. Angew Chem Int Ed Engl. Sep 15;42(35):4138-76.

Borriello L et al. (2016). More than the genes, the tumor microenvironment in neuroblastoma. Cancer Lett. Sep 28;380(1):304-14.

Bottino C et al. (2014). Natural killer cells and neuroblastoma: tumor recognition, escape mechanisms, and possible novel immunotherapeutic approaches. Front Immunol. 5:56.

Bradley A (1990). Embryonic stem cells: proliferation and differentiation. Curr Opin Cell Biol 2: 1013-1017.

Brodeur GM, Bagatell R (2014). Mechanisms of neuroblastoma regression. Nat Rev Clin Oncol. (12):704-13.

Brodeur GM et al. (1988). International criteria for diagnosis, staging, and response to treatment in patients with neuroblastoma. J Clin Oncol. 6(12):1874-81.

Bryant RJ et al. (2012). Changes in circulating microRNA levels associated with prostate cancer. Br J Cancer. 14;106(4):768-74.

Cabrera-Fuentes HA et al. (2015). Regulation of monocyte/macrophage polarisation by extracellular RNA. Thromb Haemost. Mar;113(3):473-81.

Caligiuri MA (2008). Human natural killer cells. Blood. 1;112(3):461-9.

Cameron JS et al. (2007). Toll-like receptor 3 is a potent negative regulator of axonal growth in mammals. J Neurosci 27:13033-41.

Campbell KS et al. (2013). Natural killer cell biology: an update and future directions. J Allergy Clin Immunol. 132(3):536-544.

Castriconi R et al. (2004). Identification of 4Ig-B7-H3 as a neuroblastoma-associated molecule that exerts a protective role from an NK cell-mediated lysis. Proc Natl Acad Sci U S A. 101(34):12640-5.

Cebrián C et al. (2014). Neuronal MHC-I expression and its implications in synaptic function, axonal regeneration and Parkinson's and other brain diseases. Front Neuroanat. 8:114. Published 2014 Oct 13.

Cebrián, C et al. (2014). MHC-I expression renders catecholaminergic neurons susceptible to T-cell-mediated degeneration. Nat. Commun. 5:3633.

Cerwenka A et al. (2001). Natural killer cells, viruses and cancer. Nat Rev Immunol. 1(1):41-9.

Cerwenka A et al. (2016). Natural killer cell memory in infection, inflammation and cancer. Nat Rev Immunol. 16(2):112-23.

Cheever MA et al. (2009). The prioritization of cancer antigens: a national cancer institute pilot project for the acceleration of translational research. Clin Cancer Res. 1;15(17):5323-37.

Chen X et al. (2008). Characterization of microRNAs in serum: a novel class of biomarkers for diagnosis of cancer and other diseases. Cell Res. 18(10):997-1006.

Cheung NK et al. (2012). Humanizing murine IgG3 anti-GD2 antibody m3F8 substantially improves antibody-dependent cell-mediated cytotoxicity while retaining targeting in vivo. OncoImmunology 1:477–486.

Cheung NK et al. (2012). Murine anti-GD2 monoclonal antibody 3F8 combined with granulocyte-macrophage colony-stimulating factor and 13-cis-retinoic acid in high-risk patients with stage 4 neuroblastoma in first remission. J Clin Oncol. 10;30(26):3264-70.

Cheung NK et al. (2013). Neuroblastoma: developmental biology, cancer genomics and immunotherapy. Nat Rev Cancer. 13(6):397-411.

Chiba M et al. (2012). Exosomes secreted from human colorectal cancer cell lines contain mRNAs, microRNAs and natural antisense RNAs, that can transfer into the human hepatoma HepG2 and lung cancer A549 cell lines. Oncol Rep. 28(5):1551-8.

Chinnappa P et al. (2004). Detection of thyrotropin-receptor messenger ribonucleic acid (mRNA) and thyroglobulin mRNA transcripts in peripheral blood of patients with thyroid disease: sensitive and specific markers for thyroid cancer. J Clin Endocrinol Metab 89(8):3705–9.

Chin D et al. (2006). Head and neck cancer: past, present and future. Expert Rev Anticancer Ther. 6:1111–18.

Chuang JH et al. (2011). Differential toll-like receptor 3 (TLR3) expression and apoptotic response to TLR3 agonist in human neuroblastoma cells. J Biomed Sci. 18:65.

Chuang JH et al. (2012). Preferential involvement of mitochondria in Toll-like receptor 3 agonist-induced neuroblastoma cell apoptosis, but not in inhibition of cell growth. Apoptosis. 17:335–348.

Cohn SL et al. (2009). The International Neuroblastoma Risk Group (INRG) classification system: an INRG Task Force report. J Clin Oncol. 10;27(2):289-97.

Colon NC et al. (2011). Neuroblastoma. Adv Pediatr. 58(1):297-311.

Cordeau M et al. (2016). Efficient Killing of High Risk Neuroblastoma Using Natural Killer Cells Activated by Plasmacytoid Dendritic Cells. PLoS One. 11(10):e0164401.

Corrias MV et al. (2001). Lack of HLA-class I antigens in human neuroblastoma cells: analysis of its relationship to TAP and tapasin expression. Tissue Antigens 57: 110–117.

Coughlin, C. M. et al. (2006). Immunosurveillance and survivin-specific T-cell immunity in children with high-risk neuroblastoma. J. Clin. Oncol. 24, 5725–5734.

Cullheim, S et al. (2010). Classic major histocompatibility complex classI molecules: new actors at the neuromuscular junction. Neuroscientist 16, 600–607.

Daffis S et al. (2008). Toll-like receptor 3 has a protective role against West Nile virus infection. J Virol 82:10349-58.

Delves GH et al. (2007). Prostasomes, angiogenesis, and tissue factor. Semin Thromb Hemost. 33(1):75-9.

De-Waele J et al. (2017). Poly(I:C) primes primary human glioblastoma cells for an immune response invigorated by PD-L1 blockade. Oncoimmunology. Dec 12;7(3):e1407899.

Di-Lascio S et al. (2018). Structural and functional differences in PHOX2B frameshift mutations underlie isolated or syndromic congenital central hypoventilation syndrome. Hum Mutat. 39(2):219-236.

Di-Vizio D et al. (2012). Large oncosomes in human prostate cancer tissues and in the circulation of mice with metastatic disease. Am J Pathol. 181(5):1573-84.

Downes CE et al. (2010). Neural injury following stroke: are Toll-like receptors the link between the immune system and the CNS Br J Pharmacol 160:1872-88.

Drouin-Ouellet J et al. (2012). Inflammation and neurodegeneration: the story “retolled.” Trends Pharmacol Sci 33:542-51.

El-Abd E et al. (2008). Serum metastasin mRNA is an important survival predictor in breast cancer. Br J Biomed Sci 65(2):90–4.

EL-Andaloussi S et al. (2013). Extracellular vesicles: biology and emerging therapeutic opportunities. Nat Rev Drug Discov. 12(5):347-57.

Fang F et al. (2017). NK cell-based immunotherapy for cancer. Semin Immunol. 31:37-54.

Fang Y et al. (2007). Higher-order oligomerization targets plasma membrane proteins and HIV gag to exosomes. PLoS Biol. 5(6):e158.

Farag SS et al. (2006). Human natural killer cell development and biology. Blood Rev. 20(3):123-37.

Farina C et al. (2005). Preferential expression and function of Toll-like receptor 3 in human astrocytes. J Neuroimmunol 159: 12–19.

Farkas LM et al. (2008). The cell biology of neural stem and progenitor cells and its significance for their proliferation versus differentiation during mammalian brain development. Curr Opin Cell Biol 20: 707±715.

Favrot MC et al. (1991). Expression of leucocyte adhesion molecules on 66 clinical neuroblastoma specimens. Int J Cancer. 48(4):502-10.

Forbes SA et al. (2011). COSMIC: mining complete cancer genomes in the Catalogue of Somatic Mutations in Cancer. Nucleic Acids Res. 39(Database issue):D945-50.

Foreman NK et al. (1993). Mechanisms of selective killing of neuroblastoma cells by natural killer cells and lymphokine activated killer cells. Potential for residual disease eradication. Br J Cancer. 67(5):933-8.

Frost B et al. (2009). Propagation of tau misfolding from the outside to the inside of a cell. J Biol Chem. 8;284(19):12845-52.

Fühlhuber V et al. (2015). Autoantibody-mediated cytotoxicity in paediatric opsoclonus-myoclonus syndrome is dependent on ERK-1/2 phophorylation. J Neuroimmunol. Dec 15;289:182-6.

Gailhouste L et al. (2013). Potential applications of miRNAs as diagnostic and prognostic markers in liver cancer. Front Biosci (Landmark Ed). 1;18:199-223.

Galluzzi L et al. (2014). Classification of current anticancer immunotherapies. Oncotarget. 5(24):12472-508.

Gama-Carvalho M et al. (2014). Regulation of Cardiac Cell Fate by microRNAs: Implications for Heart Regeneration. Cells. 29;3(4):996-1026.

Goethals S et al. (2010). Toll-like receptor expression in the peripheral nerve. Glia 58:1701-9.

Graus F (2017). Widening the spectrum of inflammatory disorders of the central nervous system. Curr Opin Neurol. 30(3):292-294.

Groth A et al. (2011). Mechanisms of tumor and viral immune escape from natural killer cell-mediated surveillance. J Innate Immun. 3(4):344-54.

Gupta A et al. (2014). Exosomes as mediators of neuroinflammation. J Neuroinflammation. 3;11:68.

Hammer Q et al. (2018). Natural killer cell specificity for viral infections. Nat Immunol. 19(8):800-808.

Hanson EK et al. (2009). Identification of forensically relevant body fluids using a panel of differentially expressed microRNAs. Anal Biochem. 15;387(2):303-14.

Hasan UA et al. (2005). Toll-like receptor signaling stimulates cell cycle entry and progression in fibroblasts. J Biol Chem. 280:20620–7.

Haupt R et al. (1979). Improved survival of children with neuroblastoma between 1979 and 2005 a report of the Italian Neuroblastoma Registry. J Clin Oncol. 28:2331–2338.

Hautekeete ML et al. (1997). The hepatic stellate (Ito) cell: its role in human liver disease. Virchows Arch. 430(3):195-207.

Hazenberg MD et al. (2014). Human innate lymphoid cells. Blood. 31;124(5):700-9.

Hopper C et al. (2004). mTHPC- mediated photodynamic therapy for early oral squamous cell carcinoma. Int J Cancer. 111:138–46.

Höftberger R et al. (2015). Update on neurological paraneoplastic syndromes. Curr Opin Oncol. 27(6):489-95.

Hsu WM et al. (2015). MDA5 complements TLR3 in suppression of neuroblastoma. Oncotarget. Sep 22;6(28):24935-46.

Hsu WM et al. (2013). Toll-like receptor 3 expression inhibits cell invasion and migration and predicts a favorable prognosis in neuroblastoma. Cancer Lett. 336:338–346.

Huang M et al. (2013). Neuroblastoma and MYCN. Cold Spring Harb Perspect Med. 3(10):a014415.

Huh, SG et al. (2000). Functional requirement for class I MHC in CNS development and plasticity. Science. 290, 2155–2159.

Humphries C (2013). Adoptive cell therapy: Honing that killer instinct. Nature. 504(7480):S13-5.

Iannello A et al. (2016). Immunosurveillance and immunotherapy of tumors by innate immune cells. Curr Opin Immunol 38:52-58.

Jack CS et al. (2005). TLR signaling tailors innate immune responses in human microglia and astrocytes. J Immunol 175: 4320–4330.

Jackson AC et al. (2006). Expression of Toll-like receptor 3 in the human cerebellar cortex in rabies, herpes simplex encephalitis, and other neurological diseases. J Neurovirol 12: 229–234.

Janeway CA Jr et al. (2002). Innate immune recognition. Annu Rev Immunol. 20:197-216.

Jiang Q et al. (2008). Poly I:C enhances cycloheximide induced apoptosis of tumor cells through TLR3 pathway. BMC Cancer. 8:12.

Jinek M et al. (2009). A three-dimensional view of the molecular machinery of RNA interference. Nature. Jan 22;457(7228):405-12.

Kahlert C et al. (2013). Exosomes in tumor microenvironment influence cancer progression and metastasis. J Mol Med (Berl). 91(4):431-7.

Kalaskar RR et al. (2016). Neuroblastoma in early childhood: A rare case report and review of literature. Contemp Clin Dent. 7(3):401-4.

Kannemeier C et al. (2007). Extracellular RNA constitutes a natural procoagulant cofactor in blood coagulation. Proc Natl Acad Sci U S A. Apr 10;104(15):6388-93.

Kanzler H et al. (2007). Therapeutic targeting of innate immunity with Toll-like receptor agonists and antagonists. Nat Med. 13: 552–559.

Kawasaki T et al. (2014). Toll-like receptor signaling pathways. Front Immunol 5:461.

Kembhavi SA et al. (2015). Imaging in neuroblastoma: An update. Indian J Radiol Imaging. 25(2):129-36.

Kollipara PS et al. (2014). Co-culture with NK-92MI cells enhanced the anti-cancer effect of bee venom on NSCLC cells by inactivation of NF-κB. Arch Pharm Res. 37(3):379-389.

Koppers-Lalic D et al. (2013). Virus-modified exosomes for targeted RNA delivery; a new approach in nanomedicine. Adv Drug Deliv Rev. 65(3):348-56.

Korfei M et al. (2005). Functional characterisation of autoantibodies from patients with pediatric opsoclonus-myoclonus-syndrome. J Neuroimmunol. 170:150–157.

Kosaka N et al. (2010). microRNA as a new immune-regulatory agent in breast milk. Silence. 1;1(1):7.

Kosaka N et al. (2013). Exosomal tumor-suppressive microRNAs as novel cancer therapy: "exocure" is another choice for cancer treatment. Adv Drug Deliv Rev. 65(3):376-82.

Kramer K et al. (1998). Disialoganglioside G(D2) loss following monoclonal antibody therapy is rare in neuroblastoma. Clin Cancer Res. 1998 Sep;4(9):2135-9.

Kuhnert F et al. (2008). Attribution of vascular phenotypes of the murine Egfl7 locus to the microRNA miR-126. Development. 135(24):3989-93.

Kumar S (2018). Natural killer cell cytotoxicity and its regulation by inhibitory receptors. Immunology. 154(3):383-393.

Kurt-Jones EA et al. (2004). Herpes simplex virus 1 interaction with Toll-like receptor 2 contributes to lethal encephalitis. Proc Natl Acad Sci U S A 101:1315-20.

Kuznik A et al. (2011). Mechanism of endosomal TLR inhibition by antimalarial drugs and imidazoquinolines. J Immunol. 186(8):4794–804.

LaBrosse EH et al. (1980). Urinary excretion of 3-methoxy-4-hydroxymandelic acid and 3-methoxy-4-hydroxyphenylacetic acid by 288 patients with neuroblastoma and related neural crest tumors. Cancer Res. 40(6):1995-2001.

Lacour J et al. (1992). Polyadenylic-polyuridylic acid as an adjuvant in resectable colorectal carcinoma: a 6 1/2 year follow-up analysis of a multicentric double blind randomized trial. Eur J Surg Oncol. 18:599–604.

Lafon M et al. (2006). The innate immune facet of brain: human neurons express TLR-3 and sense viral dsRNA. J Mol Neurosci 29: 185–194.

Lampson LA et al. (1983). Striking paucity of HLA-A, B, C and beta 2-microglobulin on human neuroblastoma cell lines. J Immunol 130: 2471– 2478.

Lampson LA. (1995). Interpreting MHC class I expression and class I/class II reciprocity in the CNS: reconciling divergent findings. Microsc. Res. Tech.32,267–285.

Lanier LL (2008). Up on the tightrope: natural killer cell activation and inhibition. Nat Immunol. 9(5):495-502.

Laplanche A et al. (2000). Polyadenylic-polyuridylic acid plus locoregional radiotherapy versus chemotherapy with CMF in operable breast cancer: a 14 year follow-up analysis of a randomized trial of the Federation Nationale des Centres de Lutte contre le Cancer (FNCLCC). Breast Cancer Res Treat. 64:189–91.

Lathia JD et al. (2008). Toll-like receptor 3 is a negative regulator of embryonic neural progenitor cell proliferation. J Neurosci 28:13978-84.

Letellier, M et al. (2008). Normal adult climbing fiber monoinnervation of cerebellar Purkinje cells in mice lacking MHC class I molecules. Dev. Neurobiol.68, 997–1006.

Lesterhuis WJ et al. (2011). Cancer immunotherapy--revisited. Nat Rev Drug Discov. 10(8):591-600.

Li K et al. (2018). Advances, challenges, and opportunities in extracellular RNA biology: insights from the NIH exRNA Strategic Workshop. JCI Insight. 5;3(7). pii: 98942.

Lindå, H et al. (1999). Expression of MHC class I heavy chain and beta2-microglobulin in rat brainstem motoneurons and nigral dopaminergic neurons. J. Neuroimmunol.101, 76–86.

Liu D et al. (2012). IL-15 protects NKT cells from inhibition by tumor-associated macrophages and enhances antimetastatic activity. J Clin Invest. 122(6):2221-33.

Liu G et al. (2010). miR-21 mediates fibrogenic activation of pulmonary fibroblasts and lung fibrosis. J Exp Med. 2;207(8):1589-97.

Liu J et al. (2013). The expression pattern of classical MHC class I molecules in the development of mouse central nervous system. Neurochem. Res.38, 290–299.

Long EO et al. (2013). Controlling natural killer cell responses: integration of signals for activation and inhibition. Annu Rev Immunol 31:227–258.

Louis CU et al. (2015). Neuroblastoma: molecular pathogenesis and therapy. Annu Rev Med. 66:49-63.

Luo YB et al. (2018). Advances in the Surgical Treatment of Neuroblastoma. Chin Med J (Engl). 131(19):2332-2337.

Makiguchi T et al. (2016). Serum extracellular vesicular miR-21-5p is a predictor of the prognosis in idiopathic pulmonary fibrosis. Respir Res. 5;17(1):110.

Mao L et al. (2004). Focus on head and neck cancer. Cancer Cell. 5:311–16.

Maris JM et al. (2007). Neuroblastoma. Lancet. 369:2106–2120.

Maris JM (2010). Recent advances in neuroblastoma. N Engl J Med. 362(23):2202-11.

Marleau AM et al. (2012). Exosome removal as a therapeutic adjuvant in cancer. J Transl Med. 27;10:134.

Matsumoto M et al. (2002). Establishment of a monoclonal antibody against human Toll-like receptor 3 that blocks double-stranded RNA-mediated signaling. Biochem Biophys Res Commun. 24;293(5):1364-9.

Matsumoto M et al. (2003). Subcellular localization of Toll-like receptor 3 in human dendritic cells. J Immunol. 15;171(6):3154-62.

Matsumoto M et al. (2008). TLR3: interferon induction by double-stranded RNA including poly(I:C). Adv Drug Deliv Rev. 29;60(7):805-12.

Matsumoto M et al. (2011). Antiviral responses induced by the TLR3 pathway. Rev Med Virol. 21(2):67-77.

McConnell SK (1995) Constructing the cerebral cortex: neurogenesis and fate determination. Neuron 15: 761±768.

Meany HJ (2019). Non-High-Risk Neuroblastoma: Classification and Achievements in Therapy. Children (Basel) 6(1).

Menke TB et al. (2004). Improved conditions for isolation and quantification of RNA in urine specimens. Ann N Y Acad Sci. 1022:185-9.

Ménager P et al. (2009). Toll-like receptor 3 (TLR3) plays a major role in the formation of rabies virus Negri Bodies. PLoS Pathog. 5(2):e1000315.

Michael A et al. (2010). Exosomes from human saliva as a source of microRNA biomarkers. Oral Dis. 16(1):34-8.

Millimaggi D et al. (2007). Tumor vesicle-associated CD147 modulates the angiogenic capability of endothelial cells. Neoplasia. 9(4):349-57.

Milosevic J et al. (2012). Profibrotic role of miR-154 in pulmonary fibrosis. Am J Respir Cell Mol Biol. 47(6):879-87.

Miura N et al. (2006). Clinical usefulness of serum telomerase reverse transcriptase (hTERT) mRNA and epidermal growth factor receptor (EGFR) mRNA as a novel tumor marker for lung cancer. Cancer Sci 97(12):1366–73.

Mobergslien A et al. (2014). Exosome-derived miRNAs and cellular miRNAs activate innate immunity. J Innate Immun. 6(1):105-10.

Monclair T et al. (2009). The International Neuroblastoma Risk Group (INRG) staging system: an INRG Task Force report. J Clin Oncol. 27(2):298-303.

Morandi F et al. (2012). Bone marrow-infiltrating human neuroblastoma cells express high levels of calprotectin and HLA-G proteins. PLoS One. 7(1):e29922.

Morandi F et al. (2018). Novel Immunotherapeutic Approaches for Neuroblastoma and Malignant Melanoma. J Immunol Res. 2018:8097398.

Moretta L et al. (2006). Surface NK receptors and their ligands on tumor cells. Semin Immunol. 18(3):151-8.

Morgado S et al. (2011). NK cell recognition and killing of melanoma cells is controlled by multiple activating receptor-ligand interactions. J Innate Immun. 3:365–373.

Mossé YP et al. (2008). Identification of ALK as a major familial neuroblastoma predisposition gene. Nature. 455(7215):930-5.

Müller-Hermelink N et al. (2008). TNFR1 signaling and IFN-gamma signaling determine whether T cells induce tumor dormancy or promote multistage carcinogenesis. Cancer Cell. 13(6):507-18.

Nalysnyk L et al. (2012). Incidence and prevalence of idiopathic pulmonary fibrosis: review of the literature. Eur Respir Rev. 1;21(126):355-61.

Needleman LA et al. (2010). MHC class I molecules are present both pre-a and postsynaptically in the visula cortex during postnatal development and in adulthood. Proc. Natl. Acad. Sci. U S A107, 16999–17004.

Neumann H et al. (1995). Induction of MHC class I genes in neurons. Science. 269, 549–552.

Neves AF et al. (2008). Combined analysis of multiple mRNA markers by RT-PCR assay for prostate cancer diagnosis. Clin Biochem 41(14–15):1191–8.

Newman EA et al. (2019). Update on neuroblastoma. J Pediatr Surg. 54(3):383-389.

Nilsson J et al. (2009). Prostate cancer-derived urine exosomes: a novel approach to biomarkers for prostate cancer. Br J Cancer. 19;100(10):1603-7.

Noctor SC et al. (2008) Distinct behaviors of neural stem and progenitor cells underlie cortical neurogenesis. J Comp Neurol 508: 28±44.

Ochoa-Cortes F et al. (2010). Bacterial Cell Products Signal to Mouse Colonic Nociceptive Dorsal Root Ganglia Neurons. Am J Physiol liver Physiol 299:G723-32.

Ogorevc E et al. (2013). The role of extracellular vesicles in phenotypic cancer transformation. Radiol Oncol. 30;47(3):197-205.

Palucka K et al. (2012). Cancer immunotherapy via dendritic cells. Nat Rev Cancer. 12(4):265-77.

Papaioannou G et al. (2005). Neuroblastoma in childhood: review and radiological findings. Cancer Imaging. 30;5:116-27.

Pardoll DM (2012). The blockade of immune checkpoints in cancer immunotherapy. Nat Rev Cancer. 12(4):252-64.

Parikh NS et al. (2015). SIOP-PODC adapted risk stratification and treatment guidelines: Recommendations for neuroblastoma in low- and middle-income settings. Pediatr Blood Cancer. 62(8):1305-16.

Park JH et al. (2010). Activation of TLR2 and TLR5 did not affect tumor progression of an oral squamous cell carcinoma, YD-10B cells. J Oral Pathol Med. 39:781–5.

Park JH et al. (2012). Poly I:C inhibits cell proliferation and enhances the growth inhibitory effect of paclitaxel in oral sqaumous cell carcinoma. Acta Odontol Scand. 70(3):241-245.

Park JR et al. (2007). Adoptive transfer of chimeric antigen receptor re-directed cytolytic T lymphocyte clones in patients with neuroblastoma. Mol Ther. 15(4):825-33.

Park JR et al. (2010). Neuroblastoma: Biology, prognosis, and treatment. Hematol Oncol Clin North Am. (1):65-86.

Parker BS et al. (2016). Antitumour actions of interferons: implications for cancer therapy. Nat Rev Cancer. 16(3):131–44.

Peinado H et al. (2012). Melanoma exosomes educate bone marrow progenitor cells toward a pro-metastatic phenotype through MET. Nat Med. 18(6):883-91.

Peltier DC et al. (2010). Human neuronal cells possess functional cytoplasmic and TLR-mediated innate immune pathways influenced by phosphatidylinositol-3 kinase signaling. J Immunol 184:7010-21.

Pinto NR et al. (2015). Advances in Risk Classification and Treatment Strategies for Neuroblastoma. J Clin Oncol. 20;33(27):3008-17.

Pipinikas CP et al. (2008). HIF-1alpha mRNA gene expression levels in improved diagnosis of early stages of prostate cancer. Biomarkers 13(7):680–91.

Pipinikas CP et al. (2007). Measurement of blood E2F3 mRNA in prostate cancer by quantitative RT-PCR: a preliminary study. Biomarkers 12(5):541–57.

Platanias LC et al. (1999). Signaling pathways activated by interferons. Exp Hematol. Nov;27(11):1583-92.

Pollard ZF et al. (2010). Atypical acquired pediatric Horner syndrome. Arch Ophthalmol. 128(7):937-40.

Ponzoni M et al. (1993). Uncoordinate induction and differential regulation of HLA class-I and Transfection of NB cell lines with human IFN-c gene class-II expression by gamma-interferon in differentiating human neuroblastoma cells. Int J Cancer 55: 817–823.

Pranzatelli MR et al. (2001). Controlled pilot study of piracetam for pediatric opsoclonus-myoclonus. Clin Neuropharmacol. 24(6):352-7.

Pranzatelli MR et al. (2004). B- and T-cell markers in opsoclonus-myoclonus syndrome: immunophenotyping of CSF lymphocytes. Neurology. 62:1526–1532.

Pranzatelli MR et al. (2004). CSF B-cell expansion in opsoclonus-myoclonus syndrome: a biomarker of disease activity. Mov Disord. 19:770–777.

Prehaud C et al. (2005). Virus infection switches TLR-3-positive human neurons to become strong producers of beta interferon. J Virol 79: 12893–12904.

Pries R et al. (2008). Induction of c-Myc-dependent cell proliferation through toll-like receptor 3 in head and neck cancer. Int J Mol Med. 21:209–15.

Pule MA et al. (2008). Virus-specific T cells engineered to coexpress tumor-specific receptors: persistence and antitumor activity in individuals with neuroblastoma. Nat Med. 14(11):1264-70.

Quinn JF et al. (2015). Extracellular RNAs: development as biomarkers of human disease. J Extracell Vesicles. 28;4:27495.

Rabinowits G et al. (2009). Exosomal microRNA: a diagnostic marker for lung cancer. Clin Lung Cancer. 10(1):42-6.

Raffaghello L et al. (2004). Downregulation and/or release of NKG2D ligands as immune evasion strategy of human neuroblastoma. Neoplasia. 6(5):558-68.

Raffaghello L et al. (2005). Mechanisms of immune evasion of human neuroblastoma. Cancer Lett. 228(1-2):155-61.

Rajendran L et al. (2006). Alzheimer's disease beta-amyloid peptides are released in association with exosomes. Proc Natl Acad Sci U S A. 25;103(30):11172-7.

Rajwanshi A et al. (2009). Malignant small round cell tumors. J Cytol. 26(1):1-10.

Ratner N et al. (2016). The "neuro" of neuroblastoma: Neuroblastoma as a neurodevelopmental disorder. Ann Neurol. 80(1):13-23.

Redzic JS et al. (2014). Extracellular RNA mediates and marks cancer progression. Semin Cancer Biol. 28:14-23.

Rezvani K et al. (2017). Engineering Natural Killer Cells for Cancer Immunotherapy. Mol Ther. 2;25(8):1769-1781.

Rietdijk CD et al. (2016). Neuronal toll-like receptors and neuro-immunity in Parkinson's disease, Alzheimer's disease and stroke. Neuroimmunol Neuroinflammation 3:27-37.

Rijnierse A et al. (2009). Immunoglobulin-free light chains mediate antigen-specific responses of murine dorsal root ganglion neurons. J Neuroimmunol 208:80-86.

Rojas Y et al. (2016). The optimal timing of surgical resection in high-risk neuroblastoma. J Pediatr Surg. 51(10):1665-9.

Ross CA et al. (2004). Protein aggregation and neurodegenerative disease. Nat Med. 10 Suppl:S10-7.

Rudnick E et al. (2001). Opsoclonus-myoclonus-ataxia syndrome in neuroblastoma: clinical outcome and antineuronal antibodies-a report from the Children's Cancer Group Study. Med Pediatr Oncol. 36(6):612-22.

Saman S et al. (2012). Exosome-associated tau is secreted in tauopathy models and is selectively phosphorylated in cerebrospinal fluid in early Alzheimer disease. J Biol Chem. 3;287(6):3842-9

Schulz G et al. (1984). Detection of ganglioside GD2 in tumor tissues and sera of neuroblastoma patients. Cancer Res. 1984 Dec;44(12 Pt 1):5914-20.

Seeger RC (2011). Immunology and immunotherapy of neuroblastoma. Semin Cancer Biol. 21(4):229-37.

Sen GC et al. (2005). Transcriptional signaling by double-stranded RNA: role of TLR3. Cytokine Growth Factor Rev. 16:1–14.

Seow Y et al. (2009). Biological gene delivery vehicles: beyond viral vectors. Mol Ther. 17(5):767-77.

Sharma R et al. (2018). Clinical Presentation, Evaluation, and Management of Neuroblastoma. Pediatr Rev. 39(4):194-203.

Shibamiya A et al. (2009). A key role for Toll-like receptor-3 in disrupting the hemostasis balance on endothelial cells. Blood. Jan 15;113(3):714-22.

Sivakumar PV et al. (1999). Cutting edge: expression of functional CD94/NKG2A inhibitory receptors on fetal NK1.1+Ly-49- cells: a possible mechanism of tolerance during NK cell development. J Immunol. 15;162(12):6976-80.

Skog J et al. (2008). Glioblastoma microvesicles transport RNA and proteins that promote tumour growth and provide diagnostic biomarkers. Nat Cell Biol. 10(12):1470-6.

Smith V, Foster J (2018). High-Risk Neuroblastoma Treatment Review. Children (Basel) 5(9).

Smyth MJ et al. (2006). Cancer immunosurveillance and immunoediting: the roles of immunity in suppressing tumor development and shaping tumor immunogenicity. Adv Immunol. 90:1-50.

Snoek SA et al. (2010). The enteric nervous system as a regulator of intestinal epithelial barrier function in health and disease. Expert Rev Gastroenterol Hepatol 4:637-51.

Song L et al. (2009). Valpha24-invariant NKT cells mediate antitumor activity via killing of tumor-associated macrophages. J Clin Invest. 119(6):1524-36.

Soto C (2003). Unfolding the role of protein misfolding in neurodegenerative diseases. Nat Rev Neurosci. 4(1):49-60.

Spel L et al. (2015). Natural killer cells facilitate PRAME-specific T-cell reactivity against neuroblastoma. Oncotarget. 6(34):35770-81.

Spel L et al. (2018). Nedd4-Binding Protein 1 and TNFAIP3-Interacting Protein 1 Control MHC-1 Display in Neuroblastoma. Cancer Res. 78(23):6621-6631.

Stark GR et al. (1998). How cells respond to interferons, Annu. Rev. Biochem. 67. 227–264.

Steinman L (2014). Conflicting consequences of immunity to cancer versus autoimmunity to neurons: insights from paraneoplastic disease. Eur J Immunol. 44(11):3201-5.

Sui D et al. (2016). Mucin 1 and poly I:C activates dendritic cells and effectively eradicates pituitary tumors as a prophylactic vaccine. Mol Med Rep. Apr;13(4):3675-83.

Swift CC et al. (2018). Updates in Diagnosis, Management, and Treatment of Neuroblastoma. Radiographics. 38(2):566-580.

Takeshita N et al. (2013). Serum microRNA expression profile: miR-1246 as a novel diagnostic and prognostic biomarker for oesophageal squamous cell carcinoma. Br J Cancer. 19;108(3):644-52.

Tarek N et al. (2012). Unlicensed NK cells target neuroblastoma following anti-GD2 antibody treatment. J Clin Invest. 122(9):3260-70.

Tatematsu M et al. (2013). Toll-like receptor 3 recognizes incomplete stem structures in single-stranded viral RNA. Nat Commun. 4:1833.

Tatematsu M et al. (2014). Beyond dsRNA: Toll-like receptor 3 signalling in RNA-induced immune responses. Biochem J. 1;458(2):195-201.

Taylor DD et al. (2008). MicroRNA signatures of tumor-derived exosomes as diagnostic biomarkers of ovarian cancer. Gynecol Oncol. 110(1):13-21.

Tekautz TM et al. (2006). Evaluation of IFN-gamma effects on apoptosis and gene expression in neuroblastoma--preclinical studies. Biochim Biophys Acta. 1763(10):1000-1010.

Tolbert VP et al. (2018). Neuroblastoma: clinical and biological approach to risk stratification and treatment. Cell Tissue Res. 372(2):195-209.

Trudler D et al. (2010). Toll-like receptors expression and signaling in glia cells in neuro-amyloidogenic diseases: towards future therapeutic application. Mediators Inflamm pii: 497987

Urbich C et al. (2008). Role of microRNAs in vascular diseases, inflammation, and angiogenesis. Cardiovasc Res. 1;79(4):581-8.

Valadi H et al. (2007). Exosome-mediated transfer of mRNAs and microRNAs is a novel mechanism of genetic exchange between cells. Nat Cell Biol. 9(6):654-9.

Van-Arendonk KJ, Chung DH (2019). Neuroblastoma: Tumor Biology and Its Implications for Staging and Treatment. Children (Basel) 6(1).

Van-der-Kleij HP, et al. (2003). Functional expression of neurokinin 1 receptors on mast cells induced by IL-4 and stem cell factor. J Immunol 171:2074-9.

Van-Roy N et al. (2009). The emerging molecular pathogenesis of neuroblastoma: implications for improved risk assessment and targeted therapy. Genome Med. 27;1(7):74.

Vesely MD et al. (2011). Natural innate and adaptive immunity to cancer. Annu Rev Immunol. 29:235-71.

Wadachi R et al. (2006). Trigeminal nociceptors express TLR-4 and CD14: a mechanism for pain due to infection. J Dent Res 85:49-53.

Ward E et al. (2014). Childhood and adolescent cancer statistics, 2014. CA Cancer J Clin. 64(2):83-103.

Watanabe Y et al. (1989). Exogenous expression of mouse interferon gamma cDNA in mouse neuroblastoma C1300 cells results in reduced tumorigenicity by augmented anti-tumor immunity. Proc Natl Acad Sci USA 86: 9456–9460.

Weber F et al. (2006). Double-stranded RNA is produced by positive-strand RNA viruses and DNA viruses but not in detectable amounts by negative-strand RNA viruses. J Virol. 80(10):5059-64.

Weiner LM (2007). Building better magic bullets--improving unconjugated monoclonal antibody therapy for cancer. Nat Rev Cancer. (9):701-6.

Wei Z et al. (2017). Coding and noncoding landscape of extracellular RNA released by human glioma stem cells. Nat Commun. 26;8(1):1145.

Wittmann J et al. (2010). Serum microRNAs as powerful cancer biomarkers. Biochim Biophys Acta. 1806(2):200-7.

Wolfl M et al. (2005). Expression of MHC class I, MHC class II, and cancer germline antigens in neuroblastoma. Cancer Immunol Immunother. 54:400–6.

Wong, GH et al. (1984). Inducible expression of H-2 and Ia antigens on brain cells.Nature 310, 688–691.

Wood JD. (2011). Visceral pain: spinal afferents, enteric mast cells, enteric nervous system and stress. Curr Ph Des 17(16):1573-5.

Yang M et al. (2011). Microvesicles secreted by macrophages shuttle invasion-potentiating microRNAs into breast cancer cells. Mol Cancer. 22;10:117.

Yang S et al. (2013). miR-145 regulates myofibroblast differentiation and lung fibrosis. FASEB J. 27(6):2382-91.

Yoshizawa JM et al. (2013). Salivary microRNAs and oral cancer detection. Methods Mol Biol. 936:313-24.

Yu AL et al. (2010). Anti-GD2 antibody with GM-CSF, interleukin-2, and isotretinoin for neuroblastoma. N Engl J Med. 30;363(14):1324-34.

Zernecke A et al. (2009). Delivery of microRNA-126 by apoptotic bodies induces CXCL12-dependent vascular protection. Sci Signal. 8;2(100):ra81.

Zhang J et al. (2019). Natural Killer Cells and Current Applications of Chimeric Antigen Receptor-Modified NK-92 Cells in Tumor Immunotherapy. Int J Mol Sci. 14;20(2).

Zhou Y et al. (2013). TLR3 activation efficiency by high or low molecular mass poly I:C. Innate Immun. 19(2):184-192.

Zubakov D et al. (2010). MicroRNA markers for forensic body fluid identification obtained from microarray screening and quantitative RT-PCR confirmation. Int J Legal Med. 124(3):217-26.

ACKNOWLEDGEMENTS

First and foremost, I would like to express my profound gratitude to my supervisor, Prof. Dr. Franz Blaes, who has supported me throughout my research with his knowledge, encouragement and guidance that helped me through challenging times, whilst allowing me to work in my own way. I dedicate the completion of my thesis to his insights, suggestions and wisdom.

I would like to show my gratitude to Prof. Dr. med. Karl-Herbert Schäfer, for allowing me to work in his lab in Zweibrücken, Germany and permitting me to plan and execute my experiments with continual supervision from his side. I am indebted with appreciation for his advices and support. Furthermore, I would like to thank the lab members in Zweibrücken for helping me in my experiments and especially in everyday life, making my stay in Zweibrücken memorable. Firstly, I express my heartily thanks to Eva Loris for being a great friend, the finest lab companion to work with and for being my partner in working late in the evenings and driving me back home. I deeply appreciate Dr. Manuela Gries for her scientific help and productive suggestions on the execution of my experiments. I would like to thank Cheng Xu for his help during my initial days in lab and in Zweibrücken. I thank Carolin Strutwolf and Stephanie Rommel for their friendly nature and supportive attitude towards me during my stay and afterwards. I would like to thank Anne Braun, Max Weyland, Dr. Akira Kakuta, Irfan Masood, Dr. Luca Gentile and all other lab members for their constant help in early morning dissections, productive suggestions in lab meetings, eating together in mensa and for accepting me whole heartedly in the group.

I gratefully acknowledge the Giessen Graduate school for Life Science (GGL) for providing me with three years of continuous scientific knowledge, support from mentors and opportunity to socialize with various individuals from diverse scientific and cultural backgrounds.

I had the good fortune of knowing Dr. Muhammad Khalid Shaikh and Dr. Asghar Nasir while working as a research associate in Karachi, Pakistan. Their immense admiration and scientific knowledge towards their respective fields substantiated to be the corner stone in my pursuing a PhD. I am grateful for their continuous guidance and motivation throughout my PhD.

I would use this opportunity to thank my lab colleagues, Dr. Ranjithkumar Rajendran, Vinothkumar Rajendran for providing me with a wonderful time in the lab, especially Edith Löffler for assisting me with the german translations and her friendly discussions. I am very grateful to my colleagues from my old lab, Cornelia, Marita and Thomas for their warm and welcoming attitude towards me when I was new to Germany and for helping me learn german language. My sincere thanks to Dr. Backialakshmi Dharmalingam, former post-doctoral fellow of our group for helping me settle down and providing support during my early days in Germany. My special thanks to Nabham Rai for being a constant source of motivation in my life and Vishnu for being a great friend in Giessen. I appreciate Dr. Oliver Rossbach for allowing me to work in his lab in the institute of biochemistry, Giessen and helping me plan and execute my experiment with utmost ease and for his scientific insights and suggestions.

Last but not the least; I am forever grateful to my parents, my father Zar Muhammad and my mother Milkhun Zar for having faith in me and allowing me to pursue my PhD in Germany. My deepest regards for my brothers Ashfaq Ali and Salman Ali for their unceasing support and encouragement. My sincere and heartily thanks to my sister Dr. Zahida Zar for her endless love, patience, moral support and assistance in every possible way and for being my pillar and confidant throughout the years. Finally, the one above all of us, the omnipresent Allah, for giving me the strength to continue my dream, for answering my prayers and for always being with me, I am forever grateful.

PUBLICATIONS

Publication originated from this dissertation

T. Zar, M. Tschernatsch, B.Hero, B. M. Kaps, B. Lang, K.T. Preissner, F. Blaes. NK-cell-mediated neuroblastoma cell lysis is enhanced by IgG from patients with paediatric Opsoclonus-Myoclonus-Syndrome. J of Pediatr Hematol Oncol 2020 Oct 13 PMID: 33060390 Online ahead of print.

Presentations and posters from this thesis

Tahira Zar, and Franz Blaes. NK cell-mediated neuroblastoma cell lysis is enhanced by IgG from patients with paediatric Opsoclonus Myoclonus Syndrome. 11th International Congress on Autoimmunity, Lisbon, Portugal. 2018.

Tahira Zar, Backialakshmi Dharmalingam, Franz Blaes. Tumor-immune interactions in paraneoplastic opsoclonus-myoclonus syndrome (OMS) by extracellular RNA (exRNA). Annual Retreat of GGL Section 5 (Neurosciences) at Giessen, Germany. 2017.

Tahira Zar, Backialakshmi Dharmalingam, Franz Blaes. Modification of onconeuronal antigens in the neuroblastoma of paraneoplastic OMS by free RNA. 9th International conference at the Giessen Graduate school of Life sciences (GGL), Giessen, Germany. 2016.